



Horizon 2020
Programme

Gemini Plus

Research and Innovation Action (RIA)

This project has received funding from the European Union's Horizon 2020 research and innovation programme under grant agreement No 755478.

Start date : 2017-09-01 Duration : 36 Months
<http://gemini-initiative.eu/>



Use of HTGR process heat with catalysts for dry reforming of methane using CO₂ to singas for the chemical industry

Authors : Dr. Ludwik PIENKOWSKI (AGH), Monika Motak (PROCHEM SA and AGH - University of Science and Technology, Faculty of Energy and Fuels), Radoslaw Dabek (AGH - University of Science and Technology, Faculty of Energy and Fuels) Marek Jaszczur (PROCHEM SA and AGH - University of Science and Technology, Faculty of Energy and Fuels), Ludwik Pienkowski (PROCHEM SA and AGH - University of Science and Technology, Faculty of Energy and Fuels)

Gemini Plus - Contract Number: 755478
Gemini Plus Dr. Panagiotis MANOLATOS

Document title	Use of HTGR process heat with catalysts for dry reforming of methane using CO ₂ to singas for the chemical industry
Author(s)	Dr. Ludwik PIENKOWSKI, Monika Motak (PROCHEM SA and AGH - University of Science and Technology, Faculty of Energy and Fuels), Radoslaw Dabek (AGH - University of Science and Technology, Faculty of Energy and Fuels) Marek Jaszczur (PROCHEM SA and AGH - University of Science and Technology, Faculty of Energy and Fuels), Ludwik Pienkowski (PROCHEM SA and AGH - University of Science and Technology, Faculty of Energy and Fuels)
Number of pages	65
Document type	Deliverable
Work Package	WP3
Document number	D3.6
Issued by	AGH
Date of completion	2018-05-16 15:38:47
Dissemination level	Public

Summary

The process of dry methane reforming (DRM) is an important reaction capable to convert carbon dioxide into industrially valuable synthesis gas, contributing in this way to valorization of CO₂ emissions. Energy to power the reaction may be supplied from the excess heat energy from small nuclear reactors (e.g. HTGR). Currently, the lack of stable catalyst is the main limiting factor for DRM commercialization. Therefore, various materials for efficient DRM catalysts have been intensively studied since last few decades. Since CO₂ is a stable and non-reactive molecule it requires highly active metal catalyst. For this reason noble metals were very promising materials. However, their high price and limited availability focused the research on nickel containing catalysts. Nickel-based catalysts show similar activity to those of noble metals, however, they tend to undergo deactivation due to formation of carbon deposits. Thus, the main challenge concerning DRM catalyst is to increase their stability. Various approaches and solutions have been proposed, including increasing nickel-support interactions, increasing surface basicity, decreasing nickel particle size and increasing nickel dispersion, which may be realized via application of appropriate support or addition of promoters. In view of these facts hydrotalcite-derived materials have been proposed as potential catalysts of dry reforming reaction. The catalytic properties of hydrotalcite-derived materials in DRM may be tailored by controlling composition of the catalyst precursor, synthesis method and promotion by various metal species as confirmed by studies carried out by The Group for Catalytic and Adsorption Processes in Energy and Environmental Protection from Faculty of Energy and Fuels, AGH University of Science and Technology. Further development of proposed catalysts, as well as tests on semi-industrial scale are important and may contribute to commercialization of dry reforming reaction.

Approval

Date	By
2018-05-16 15:49:23	Dr. Michael FÜTTERER (EC-JRC)

Use of HTGR process heat with catalysts for dry reforming of methane using CO₂ to syngas for the chemical industry

**Monika Motak¹², Radosław Dąbek², Marek Jaszczur¹²,
Ludwik Pieńkowski¹²**

1) *PROCHEM SA*

**2) *AGH - University of Science and Technology,
Faculty of Energy and Fuels***

Contents

1. Motivation for the research	3
1.1 Greenhouse gas emissions (GHGs) and Emissions reduction policies	3
1.2 Solutions for the reduction of CO ₂ emissions	4
2. Dry reforming of methane – applications	6
2.1 Synthesis gas production – comparison to other processes	6
2.2 Industrial experience with large scale reforming of CO ₂ -rich gas	8
2.2.1 CALCOR process	10
2.3 Potential future applications of DRM reaction	10
3. Thermodynamic analysis of CO₂ methane reforming	13
3.1 Thermodynamics of side reactions	15
3.2 Optimal conditions for DRM reaction	16
4. Catalysts for DRM	18
4.1 The role of active component	18
4.2 Nickel-based catalysts	21
4.3 Hydrotalcites	35
4.4 Hydrotalcites as DRM catalysts	35
5. Future plans	53
5.1 Bimetallic hydrotalcite-derived catalyst	53
5.2 Long-term stability tests and catalysts regeneration	54
References	56

1. Motivation for the research

1.1 Greenhouse gas emissions (GHGs) and Emissions reduction policies

The growing concerns about global climate change and increasing social awareness of the environmental problems have created a need for more sustainable development. Thus, our society needs to face new challenges, such as mitigation of climate change, preservation of the environment, usage of renewable energy and replacement of fossil fuels. The realization of these challenges requires new breakthrough solutions in order to be successfully addressed. There is no doubt that carbon dioxide (CO₂) is a common factor in these great challenges. The increasing emissions of this greenhouse gases (GHG) are of large concern and therefore nowadays a huge effort is dedicated to reduce emissions of GHG, especially carbon dioxide, which contributed in total to ca. 67% of 53 GtCO₂eq (in 2012) GHG emission [1,2].

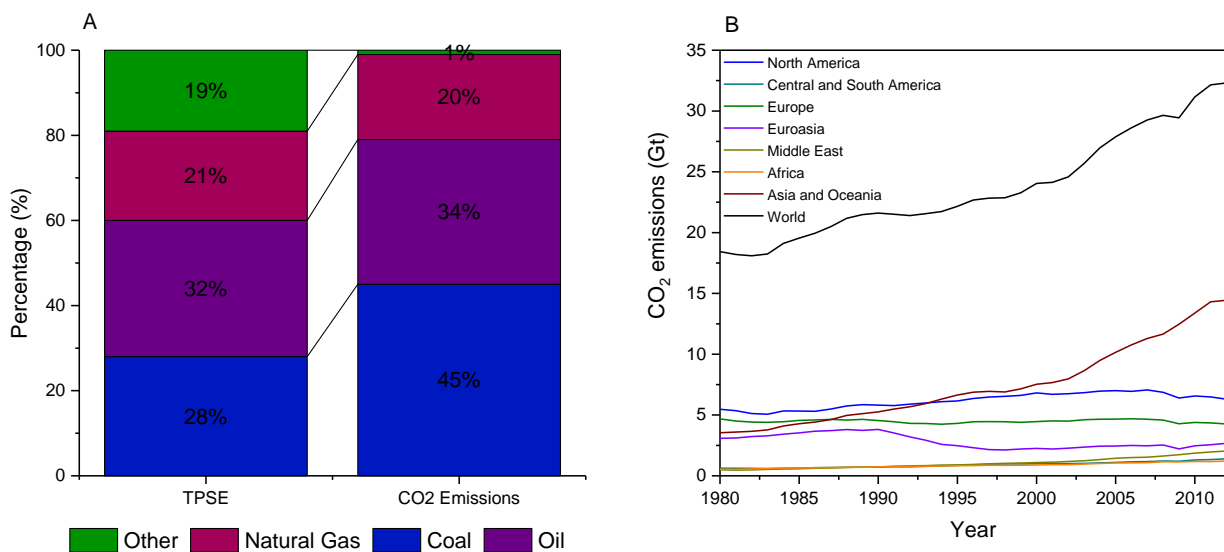


Fig. 1 (A) World primary energy supply (TPSE) and CO₂ emissions – shares by fuel in 2015 (adapted from [3]) and (B) global CO₂ emissions by region in 1980-2013 [2]

Carbon dioxide emissions have been constantly growing worldwide since pre-industrial era reaching the level of 36.2 Gt in 2016 [4]. This caused the increase of CO₂ concentration from ca. 280 ppm (parts per million) in the mid-1800s to 397 ppm in 2014, with an average growth of 2 ppm/year in the last 10 years [5]. More than 60% of anthropogenic greenhouse gas emissions, for which over 90% is associated with CO₂, are coming from energy sector. Between 1971 and 2013 an increase by 150% in global total primary energy supply (TPSE) has been observed, which is mainly caused by worldwide economic growth and development. Although for last few decades a huge development of renewable and nuclear energy sources was observed (which are considered non-emitting sources of energy), the world energy supply was relatively unchanged over past 42 years and fossil fuels still account for ca. 81% (in 2015) of world primary energy supply (Fig. 1A) [5]. Therefore, carbon dioxide emissions are strongly associated with the combustion of fossil fuels. Two fuels which accounted for the highest CO₂ emissions are coal and oil. Till early 2000s the shares of oil in global CO₂ emissions was exceeding those from coal. The situation changed in the beginning of 2000s, due to the higher consumption of coal by developing countries, such as India and China, where energy-intensive industrial processes are growing rapidly and large coal reserves are present.

At the same time worldwide natural gas consumption increases. In 2014 world natural gas consumption was equal to 12.9 Gtoe, which was 22.5% higher with the respect to year 2004. Only to the last year an increase of 1% in natural gas consumption was observed [6]. This trend is predicted to develop even faster as natural gas is the cheapest fossil fuel and possesses the highest H/C ratio, which contributes to lower CO₂ emissions with respect to other fossil fuels [7]. At the same time CO₂ emissions connected with the consumption of natural gas were equal to ca. 6.38 Gt in 2015, which accounted for ca. 20% of total CO₂ emissions [8]. Whence, natural gas and carbon dioxide are closely connected. Finding an appropriate solution

to ease an environmental impact of these two gases is crucial for sustainable development towards low-carbon economy and can be realized for instance via dry reforming of methane process.

It is also important to keep in mind, that the efforts to reduce CO₂ emissions are not only necessary from the environmental point, but also there are several law regulations demanding significant improvement in GHG emissions i.e. Kyoto protocol [9], Paris COP21 climate agreement [10] and European Union Policies [11,12]. The latter turned out to be very effective as the CO₂ emissions from EU countries by 0.4, 1.4 and 5.4%, respectively in 2012, 2013 and 2014 [5].

1.2 Solutions for the reduction of CO₂ emissions

The generally accepted solution for reducing CO₂ emissions into the atmosphere involves the implementation of three strategies [13]: (1) a reduction in energy consumption, (2) a change in what we consume, or (3) a change of our attitude towards the resources and waste. Currently, the most developed strategies are (1) and (2). These two strategies are resulting in lower carbon consumption by development of technologies with higher efficiency, the decrease in consumption of energy per capita and replacement of fossil fuel-based energy sources by renewables, such as wind, solar, biomass etc. However, there is a huge potential in changing our attitude towards greatly produced waste – carbon dioxide. **The implementation of carbon dioxide utilization processes is a key element to sustainable development, as strategies (1) and (2) have a limited capacity, and, as it is predicted, fossil fuels will still be our main source of energy in coming decades.** The reduction of carbon dioxide can be realized either by carbon capture and storage (CCS) technologies or via utilization of carbon dioxide as a chemical feedstock – CCU (Carbon Capture and Utilization). These two approaches are complementary, and while CCS technologies are aiming at capturing and subsequently storing huge quantities of carbon dioxide, **the chemical utilization of CO₂ aims at generating added-value products.** Moreover, most technologies, which are currently developed as future CO₂ utilization processes, require pure streams of CO₂. Thus, implementation of both solutions CCS and chemical utilization of CO₂ is required. CO₂ already finds a number of applications. However, its use as chemical feedstock has still a huge potential with a number of industrial opportunities and advantages [14,15]:

- CO₂ becomes an interesting raw material with almost zero or even negative costs.
- CCU technologies can create a positive public image of companies, as with the increasing political and social pressure on reducing CO₂ emissions, carbon dioxide will be utilized to valuable products.
- Instead of inactive storage of carbon dioxide (CCS), CO₂ will be recycled. It will also reduce the costs of CO₂ transport.
- With the production of new chemicals companies can gain new market shares.
- CCU gives opportunities to produce organic chemicals in a safer way, as many organic synthesis produce pollutants as e.g. CO₂ is 'green' alternative for toxic phosgene in organic synthesis of polycarbonates.

Fig. 2 presents current and potential technologies which use CO₂ for the production of synthetic fuels and added-value chemicals. It is predicted that processes involving CO₂ conversion will be developed on industrial scale in the coming decades, creating in this way a **new carbon dioxide based economy** [16]. Since all of these reactions require the presence of catalysts, this clearly points to the importance of catalytic studies of these chemical reactions on laboratory and pilot scale.

CO₂ conversion to fuels, rather than organic chemicals, is expected to play a major role in CO₂ emission management strategies. Firstly, because fuels market is much larger than the market of organic chemicals. Secondly, CO₂ emissions are mainly associated with the production of energy from fossil fuels. As reported by Centi et al. [15] around 5-10% of current total CO₂ emissions is suitable for the production of fuels, which corresponds to reduction of ca. 1.75-3.5 Gt CO₂ emissions per year. As the processes of CO₂ conversion into fuels are energy demanding, there is a need to apply and develop renewable technologies in order to supply energy for these chemical reactions. Thus, carbon dioxide and CCU technologies are a key element of our

sustainable development. This report is focusing on presenting the current state of knowledge and the developments achieved during the realization of NCBiR project 'Technologies supporting Development of Safe Nuclear Energy' concerning process of CO₂ methane reforming (DRM). The DRM process has already been proven to may have a significant environmental and economic impact in the future. **Therefore the research in this area may be crucial for future development towards low-carbon economy.**

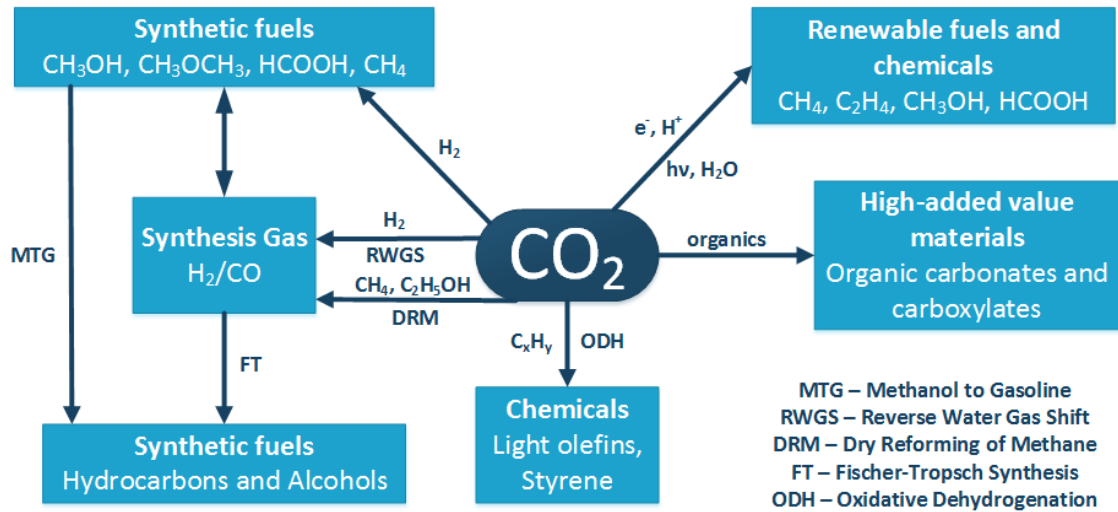


Fig. 2 Catalytic routes for CO₂ transformation into fuels and chemicals (adapted from [16])

2. Dry reforming of methane – applications

The first investigations concerning converting CO₂ and CH₄ into synthesis gas were reported in 1888. The process was further investigated by Fischer and Tropsch in 1928 [17]. Thus DRM process is not a new concept. Nowadays, dry reforming reaction has again gained much attention due to the possibility of utilizing two greenhouse gases (carbon dioxide and methane) and the production of a very valuable mixture of H₂ and CO – a building block for the production of liquid fuels and chemicals. Moreover, DRM can utilize natural gas fields which contain high amounts of CO₂ and are currently economically unprofitable to be extracted. Such gas fields often contain, apart from hydrocarbons, also carbon dioxide, whose concentration can vary from a few percent up to even 70%, as reported e.g. for Natuna natural gas field in Indonesia [18]. Studies carried out by Suhartanto et al. [18] confirmed possible application of DRM technology for this field, which, as confirmed, contains ca. 1302 billion cubic meters of gaseous hydrocarbons.

2.1 Synthesis gas production – comparison to other processes

In 2010 syngas production was over 70 000 MW_{th}, 45% of which was used to produce chemicals and 38% to produce liquid fuels [14]. Synthesis gas is currently produced on industrial scale via steam reforming of methane (eq. 1) on nickel-based catalysts, or gasification and pyrolysis of carbonaceous materials. However, very interesting alternative is to produce synthesis gas from methane in **dry reforming process (DRM)** (eq. 3). Another alternative is to perform partial oxidation of methane (POM) (eq. 2). The reforming routes for production of synthesis gas are summarized in Table 1.

Table 1 Methane reforming processes resulting in synthesis gas production

Process	Main reaction	ΔH_{298}^0 (kJ/mol)	E quation
Steam Reforming of Methane (SRM)	$\text{CH}_4 + \text{H}_2\text{O} \rightleftharpoons \text{CO} + 3\text{H}_2$	20 6	(1)
Partial Oxidation of Methane (POM)	$\text{CH}_4 + \frac{1}{2}\text{O}_2 \rightleftharpoons \text{CO} + 2\text{H}_2$	-36	(2)
Dry Reforming of Methane (DRM)	$\text{CH}_4 + \text{CO}_2 \rightleftharpoons 2\text{CO} + 2\text{H}_2$	24 7	(3)
Autothermal reforming	$\text{CH}_4 + \text{CO}_2 \rightleftharpoons 2\text{CO} + 2\text{H}_2$	24 7	(4)
	$\text{CH}_4 + \text{H}_2\text{O} \rightleftharpoons \text{CO} + 3\text{H}_2$	20 6	(5)
	In excess of methane, heat from CH ₄ combustion: $\text{CH}_4 + 2\text{O}_2 \rightleftharpoons \text{CO}_2 + 2\text{H}_2\text{O}$	- 880	(6)
Tri-reforming	Combination of SRM, DRM and POM		
Accompanying and side reactions:			
Water Gas Shift (WGS)	$\text{H}_2\text{O} + \text{CO} \rightleftharpoons \text{CO}_2 + \text{H}_2$	-41	(7)
Reverse Water Gas Shift (RWGS)	$\text{H}_2 + \text{CO}_2 \rightleftharpoons \text{H}_2\text{O} + \text{CO}$	41	(8)
Boudouard reaction	$2\text{CO} \rightleftharpoons \text{C} + \text{CO}_2$	- 172	(9)
CH ₄ decomposition	$\text{CH}_4 \rightleftharpoons \text{C} + 2\text{H}_2$	75	(

			10)
Oxidation of methane (OM)	$\text{CH}_4 + 2\text{O}_2 \rightleftharpoons \text{CO}_2 + 2\text{H}_2\text{O}$	802	11)

As presented in Table 1 synthesis gas can be produced from methane through different routes such as steam reforming of methane (SRM), DRM, partial methane oxidation (POM), autothermal reforming or tri-reforming process. The obtained H_2/CO molar ratio varies depending on the type of oxidant applied in a given process. The commercialization of DRM would be beneficial not only from the environmental perspective, but also because DRM could become a good alternative for other syngas producing reactions.

Steam reforming has been developed on the industrial scale in 1930s, and since then was strongly developed, becoming nowadays the main technology of syngas production which operates at or near its theoretical limits [19,20]. SRM process gives the highest H_2/CO molar ratio around 3, making it a suitable method for hydrogen production via water gas shift WGS. In this way e.g. H_2 for ammonia synthesis plants is produced. However, WGS reaction produces high amounts of CO_2 . On the other hand, such high H_2/CO molar ratio makes syngas from SRM unsuitable for other chemical process, such as synthesis of organic oxygenated compounds (methanol, acetic acid) or hydrocarbons. In Fischer-Tropsch (FT) synthesis high H_2/CO ratios limit carbon chain growth [19]. In this way **DRM reaction, which gives H_2/CO molar ratio around unity, can be considered more suitable for FT synthesis for production of long chain hydrocarbons or valuable oxygenated chemicals.**

SRM and DRM reactions are both endothermic and thus require high energy inputs, which are currently supplied for SRM process by the combustion of fossil fuels, contributing in this way to the growth of CO_2 emissions [21]. The generally accepted solution, in order to contribute to CO_2 emissions reduction, is to power DRM process by either renewables or nuclear energy. Moreover, SRM process is considered rather expensive, as it operates at high pressures (higher than DRM [22]) and requires high-temperature steam, which generates additional costs. Er-rbib et al. [22] compared SRM and DRM processes in terms of energy balance and CO_2 emissions for the production of synthesis gas and further H_2 production via WGS reaction (Table 2). Their studies clearly show, that **DRM can contribute to reduction of CO_2 emissions while producing synthesis gas.** On the other hand, DRM is rather not suitable for H_2 production, as production of 1kg of H_2 via DRM requires ca. 1.5 times more energy than SRM. At the same time application of DRM is connected to lower or negative CO_2 emissions with respect to SRM for both syngas and H_2 production. Although both processes give synthesis gas, the composition of the obtained product differs. Thus SRM and DRM can be used to supply syngas for different chemical processes and markets.

Table 2 Energy and CO_2 balances of steam and dry reforming of methane processes (adapted from [22])

	Steam reforming of Methane (SRM)		Dry reforming of Methane (DRM)	
	Energy balance	CO_2 balance	Energy balance	CO_2 balance
Synthesis gas production	6.65 MJ/kg($\text{CO}+3\text{H}_2$)	0.45 kg CO_2 /kg($\text{CO}+3\text{H}_2$)	4.35 MJ/kg($2\text{CO}+2\text{H}_2$)	-0.44 kg CO_2 /kg($2\text{CO}+2\text{H}_2$)
Hydrogen production	27 MJ/kg H_2	7 kg CO_2 /kg H_2	42.7 MJ/kg H_2	2.34 kg CO_2 /kg H_2

Syngas can be also produced via partial methane oxidation, which was first investigated in the 1930's and 1940's [19]. POM is an exothermic process, and thus does not require such high energy inputs as SRM and DRM. On the other hand, the process requires pure stream of O_2 , which generates additional costs. The performance of POM process in the stream of air, is considered not beneficial due to the high content of balance N_2 . Moreover, high exothermicity of the reaction can generate additional problems, such as hot spots in catalysts, and thus make process control difficult. At the same time, it is very important to control POM, as CH_4 and O_2 can form an explosive mixture [19]. The process gives H_2/CO molar ratio around 2, making it suitable for the market competition with DRM.

In order to eliminate high energy demand for SRM and DRM reactions, the concept of autothermal reforming (ATR) was developed. ATR technology is a combination of POM and SRM, or POM and DRM, so it includes both exothermic and endothermic reactions. The energy released in POM is consumed by the endothermic reaction, making the process autothermal. The feed gas composition influences the obtained H₂/CO molar ratio. Typically, the values of H₂/CO between 1 and 2 are obtained. The main drawback of ATR process is high cost of oxygen separation [23].

Tri-reforming (TRM) process seems to be the most advantageous method of syngas production. The combination of SRM, DRM and POM makes the process suitable for direct conversion of flue gases from fossil fuelled power plants to synthesis gas. Typically, flue gas from fossil fuelled power plant contains 12-14% CO₂, 8-10% H₂O, 3-5% O₂ and 72-77% N₂, while that from natural-gas fired one contains 8-10% CO₂, 18-20% H₂O, 2-3% O₂ and 67-72% N₂ [24–26]. However, there is still a problem of high concentration of balance N₂. This issue can be resolved by implementation of oxyfuel combustion, which results in the decrease of N₂ concentration of flue gases. Depending on the applied conditions, such as temperature and feed gas composition, it is possible to tailor thermal effect of the process to obtain mildly endothermic, almost thermoneutral or mildly exothermic process, and an appropriate distribution of the obtained products (H₂/CO molar ratio) [27]. It must be stressed, however, that TRM process, due to the presence of a large number of reagents, is influenced by the occurrence of a large number of side reactions, which makes the chemistry of the process hard to study.

2.2 Industrial experience with large scale reforming of CO₂-rich gas

The industrial applications of dry reforming process are so far limited to a combination of steam reforming and dry reforming reactions. The addition of CO₂ into a feed allows to control distribution of obtained products, i.e. H₂/CO molar ratio. Depending on the subsequent application of obtained synthesis gas, processes differ in operating parameters and feed composition. The comparison of different large-scale reforming processes which apply CO₂-rich gas is compared in Table 3 [28].

In a typical large-scale combined SRM-DRM reforming plant, feedstock, which may be composed from lean natural gas to heavy naphtha, is first heated to ca. 400°C and undergoes desulphurization process in order to remove sulphur species. Higher hydrocarbons which may be present in the feed, are converted into a mixture of H₂, CO₂, CH₄ and traces of CO in a pre-reformer. This stage is usually realized in the temperature range 400-550°C in order to avoid deactivation by carbonaceous deposits from higher hydrocarbons. In the next stage, the feed gas is introduced into a tubular reactor where actual reforming takes place and a mixture of CH₄/CO₂/H₂O is converted into synthesis gas. The reactor tubes are placed in the furnace powered by the combustion of fuels to supply heat for endothermic reforming process. The temperature in the reformer may differ, depending on the process. Usually it is performed at high temperatures, up to 1000°C.

The commercialization of such reforming plants is dependent on carbon-free operation. It is essential because of the problems connected with high pressure drop or expensive costs of loading of a new batch of catalyst. As it can be seen from Table 3, so far, large-scale reforming plants apply nickel catalyst supported on **alumina-magnesia**. This, clearly points that the search for a **catalyst for DRM reaction should be focused on similar systems**.

The two most often mentioned in literature large-scale reforming technologies, which apply DRM reaction, are CALCOR and SPARG processes [29].

Table 3 Comparison of full size monoreactor pilot experiments (HOU) and industrial plants (referenced with the country where they were constructed) of CO₂ rich reforming with different catalysts under different conditions. (adapted from [28]).

Process	Operating conditions				Primary reformer feed				Outlet	
	Catalyst	Feed	P (Bar)	T _{EXIT} (°C)	H ₂ O/CH ₄ (-)	CH ₄ (mol %)	CO ₂ (mol %)	H ₂ (mol %)	H ₂ /CO (-)	TOS (h)
HOU-1	Ni/MgAl ₂ O ₄	Natural Gas	23	945	1.4	74	18	9	2.6	400
HOU-2	Ni/MgAl ₂ O ₄	Natural Gas	24	945	1.6	56	44	0	1.8	380
Iran	Ni/MgAl ₂ O ₄	Natural Gas	20	960	1.3	70	12	17	3.0	-
Indonesia	Ni/MgAl ₂ O ₄	Natural Gas	12	960	2.1	74	23	2	2.7	-
Malaysia	Ni/MgAl ₂ O ₄	Natural Gas	25	950	1.5	63	20	16	2.7	-
South Korea	Ni/MgAl ₂ O ₄	Naphtha	25	900	1.7	47	38	15	2.1	-
India	Ni/MgAl ₂ O ₄	Naphtha	22	920	1.7	40	41	17	1.9	-
UK	Ni/MgAl ₂ O ₄	Naphtha	20	900	2.0	32	56	12	1.7	-
Netherlands	Ni/MgAl ₂ O ₄	Natural Gas	15	815	2.0	28	71	1	1.2	-
Sulphur-Passivated Reforming (SPARG):										
HOU-3	Ni/MgAl ₂ O ₄	Natural Gas	6	890	1.0	57	37	6	1.9	500
HOU-4	Ni/MgAl ₂ O ₄	Natural Gas	6	930	0.4	40	59	1	0.9	500
HOU-5	Ni/MgAl ₂ O ₄	Natural Gas	14	930	0.7	38	61	1	0.9	160
USA	Ni/MgAl ₂ O ₄	Natural Gas	7	900	0.9	61	33	6	1.8	-
HOU-7	Ru/MgAl ₂ O ₄	Natural Gas	32	940	0.9	51	44	5	1.4	490
Japan	Ru/MgAl ₂ O ₄	Natural Gas	2	850	1.8	10	56	32	1.0	-

2.2.1 CALCOR process

The production of carbon monoxide realized via CALCOR process combines SRM with DRM. The first pilot plants which applied this process were built in the 40s of the last century [30]. Laboratory scale studies carried out by Reitmeier et al. [30] showed that it is possible to obtain synthesis gas with high excess of CO (H_2/CO around 0.5) by a combination of steam and dry reforming reactions without any difficulties arising from the deposition of carbon. Currently, CALCOR process is a well-established technology for production of pure CO, which can be further utilized on-site for the conversion to organic compounds, such as phosgene.

In CALCOR process carbon monoxide is obtained by steam reforming of natural gas mixed with recycled CO_2 at high temperatures and high pressures in the presence of an undisclosed catalyst. It is believed, that high resistance to coking in CALCOR process is obtained via application of a few catalysts with various activities and shapes, which are placed in a different parts of reformer tubes. The process requires highly cleaned feed in order to protect the catalysts from sulphur poisoning. Usually in standard CALCOR process syngas with H_2/CO molar ratio around 0.42 is obtained [31]. The required heat comes from the combustion of fossil fuels and tail gas from CO purification units. It should be mentioned, however, that the application of DRM reaction in CALCOR process does not result in CO_2 emissions reduction. The analysis showed that for every ton of CO produced, ca. 1.8 tons of CO_2 is emitted to the atmosphere.

2.2.2 SPARG process

Sulphur Passivated Reforming (SPARG) process was commercialized in 1987 [29]. It combines steam and dry reforming with the aim to obtain synthesis gas with H_2/CO molar ratio around 1.8, which can be further used to produce acetic acid, dimethyl ether or oxo-alcohols. SPARG utilizes nickel-based catalyst, which resistance to coking was increased by passivation of nickel surface by sulphur. In this way active sites for carbon-forming reactions are poisoned, while catalytic activity towards reforming is maintained ('promotion by poisoning') [32]. The poisoning of Ni active sites is performed by co-feeding small amounts of H_2S and H_2 and needs to be carried out carefully in order to avoid the formation of nickel sulphides, which inhibit catalyst activity towards SRM/DRM [28]. SPARG process proceeds at high temperatures around 1000°C.

2.3 Potential future applications of DRM reaction

2.3.1 Chemical Energy Transmission and/or Storage Systems (CETS)

Dry reforming reaction may be applied in exothermic-endothermic reaction-cycle systems for transport and storage of energy. The schematic concept of the so called chemical energy transmission systems is presented in Fig. 3. Endothermic reaction is powered by fossil, nuclear or renewable energy. The products of the reaction, which store energy, are saved for later use or transported through pipelines to a location where exothermic reaction releases energy [33].

So far several concept of this CETS system has been considered for industrial application. The most advanced developments have been made in the nuclear ADAM-EVA process [33]. The application of DRM reaction in CETS systems has a huge potential. McCrary et al. [34] and Chubb [35] proposed SOLCHEM technology. In this concept, reversible closed-cycle chemical reactions are carried out in order to transport solar energy from solar collectors to a central station, where the energy could be released in case of increased demand. The process investigated CO_2 reforming-methanation cycle, in which a mixture of CH_4 and CO_2 underwent dry reforming reaction at temperatures higher than 700°C, giving H_2 and CO. The energy for the DRM reaction was supplied from the solar collectors. Obtained syngas can be transported and subsequently undergoes methanation at temperatures below 600°C, to form methane and carbon dioxide. The stored energy is released in this exothermic reaction. Although, the SOLCHEM concept has not been developed on the industrial scale, it proposes an alternative way to use DRM reaction as an energy carrier.

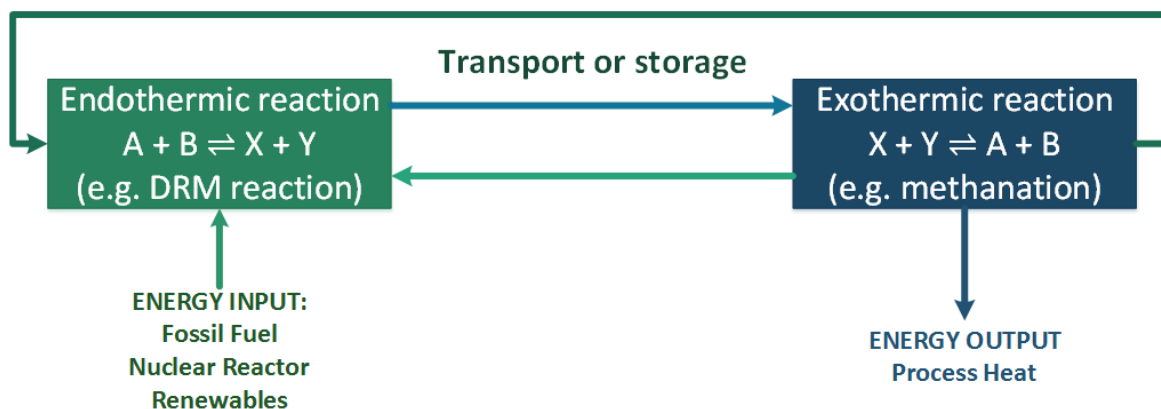


Fig. 3 The scheme of chemical energy transmission system (CETS) for transport and storage of energy

Similarly as proposed in SOLCHEM technology, DRM reaction can be powered by other renewables or nuclear energy. The only limitation concerning the application of DRM in CETS is the offer of a stable catalyst.

2.3.2 DRM for production of chemicals

Apart from the application of DRM as a way of transport and storage of energy, the main potential future application of this process is associated with the production of synthesis gas to be used in subsequent synthesis of fuels or chemicals.

Table 4 The comparison of different concepts of CO₂ conversion to varied products, implementing DRM reaction (adapted from [21])

Route	Moles of CO ₂ mitigated per mole of CO ₂ consumed	Conclusions
CH₄ to higher hydrocarbons (HC)		
Reactions: $\text{CH}_4 + \text{CO}_2 \rightleftharpoons 2\text{CO} + 2\text{H}_2$ $\text{CH}_4 + \text{H}_2\text{O} \rightleftharpoons \text{CO} + 3\text{H}_2$ $6\text{CO} + 13\text{H}_2 \rightleftharpoons \text{C}_6\text{H}_{12} + \text{H}_2\text{O}$	A net reduction of 0.95 moles of CO ₂	This is an effective method of CO ₂ mitigation
CH₄ to methanol		
Reactions: $\text{CH}_4 + \text{CO}_2 \rightleftharpoons 2\text{CO} + 2\text{H}_2$ $\text{CH}_4 + \text{H}_2\text{O} \rightleftharpoons \text{CO} + 3\text{H}_2$ $\text{CO} + 2\text{H}_2 \rightleftharpoons \text{CH}_3\text{OH}$	A net reduction of 0.66 moles of CO ₂	Provides a trap for some CO ₂ . The methanol production by combined SRM-DRM process will contribute only to small global CO ₂ emissions reduction.
CH₄ to carbon		
Reactions: $\text{CH}_4 + \text{CO}_2 \rightleftharpoons 2\text{CO} + 2\text{H}_2$ $2\text{CO} + 2\text{H}_2 \rightleftharpoons 2\text{C} + 2\text{H}_2\text{O}$	A net reduction of 1 mole of CO ₂	Offers an energy efficient means of CO ₂ mitigation. Carbon can be used as adsorbent or as catalyst support.

It has been proven that there is a need on the market for synthesis gas with H₂/CO molar ratio lower than that obtained via SRM process [28]. In this way not only added-value products could be obtained, but also CO₂ emissions could be reduced.

Ross et al. [21] analysed CO₂ mitigation connected with potential future applications of DRM reaction as the means of producing hydrocarbons via FT synthesis, methanol and carbon (via reduction of CO). The results presented in Table 4, showed that the combination of DRM and SRM could attribute to the reduction of

CO₂ emissions, if powered by non-fossil fuel energy source. The application DRM process alone might be thus even more beneficial.

The main problem limiting the application of DRM reaction is the formation of carbon deposits on the catalyst surface. **Therefore, the commercialization of DRM reaction on industrial scale is depended on the offer of new stable and active catalyst** and price of ton of CO₂ (around 8€ nowadays).

3. Thermodynamic analysis of CO₂ methane reforming

The dry reforming of methane is highly endothermic reaction and high temperatures are required in order to obtain considerable conversions of CH₄ and CO₂. Additionally, there is a number of possible side reactions which may occur during DRM process, and thus thermodynamic analysis of the process is important. Partial information concerning thermodynamic equilibrium calculations studied based on the minimization of Gibbs free energy is available in literature [36–43]. Nikoo et al. [36] studied the thermodynamics of DRM reaction in the view of carbon formation. Istadi et al. [37] investigated the possibilities of the formation of C₂ hydrocarbons, but the possible C-forming reactions were not analysed. Li et al. [38] compared thermodynamic calculations for autothermal, steam and dry reforming processes. The analysis of DRM at high pressures was performed by Chien et al. [39]. Shamsi et al. [40] reported thermodynamic data of two carbon-forming reactions in DRM process: CH₄ decomposition and Boudouard reaction. Sun et al. [41] analysed the thermodynamics of steam and dry reforming in a view of their solar thermal applications. Soria et al. [42] and Ozkara-Aydinoglu [43] carried out the thermodynamic analysis of combined SRM-DRM systems. Propane dry reforming was analysed by Wang et al. [44].

The thermodynamics of DRM was also analyzed by the authors of this report. The thermodynamic equilibrium concentration analysis of DRM reaction was performed with HSC Chemistry 5 software based on minimization of Gibbs free energy method. The effects of temperature and concentration of substrates were considered while calculating equilibrium compositions. The possible reactants in the DRM reaction, which were taken into account during analysis, were: Ar_(g), CH_{4(g)}, C₂H_{2(g)}, C₂H_{4(g)}, C₂H_{6(g)}, CO_(g), CO_{2(g)}, H_{2(g)}, CH₃OH_(g), CH₃OCH_{3(g)}, C_(s) and H₂O_(g). Ar_(g), CH_{4(g)} and CO_{2(g)} were introduced into the system as the substrates, while other reactants were considered as possible products of DRM and side reactions. The summary of this analysis is presented below and in the Fig. 4.

CH₄ conversion was increasing with temperature and reached ca. 100% at 800°C. CO₂ conversion decreased with temperature till it reached minimum in the temperature range 500-600°C and then an increase in conversion was observed. CO₂ conversions reached ca. 100% at temperatures higher than 950°C. In the whole temperature range CH₄ conversions were higher than for CO₂, especially in the low temperature range. This clearly indicates that both methane and carbon dioxide are involved in side reactions. It is reflected also in the excess of produced H₂, especially at low temperature as illustrated by Fig. 4 B, where the values of H₂/CO molar ratio reached unity above 850°C. Apart from the products of DRM reaction, H₂ and CO, carbon and water were formed. The concentration of other chemical compounds that were included in the study, such as CH₃OH, C₂H₆, C₂H₄, CH₃OCH₃, HCOOH, were observed at the level of ca. 1·10⁻³ -1·10⁻⁴ moles for C₂ hydrocarbons, and were even lower for the other considered chemicals, and thus the influence of reactions involving these chemicals on DRM process may be neglected and will not be discussed further.

The equilibrium water content was decreasing with the increase of temperature and only negligible amounts of water were present in the system at temperatures higher than 900°C. Water can be formed in RWGS reaction, reduction of CO and CO₂ with hydrogen and methanation processes. It is most probable that in the low temperature range RWGS contributes the most to the water formation. The same conclusion was reported by Soria et. al. [42].

Equilibrium carbon content was decreasing with the increase of temperature and almost no carbon formation may be observed at temperatures higher than 900°C (cp. Fig. 4 A and E). Up to 550°C the amount of carbon deposits decreased slowly, and above 550°C the decrease was rapid. As is reported in literature [36], carbon formation at low temperatures may be mainly associated with the disproportionation of CO. The reverse reaction is highly endothermic, and thus promoted at high temperatures, which can contribute to the oxidation of carbon deposits and results in the decrease of equilibrium carbon content. On the other hand, endothermic direct CH₄ decomposition is responsible for carbon formation at high temperatures.

A

B

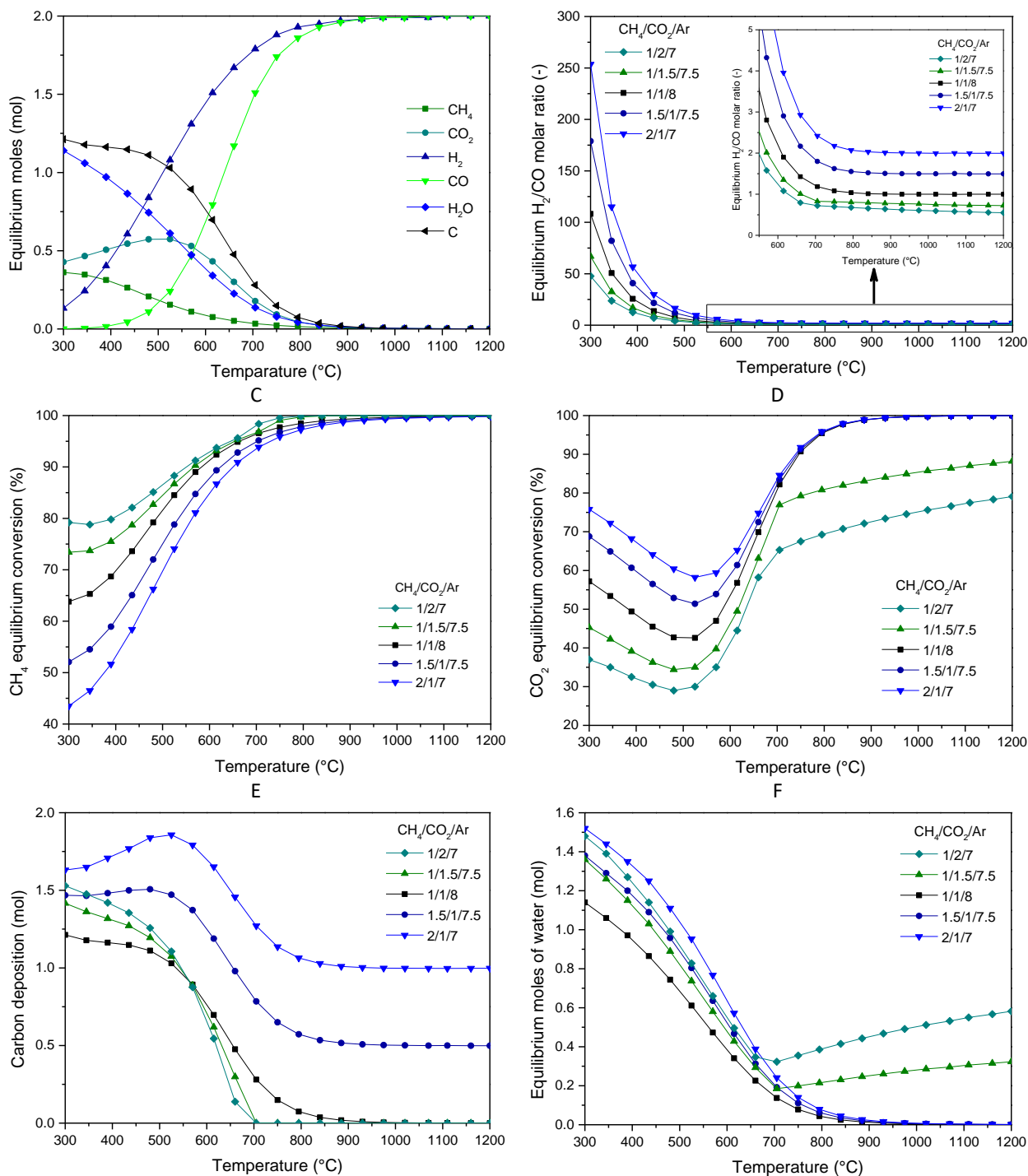


Fig. 4 The influence of temperature on the equilibrium concentration of reactants during DRM. Temperature range 300-1200°C. Atmospheric pressure.

- (A) equilibrium conversions of reactants for $\text{CH}_4/\text{CO}_2/\text{Ar}=1/1/8$; (B) equilibrium H_2/CO molar ratio;
 (C) CH_4 equilibrium conversion; (D) CO_2 equilibrium conversion;
 (E) Equilibrium moles of carbon; (F) equilibrium moles of H_2O ;

The obtained values of H_2/CO ratio showed an excess of hydrogen in the system (Fig. 4 B), which is decreasing with the increase of temperature. This effect may be explained by the occurrence of direct methane decomposition and SRM reactions. As reported by Ozkara-Adinoglu [43] for the combined SRM-DRM process, CH_4 reacts more easily with water than CO_2 , since the latter is a very stable molecule. Additionally, in the low temperature range exothermic water gas shift (WGS) can influence DRM process and contribute to H_2 production.

3.1 Thermodynamics of side reactions

Table 5 presents the list of possible reactions which may occur in DRM process. The reactions (or group of reactions) are [7,36,37,40,41,43]:

- Reverse water gas shift – RWGS (eq. 2) – accompanies DRM reaction in whole temperature range
- Carbon forming reactions (eq. 3-6):
 - CH₄ decomposition (eq. 3) – favored at high temperatures;
 - Boudouard reaction (eq. 4) – favored below 550°C;
 - Hydrogenation of CO and CO₂ (eq. 5-6) – do not influence process significantly;
- Oxidative coupling reactions (eq. 7-8) – occur at high temperatures;
- Dehydrogenation (eq. 9) – occurs at high temperatures;
- Hydrogenation of CO and CO₂ (eq. 10-12) – at high temperatures favorable towards reverse side
- Methanation (eq. 13-14) – favorable at temperatures below 550°C
- Dehydration (eq. 15) – highly influenced by equilibrium limitations;
- Reforming reactions (16-22) – tent to occur at high temperatures.

The influence of each reaction presented in Table 5 on the overall DRM process is different. In general, as the main side reactions are considered RWGS (eq. 2), CH₄ decomposition (eq. 3) and disproportionation of CO (eq. 4). The influence of other reactions is rather insignificant [36,37]. However, they still need to be taken into account, as e.g. reforming reactions (eq. 16-22) can contribute to the syngas production. The temperature ranges in which the main DRM side reactions are favored are presented in Fig. 5.

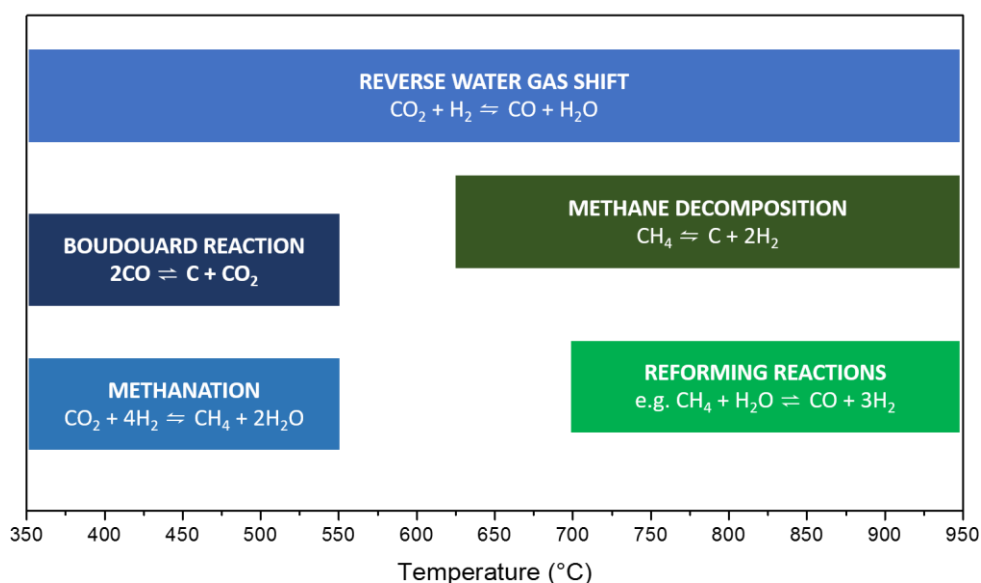


Fig. 5 Temperature ranges in which the main side reactions during DRM process are favourable

Table 5 The main reactions which may occur during dry reforming of methane (adapted and modified from [36])

Reaction number	Reaction	ΔH_{298}^0 (kJ/mol)
	Dry reforming	

1	$\text{CH}_4 + \text{CO}_2 \rightleftharpoons 2\text{CO} + 2\text{H}_2$	+247
Reverse Water Gas Shift		
2	$\text{CO}_2 + \text{H}_2 \rightleftharpoons \text{CO} + \text{H}_2\text{O}$	+41
Carbon forming reactions		
3	$\text{CH}_4 \rightleftharpoons \text{C} + 2\text{H}_2$	74.9
4	$2\text{CO} \rightleftharpoons \text{C} + \text{CO}_2$	-172.4
5	$\text{CO}_2 + 2\text{H}_2 \rightleftharpoons \text{C} + 2\text{H}_2\text{O}$	-90
6	$\text{CO} + \text{H}_2 \rightleftharpoons \text{C} + \text{H}_2\text{O}$	-131.3
Oxidative coupling of methane		
7	$2\text{CH}_4 + \text{CO}_2 \rightleftharpoons \text{C}_2\text{H}_6 + \text{CO} + \text{H}_2\text{O}$	+106
8	$2\text{CH}_4 + 2\text{CO}_2 \rightleftharpoons \text{C}_2\text{H}_4 + 2\text{CO} + 2\text{H}_2\text{O}$	+284
Dehydrogenation		
9	$\text{C}_2\text{H}_6 \rightleftharpoons \text{C}_2\text{H}_4 + \text{H}_2$	+136
Hydrogenation of CO and CO ₂		
10	$\text{CO} + 2\text{H}_2 \rightleftharpoons \text{CH}_3\text{OH}$	-90.6
11	$\text{CO}_2 + 3\text{H}_2 \rightleftharpoons \text{CH}_3\text{OH} + \text{H}_2\text{O}$	-49.1
12	$\text{CO}_2 + \text{H}_2 \rightleftharpoons \text{HCOOH}$	15
Methanation		
13	$\text{CO}_2 + 4\text{H}_2 \rightleftharpoons \text{CH}_4 + 2\text{H}_2\text{O}$	-165
14	$\text{CO} + 3\text{H}_2 \rightleftharpoons \text{CH}_4 + \text{H}_2\text{O}$	-206.2
Dehydration		
15	$2\text{CH}_3\text{OH} \rightleftharpoons \text{CH}_3\text{OCH}_3 + \text{H}_2\text{O}$	-37
Reforming		
16	$\text{CH}_3\text{OCH}_3 + \text{CO}_2 \rightleftharpoons 3\text{CO} + 3\text{H}_2$	+258.4
17	$\text{C}_2\text{H}_6 + 2\text{H}_2\text{O} \rightleftharpoons 2\text{CO} + 5\text{H}_2$	+350
18	$\text{C}_2\text{H}_6 + 2\text{CO}_2 \rightleftharpoons 4\text{CO} + 3\text{H}_2$	+430
19	$\text{C}_2\text{H}_4 + 2\text{CO}_2 \rightleftharpoons 4\text{CO} + 2\text{H}_2$	+290
20	$\text{C}_2\text{H}_4 + 2\text{H}_2\text{O} \rightleftharpoons 2\text{CO} + 4\text{H}_2$	+210
21	$\text{CH}_3\text{OCH}_3 + 3\text{H}_2\text{O} \rightleftharpoons 2\text{CO}_2 + 6\text{H}_2$	+136
22	$\text{CH}_3\text{OCH}_3 + \text{H}_2\text{O} \rightleftharpoons 2\text{CO} + 4\text{H}_2$	+204.8

3.2 Optimal conditions for DRM reaction

Basing on the thermodynamic analysis of DRM process presented in literature [36–44], some general remarks concerning optimal conditions for dry reforming of methane can be formulated:

- Considerable conversions of both CH₄ and CO₂ and H₂/CO molar ratios around unity can be reached at temperatures higher than 700°C and atmospheric pressure. (DRM is thermodynamically favourable above 700°C).
- Carbon formation can be suppressed by introducing the excess of CO₂ into reaction system and carrying out the process at high temperatures.
- The reaction is favourable at low pressures, as at high pressures carbon formation increases and CO₂ and CH₄ conversions decreases.

- Introduction of other oxidizing agents such as water or O₂ can also decrease carbon formation [38,41–44].

The above remarks are very general. The high temperatures of reaction promote DRM route and inhibit side reactions. However, from the economic and technical perspective it would be more beneficial to perform DRM process at temperatures lower than 700°C. In order to do that, active, stable and selective catalysts needs to be introduced into the DRM reaction system, which **can promote a kinetic inhibition of carbon formation and shift selectivity of the process towards DRM.**

4. Catalysts for DRM

Carbon dioxide is a stable molecule, thus its chemical activation requires highly active metal catalysts. The catalytic performance of the material may be affected by numerous variables, such as active material, support, promoter, calcination temperature and conditions, reducing environment, preparation method, particle size, shape, and reactor selection.

During last decades great efforts have been undertaken to develop of highly active and stable DRM catalysts. The deactivation of DRM catalysts is mainly caused by: (i) the formation of catalytic coke, which may result in the blockage of pores and active sites, (ii) sintering of active material, as DRM is carried out rather at high temperatures, or (iii) oxidation of metallic active sites. The application of different types of materials, preparation methods and application of promoters may lead to overcoming these problems. The following part of the report discusses the literature information on the influence of these variables on catalytic activity of materials tested in DRM process.

4.1 The role of active component

It has been reported that in general transition metals of 8, 9 and 10 groups of periodic table (VIII group metals in old classification) are active materials for DRM reaction i.e. iron, cobalt, nickel, ruthenium, rhodium, palladium, osmium, iridium and platinum (Fig. 6). There are no reports regarding Os-based catalyst. Table 6 lists different sequences of catalytic activity in DRM reaction reported for these transition metals. Moreover, it is important to stress, that the selection of active phase in catalysts affects, besides activity, also catalyst selectivity and stability, which can be more critical properties where commercialization of catalytic process is concerned.

Periodic Table of the Elements

The periodic table shows the following elements highlighted for catalytic activity in DRM reaction:

- Noble Metals (Green):** Pt, Pd, Rh, Ru, Ir, Ni, Co, Fe, Ni, Cu, Ag, Au.
- Non-noble Transition Metals (Blue):** Fe, Co, Ni, Ru, Rh, Pd, Ir, Pt, Os, Ir, Pt, Au, Hg, Tl, Pb, Bi, Po, At, Rn, Fr, Ra, Ac, Th, Pa, U, Np, Pu, Am, Cm, Bk, Cf, Es, Fm, Md, No, Lr.

Legend:

- Noble metals (Green)
- Non noble transition metals (Blue)

Element Information Box:

- Atomic Number
- Valence Charge
- Symbol
- Name
- Atomic Mass

Lanthanide Series: La, Ce, Pr, Nd, Pm, Sm, Eu, Gd, Tb, Dy, Ho, Er, Tm, Yb, Lu.

Actinide Series: Ac, Th, Pa, U, Np, Pu, Am, Cm, Bk, Cf, Es, Fm, Md, No, Lr.

Fig. 6 The metals which showed catalytic activity in dry reforming reaction

Solymsi et al. [45] investigated the catalytic activity of noble metals supported on alumina (Pt, Pd, Rh, Ru, Ir), which, in terms of turnover numbers, followed the sequence: Ru>Pd>Rh>Pt>Ir. This sequence was the same as the ability of noble metals to dissociate CO₂. The largest amount of coke deposits was observed for Rh and Pt catalysts and the least for Pd-containing one. The authors found that methane alone showed little reactivity towards supported noble metals. Their conclusion was that activity of noble metals in DRM reaction was associated with their ability to dissociate CO₂ to adsorbed CO and O species, which in turn, can promote dissociation of methane to adsorbed CH_x and H species, and thus DRM reaction. Ashcroft et al. [46] compared

activity of noble metals with non-noble nickel supported on alumina. The highest activity towards DRM was observed for Ir- and Rh-based catalysts, which did not exhibit the formation of coke deposits during 200h tests, and showed conversions of CH₄ and CO₂ equal to almost 90% at 777°C. The high conversions of CH₄ and CO₂ over Ni/Al₂O₃ catalyst (higher than for Pd and Ru) were observed due to the higher loading of active phase. However, Ni-based catalyst showed the highest amount of coke deposits after catalytic tests. Similar effect was observed by Barama et al. [47] and Hou et al.[48].

CO₂ reforming of methane over Pt, Rh, Rd, Ir, Pd and Ni supported magnesia catalysts was examined by Rostrup-Nielsen et al.[49]. The catalytic performance of prepared materials was compared in SRM and DRM reaction. The obtained results showed that Rh- and Ru-based catalysts were the most active ones in DRM reaction, with high reaction rates and no carbon deposition. A similar catalytic activity was registered by Ni, Pt and Pd catalysts. However, Ni-based catalysts exhibited high amounts of carbon whiskers-like deposits. The authors showed that passivation of Ni-based catalyst by sulphur could enhanced its resistance to coke formation, but in order to obtain high reaction rates higher temperatures than those for Rh- and Ru-based catalysts were required.

Tsyganok et al. [50] proposed an efficient method of introducing precious metals (Ru, Rh, Ir, Pt, Pd, Au) into the structure of hydrotalcite-derived Mg(Al)O mixed-oxides. Ru or Rh containing catalysts showed the highest conversions of CH₄ and CO₂. Over these two catalysts conversions of CO₂ were a few percent higher than those of CH₄, pointing to the occurrence of RWGS. The highest catalytic activity and resistance to coke formation was observed for Ru-based catalyst which was additionally tested over 50h timer on stream (TOS). The good performance was ascribed to high dispersion of very small (under 1.5 nm) Ru crystallites on the catalyst surface. Pt-containing catalyst showed much lower activity and the activity of Pd catalyst was suppressed by heavy formation of coke deposits. Au turned out to be practically inactive in DRM.

The performance in DRM reaction of Fe, Co and Ni supported on ceria was compared by Asami et al. [51]. The highest activity at 850°C was observed for Ni/CeO₂ catalysts. As over 20h on stream, no change in CO₂ and CH₄ conversions, as well as H₂/CO molar ratios close to unity were observed. It was stated that Ni/CeO₂ catalyst did not undergo deactivation. This was ascribed to strong metal-support interactions. However, at 700°C deactivation of Ni/CeO₂ catalyst was observed. Co-based catalyst also showed good conversion of CH₄ and CO₂. However, the initial values of CH₄ conversion were low, due to incomplete reduction of cobalt species. Fe/CeO₂ catalyst had the lowest activity and poor selectivity, caused by the deactivation of catalyst.

The theoretical calculations considering activity in DRM on (111) planes of transition metal surfaces (Cu, Ni, Pd, Pt, Rh, Ru, Ir and Fe) were performed by Hei et al. [52]. The authors studied heats of chemisorption, activation barriers and enthalpy changes for different species involved in DRM reaction on transition metal surfaces, and based on obtained results proposed the mechanisms of DRM reaction, and the activity sequence: Fe > Ni > Rh > Ru > Ir > Pd > Pt > Cu. Authors stated that noble metals could desorb CO before its decomposition to carbon, while Fe and Ni tended to dissociate CO to carbon and oxygen. Thus non-noble metals catalysts promoted carbon forming reactions, which affected their stability.

It must be mentioned, however, that the direct comparison of activity of transition metals in DRM reaction as reported in literature [45,51,53,54], is rather difficult as the reported catalysts (Table 6) were tested under different reaction conditions (temperature, contact time, feed gas composition), as well as different supports were used, which may influence metal-support interactions. Thus only general conclusions may be withdrawn. The noble metal-based catalysts show good activity and selectivity in DRM reaction. Among noble metals, Rh- and Ru-based catalysts are the most active ones [45,47–52], but the better chances of industrial applications the latter, as ruthenium is cheaper than rhodium [52].

Table 6 The influence of the type of metal on catalysts activity in DRM. Catalytic tests carried out in fixed-bed reactor at atmospheric pressure.

Active material	Support or carrier	Reaction conditions	Activity Sequence	Ref.
1 wt.% Pd, Rh, Ir, Ru, 2 wt.% Pt; IMP	Al ₂ O ₃	Temp. 500°C m _{cat} = 300mg; CH ₄ /CO ₂ =1/1; GHSV = 3000-6000h ⁻¹ Reduction: 1h at 500°C	Ru > Pd > Rh > Pt > Ir	[45]
1wt.% Pd, Ru, Rh, Ir, Ni*; IMP	Al ₂ O ₃	Temp. 777°C; m _{cat} =50mg; CH ₄ /CO ₂ =1/1; GHSV=40000h ⁻¹	Ir > Rh > Ni > Pd > Ru	[46, 53,5 4]
0.9-1.4 wt% Ni, Ru, Rh, Pd, Ir, Pt 16 wt.% Ni; IMP	MgO-Al ₂ O ₃ alumina-stabilized magnesia, MgAl ₂ O ₄	Temp. 500, 650°C; m _{cat} = 10-50mg; CH ₄ /CO ₂ /H ₂ =4/16/1.6	Ru > 16 wt.% Ni/MgAl ₂ O ₄ > Rh ≈ Ni > Ir > Pt > Pd	[49]
Rh, Ru, Pt, Pd, Ir (5 wt.%); Ni, Co (10 wt.%); IMP	α-Al ₂ O ₃ mesoporous Al ₂ O ₃	Temp. 800°C; CH ₄ /CO ₂ =1/1; GHSV=60000 or 120000 cm ³ /g _{cat} h; Reduction: 800°C for 1h;	Ni > Rh > Ru > Co > Ir > Pt > Pd	[48]
3, 5 and 10 wt.% Ni, Rh, Pd, Ce; IMP	Al-pillared montmorillonites	Temp. 650°C; CH ₄ /CO ₂ /He=1/1/8; mcat=500mg; flow 12 dcm ³ /h;	3% Rh ≈ 10%Ni >>Pd >> 3%Ni >> Ce	[47]
2 wt.% Ru, Rh, Ir, Pt, Pd, Au,	Hydrotalcite-derived Mg(Al)O mixed- oxides	Temp. 800°C CH ₄ /CO ₂ /N ₂ =23/23/35; Flow/Weight = 92727 cm ³ /g _{cat} h	Ru ≈ Rh > Ir > Pt >> Pd >> Au	[50]
5 wt.% Fe, Co, Ni; IMP	CeO ₂	Temp. 700°C; CH ₄ /CO ₂ /Ar=1/1/3 Reduction: in H ₂ /Ar (2/3 vol/vol) at 700°C for 1h	Ni > Co >> Fe	[51]

*Ni-based commercial steam reforming catalyst from British Gas (ca. 63 wt.%Ni)
IMP – metals introduced on the support via incipient wetness impregnation method

From non-noble metals, only nickel-based catalysts showed similar activities and selectivities to those reported for noble metals. Activity of nickel-based catalyst may be enhanced by introduction of higher loadings of active phase than noble metals [47–49]. On the other hand, non-noble metals show tendency to promote carbon-forming reactions which can cause catalyst deactivation and reactor plugging. In general high resistance of noble metals to coke formation can be explained by the fact that they do not dissolve carbon to such high extent as in e.g. Ni, which is responsible for the formation of carbon deposits, in the latter case.

Noble metals are usually introduced onto catalyst support in small amounts, due to their high price, and thus form small crystallites which promotes carbon-free operation [55,56].

Despite better performance of noble-metal-based catalysts, most of the reported research is focused nowadays on **nickel-based ones**, as Ni is much cheaper and more available [56]. In comparison to other non-noble metals, e.g. Fe, Co, nickel-based catalysts are less prone to coking [52]. This is why, the next part of this report will be focused on nickel-based catalysts tested in dry reforming of methane.

4.2 Nickel-based catalysts

Nickel was found to be the most suitable non-noble catalyst in DRM reaction. The research on nickel-based catalyst is currently focused mainly on increasing catalysts stability. The high endothermicity of dry reforming of methane requires high reaction temperatures. This unavoidably leads to the sintering of nickel particles, as its Tammann temperature is equal to 600°C [57]. Moreover, it also accelerates the deactivation via carbon deposition, as carbon-forming reactions proceed more easily on large nickel crystallites [55]. Therefore, several approaches have been proposed in order to increase stability of Ni-based catalysts, such as [58]:

- Employing appropriate catalysts preparation method to inhibit coke growth.
- Using metal oxides with strong Lewis basicity as supports or promoters, as basic sites enhance CO₂ adsorption. Metal oxides can promote oxidation of carbon deposits (reverse Boudouard reaction), but, on the other hand, supports which exhibit Lewis acidity enhance formation of coke deposits.
- The addition of second metal, i.e. noble metal, which can enhance the transport of hydrogen and/or oxygen between active site and support by spillover, and can influence the mechanism of coke formation.
- Sulphur passivation of Ni catalysts, which blocks the step edge sites where coke build-up is initiated.
- Changing reaction conditions by the addition of oxidizing agents, such as water or oxygen which can help to oxidize carbon deposits.

In this subchapter an overview of the research for Ni-based catalyst carried out during ca last 20 years is presented. More general reviews of catalysts for dry methane reforming were discussed by Edwards and Maitra [59], Wang and Lu [60], Bradford and Vannice [17], Hu and Ruckenstein [55], Fan et al. [61], Lavoie [7] and recently by Usman et al. [62], Abdullah et al. [63], Wang et al. [64] and Aramouni et al. [65].

4.2.1 The role of support

The role of support in the catalyst is very important. It determines the dispersion of catalytically active metal particles and resistance to sintering, stabilizes and promotes active sites, provides large active surface area, may participate in the reaction itself and can modify catalytic properties of active phase and thus in e.g. increase resistance to coking [20,55]. In DRM reaction, nickel-based catalysts on various supports were tested, such as single oxides (Al₂O₃ [66–72], MgO [73–78], CeO₂ [79–81], ZrO₂ [82], SiO₂ [57,83,84], ordered mesoporous silica – SBA-15 [85], La₂O₃ [86], TiO₂ [87]), mixed oxides (MgO-Al₂O₃ [88–91], CeO₂-ZrO₂ [92,93], CeO₂-Al₂O₃ [94]), zeolites (zeolite Y, zeolite A, zeolite X, ZSM-5) [95], clays (clinoptolite [96], diatomite [97], vermiculite [98], montmorillonite [99]) and carbon-based materials (carbon nanotubes, activated carbon) [100] (Table 7).

Alumina – Al₂O₃

Alumina is one of the most commonly studied supports for nickel catalysts [55,56]. It is relatively cheap and possesses high specific surface area, basic character and α -Al₂O₃ phase possesses high thermal stability. However, the catalytic properties of Ni/Al₂O₃ catalyst in DRM reaction and its resistance to carbon formation depends on the catalyst structure, composition, calcination conditions and preparation method. Beccera et al. [66] studied the influence of calcination temperature on activity of impregnated Ni/Al₂O₃ catalysts. With increase of calcination temperature higher amounts of NiAl₂O₄ spinel phase were formed, which suppressed catalytic activity at low temperatures (below 700°C). At reaction temperatures higher than 700°C this effect was not so evident, as calcination temperature did not influence the activity of Ni/Al₂O₃ catalyst. At the same time, the formation of spinel phase increased catalyst resistance to coke formation. As explained by Hu et al. [55] this was the result of strengthening of the Ni-O bond in NiAl₂O₄ with respect to NiO crystal, thus increasing the difficulty of Ni²⁺ reduction to Ni⁰, and resulting in the formation of smaller nickel crystallites on the surface. Similar results were reported by Chen and Ren [68]. Bhattacharyya and Chang [69] also reported that NiAl₂O₄ catalysts prepared via co-precipitation exhibited higher activity and much more stable performance than Ni/Al₂O₃ prepared by physically mixing of NiO and α -Al₂O₃ powders.

Table 7 Catalytic activity of Ni-based catalysts in DRM reaction. Effect of the support.

Ni (wt.%)	Support	PM ¹⁾	Reaction conditions				Conversion		H ₂ /CO (-)	Ref.
			Temp. (°C)	CH ₄ / CO ₂	GHSV (h ⁻¹)	TOS (h)	CH ₄ (%)	CO ₂ (%)		
10.3	γ -Al ₂ O ₃	IMP	800	1/1	nd	6	92	94	0.98	[66]
ca. 10	Al ₂ O ₃ aerogel	SG	700	1/1 ²⁾	nd	30	55	62	nd	[67]
10	γ -Al ₂ O ₃	IMP				4-5	66	68	nd	
13	γ -Al ₂ O ₃	IMP	750	1/2	3000	nd	94	83	0.81	[68]
5	Al ₂ O ₃	IMP	700	1/1	nd	24	64	70	nd	[72]
10	MgO	IMP	650	1/1	36000	10	63	75	0.85	[73]
10	MgO	CP	700	1/1	14000	5	67	77	0.87	[76]
nd	MgO	IMP	650	1/1 ²⁾	nd	12	23	nd	0.5	[74]
			800				66	nd	0.9	
10	MgO	SG/E	750	1/1	30000	25	54	69	1.12	[77]
10	MgO	IMP	700	2/1	12000	20	45	nd	nd	[78]
15	MgO-Al ₂ O ₃	SG	800	1/1 ²⁾	36000	40	84	89	nd	[88]
		CP					84	89	nd	
10	MgO-Al ₂ O ₃	SCH	700	1/1	24000	53	74	84	1	[91]
5	MgO-Al ₂ O ₃	EISA	700	1/1	15000	100	77	79	0.8	[89]

Table 7 Continuation

Ni (wt.%)	Support	PM ¹⁾	Reaction conditions				Conversion		H ₂ /CO (-)	Ref.
			Temp. (°C)	CH ₄ / CO ₂	GHSV (h ⁻¹)	TOS (h)	CH ₄ (%)	CO ₂ (%)		
10 ³⁾	CeO ₂	IMP	760	1/1 ²⁾	13400	100	65	80	0.83	[79]
5	CeO ₂ (NR)	IMP	700	1/1	18000	30	63	77	0.9	[80]
	CeO ₂ (NP)						58	70	0.9	

5	CeO ₂	IMP	700	1/1	38400	12	37	68	0.6	[81]
3	ZrO ₂	IMP	600	2.2/1 ²⁾	nd	2	53	15	0.75	[82]
2	ZrO ₂	IMP	650	1/1 ²⁾	nd	2	22	14	1.1	[101]
10	CeO ₂ -ZrO ₂	IMP	550	1/1 ²⁾	20000	5	38	37	1	[92]
5	CeO ₂ -ZrO ₂	IMP	700	1/1	30000	24	39	52	0.7	[93]
10	CeO ₂ -Al ₂ O ₃	IMP	800	1/1 ²⁾	90000	25	75	85	0.88	[94]
10	SiO ₂	IMP	700	1/1	36000	30	68	69	nd	[83]
4	SiO ₂	IMP	700	1/1 ²⁾	nd	65	62	76	nd	[57]
31.5	SiO ₂	SG	750	1/1 ²⁾	48000	25	54	66	0.68	[84]
8	SBA-15	CP	600	1/1 ²⁾	20000	24	68	89	0.87	[102]
10	TiO ₂	IMP	750	1/1	nd	10	33	nd	nd	[87]
	CeO ₂ -TiO ₂	IMP	750	1/1	nd	10	87	nd	nd	[87]
8	Clinoptilolite	IMP	700	1/1	nd	6	69	72	0.9	[96]
5	diatomite	TSD	650	1/1	21120	12	31	41	0.76	[97]
12	Vermiculite	IMP	750	2.8/1 ⁴⁾	19000	24	96	71	1.1	[98]
10	Montmorillonite	IMP	700	1/1 ²⁾	30000	-	77	75	nd	[99]
10	CNs	IMP	750	1/1 ²⁾	Nd	8	66	78	0.85	[100]
	AC	IMP	750	1/1 ²⁾	Nd	-	50	65	0.85	[100]

¹⁾ PM – Preparation Method: IMP – Impregnation, SG – Sol-Gel, CP – Co-Precipitation, SG/E – one-pot sol-gel/evaporation, EISA – One-pot evaporation induced self-assembly, SCH – Sonochemistry method, TSD – two-solvent deposition method, MIMP – Melt-impregnation;

²⁾ CH₄ and CO₂ were diluted by inert gas

³⁾ mol %

⁴⁾ tests carried out in the presence of oxygen;

nd-no data

Kim et al. [67] compared catalytic performance of impregnated Ni/ γ -Al₂O₃ and Ni supported on alumina aerogel prepared by sol-gel method. The preparation method influenced morphology and size of metal particles distributed on catalyst surface, and the catalyst prepared via the latter method exhibited very high specific surface area, high porosity and narrow distribution of nickel particle size. In contrast the former, showed larger size of Ni particles distributed irregularly. This affected catalytic performance in DRM reaction. Ni supported on alumina aerogel was stable up to 30h TOS and its activity was comparable to the reference 5wt.%Ru/Al₂O₃ catalyst. On the other hand, nickel-impregnated catalyst lost its catalytic activity during first 4-5h TOS, due to the formation of carbon deposits. According to the authors, the minimal size of nickel crystallites needed for the formation of whisker-type carbon deposits was 7nm, and thus coking was unavoidable for Ni/Al₂O₃ catalyst prepared by impregnation method. Additionally, due to the weak metal-support interactions sintering of active phase occurred during DRM reaction for such catalysts.

A different approach was applied by Baktash et al. [70], who prepared so called 'inverse catalyst'. Aiming at stabilizing the structure and inhibiting sintering of active Ni crystallites, they coated NiO nanopowder with a thin layer (around few nm) of porous alumina via atomic layer deposition technique. NiO powder covered with alumina layers showed stable CH₄ conversion of ca. 80%. at 800°C up to 12h TOS. However, catalytic activity decreased with the increase of alumina layer thickness. Additionally, alumina coating prevented sintering of active phase and lead to decreased coking with respect to uncoated catalyst.

Magnesia – MgO

Magnesia was another commonly studied support for DRM nickel-based catalysts. The high Lewis basicity of MgO has beneficial effect, as CO₂ adsorption is enhanced on basic supports, therefore accelerating reaction between CO₂ and deposited carbon species. Another advantage of MgO as a support in DRM arises from the possibility of formation of NiO-MgO solid solution at any molar ratio because of similar anion radii (Mg²⁺ 0.065nm, Ni²⁺ 0.072nm [77]) and lattice parameters. This in turn increases metal-support interactions, and thus prevents catalysts deactivation via sintering.

The effect of nickel loading on (111) magnesia nano-sheets supported catalyst prepared via impregnation was studied by Li et al. [73]. The stability and activity was reported to be closely related to Ni loadings. The catalytic activity in DRM was increasing with Ni loading up to 10wt.% and then decreased with further increase of Ni content to 20wt.%. Stability for the catalyst with loading higher than 50wt.% was poor. Similar results were reported by Zanganeh et al. [75,76]. In both studies, the best performance was registered for 10wt.%Ni/MgO catalysts, which was attributed to high basicity of the studied materials and the formation of small nickel crystallites, due to the strong metal-support interactions. It must be mentioned, however, that in both studies the most active catalysts still exhibited the presence of carbon deposits after reaction. The catalysts with low nickel loading (2wt.%) showed decrease in CH₄ and CO₂ conversions which was ascribed to sintering of active nickel phase or oxidation of Ni species. At the same time insignificant amount of catalytic coke was present on the catalyst surface after reaction. In terms of catalyst stability and activity Jafarbegloo et al. [77] also stated that the catalyst loaded with 10wt.% Ni on MgO prepared via one-pot sol-gel/evaporation technique exhibited the best performance with respect to catalysts loaded with higher or smaller amount of Ni. The studies presented in ref. [73,75–77] showed that CO₂ conversion were always higher than CH₄ conversions in tested temperature range, pointing to the occurrence of RWGS reaction, which decreases H₂/CO molar ratio in the products, over Ni/MgO catalyst. However, only in studies carried out by Jafarbegloo et al. [77] the excess of H₂ in the products of the reaction was observed, which clearly indicates that the method of catalyst preparation influences the occurrence of side reaction and thus the distribution of the obtained products.

Alumina-Magnesia

The beneficial effects of magnesia (enhanced chemisorption of CO₂) and alumina (enhanced thermal stability, high specific surface area) can be combined in mixed MgO-Al₂O₃ support. It has been reported that the addition of MgO into Ni/Al₂O₃ catalyst resulted in the increase of basicity [88,89], specific surface area and total pore volume [88], due to the formation of MgAl₂O₄ spinel phase. The catalytic activity of Ni supported on mixed magnesia alumina depends on the support preparation method, reaction conditions and pretreatment of the catalyst. Min et al. [88] compared the performance of the catalyst synthesized via sol-gel and co-precipitation methods. Both catalysts showed high conversions of CH₄ and CO₂ and were stable for to 40h TOS. Although, the catalysts did not differ in activity, the characterization of catalyst after reaction proved the presence of Ni crystallites of larger size for co-precipitated catalyst than for that prepared via sol-gel method clearly pointing to higher deactivation by sintering. Thus, co-precipitated catalyst was less resistant to coke formation. The authors examined also the effect of Mg/Al molar ratio. The catalysts with medium concentrations of MgO exhibited highest activity. On the other hand, the investigation carried out by Alipour et al. [90] and Xu et al. [89] showed that only a small addition of MgO (up to 5 wt.%) to Ni/Al₂O₃ enhanced its stability and activity.

The formation of Mg(Al)O supported-nickel catalyst may be also realized via thermal decomposition of hydrotalcite-like compounds. These types of catalysts were reported to be very active and stable in DRM reaction and will be in the separate section of this report.

Ceria – CeO₂

Ceria is well known for its high oxygen storage capacity associated with electron transformation between Ce³⁺ and Ce⁴⁺ [79,92]. Therefore, the application of ceria support in DRM reaction may be beneficial, due to easier removal of carbon deposits via oxidation by oxygen anions. Moreover, nickel can dissolve in fluorite structure of CeO₂. The Ni-O-Ce bond is stronger than Ni-O bond in NiO crystal, thus leading to increased metal-support interactions of ceria-supported Ni, resulting in the formation of small Ni particles. The solubility of nickel in CeO₂ is limited to 10-12 mol.% due to the structure limitations, and Ni loadings higher than the

solubility limit may result in the loss of its coke-resistance properties, as reported by Yu et al. [79]. The other important factor is morphology of ceria support, as different morphologies are characterized by different oxygen mobility and intensity of interactions with active metal particles. Du et al. [80] compared the DRM performance of ceria nanorods (NR) and nanopolyhedra (NP) structures with that of commercial CeO₂ support. Both nanomaterials exhibited enhanced catalytic activity and stability in comparison to commercial CeO₂. The best catalytic performance was shown by Ni/CeO₂-NR catalyst, which was attributed to concentration of surface Ce³⁺ species higher than that for Ni/CeO₂-NP catalyst. Ce³⁺ species were associated with the amount of oxygen vacancies and influenced the type of Ni species present on the catalyst surface, pointing to the importance of oxygen mobility.

Ceria-Zirconia

Another tested support for DRM catalysts was ceria-zirconia. The increase in the number of oxygen vacancies in ceria may be realized via introduction of ZrO₂ into its structure [92]. Zirconia stabilizes ceria by the formation of ceria-zirconia solid solution in the whole composition range. Moreover, ceria-zirconia possesses higher basicity, improved textural features and thermal stability with respect to CeO₂ [93]. However, catalytic activity for zirconia supported Ni catalyst [82,101] was lower than that reported for Ni/alumina. The effect of Ni loading on Ce_{0.62}Zr_{0.38}O₂ was studied by Radlik et al. [92]. The highest conversions of CH₄ and CO₂ and H₂/CO molar ratio close to unity were observed for the catalyst with 10 wt.% Ni loading. However, this sample exhibited the highest weight loss during TG experiment after reaction, suggesting the lowest resistance to coke formation, which was explained by the largest size of Ni particles on the ceria-zirconia surface. Therefore, it may be beneficial to use lower Ni loadings than 10 wt.%.

Kambolis et al. [93] studied ceria-zirconia binary oxides prepared via co-precipitation with different zirconia content. Mixed CeO₂-ZrO₂ exhibited better performance than CeO₂ and ZrO₂ alone. The catalytic activity and resistance to the formation of carbonaceous deposits increased with zirconia content and was the highest for the sample with 28 mol % of ceria. As explained by authors, in the presence of Zr⁴⁺ cations ceria lattice undergoes extensive distortion, which results in the increase of both oxygen mobility and anion vacancies on the surface of binary oxide. The latter may be the active sites for the dissociative adsorption of CO₂ molecule and thus with the introduction of ZrO₂ into ceria structure, the number of DRM active sites increases.

Silica – SiO₂

Silica is another material used typically in catalysis as a support. Huang et al. [83] studied the effect of the preparation conditions of silica support on its catalytic activity in DRM reaction at 700°C. Silica supports prepared via sol-gel method exhibited various types of morphologies and texture such as: yielded sphere, shell-like shape and peanut-like shape. The best activity and resistance to coking was registered for shell-type silica structure. This type of silica carrier exhibited the highest dispersion and the lowest size of Ni particles, as Ni crystallite size depended primarily on the pore size of silica support. It must be mentioned, however, that although the shell-like catalyst showed high conversions of CH₄ and CO₂ (Table 7), a huge amount of carbon deposits was present on the catalyst surface after reaction, as spent catalyst exhibited around 60% weight loss. The type of carbon deposits formed on the catalyst surface also depended on silica morphology. Similar results were reported by Zhang and Li [84], who studied core-shell type Ni catalyst in DRM reaction. According to their studies, the micro- and mesopores present in amorphous silica and formed upon material calcination, served as channels through which gas molecules diffused and silica shell structure (narrow pores) suppressed carbon filament growth.

The influence of pre-treatment conditions (reduction and calcination conditions) of Ni impregnated silica catalyst was examined by Kroll et al. [57]. Initial activity of catalyst did not depend on the pretreatment conditions but, with the increase in TOS the differences in catalysts performance were visible. The samples calcined and reduced at high temperatures (700-900°C) exhibited significant loss in catalytic activity, while the unpretreated catalyst showed enhanced stability. Based on the obtained results authors proposed that the active phase for DRM reaction is not metallic nickel, but nickel-carbide-like layer formed at particle surface immediately after contact with the reacting mixture, which explained similar initial activity. The subsequent

morphological changes of active phase were depended on the pretreatment procedure and thus influenced activity of catalysts and differences between activity of catalysts were observed.

The catalytic activity of nickel supported on ordered mesoporous silica (SBA-15) prepared via impregnation, precipitation and ascorbic acid-assisted precipitation methods was studied by Galvez et al. [102]. The application of ascorbic acid as a reducing agent, resulted in the formation of a catalyst where Ni species were present in the mesopores of SBA-15, and thus enhanced catalyst activity and stability.

Titania – TiO₂

Titania was also reported as a good support for DRM reaction [87], due to its ability to suppress carbon deposition. TiO_x species, which are formed during reduction with H₂ can migrate to nickel particles and create new active site of Ni-O-Ti³⁺. These new active sites formed at the boundary between active phase and support increase metal-support interactions and promote oxidation of the deposited carbon to CO. Ni/TiO₂ was examined in DRM reaction by Bradford et al. [103] and Ni supported on mixed CeO₂-TiO₂ systems by Kim et al. [87]. The latter catalyst exhibited enhanced performance as compared to Ni/CeO₂ and TiO₂, due to its redox characteristics and higher dispersion of nickel species.

Natural clays and zeolites

Zeolites and natural clays which can be considered a 2D zeolite-like relatively cheap materials, were also studied. Their properties, such as acid-basic properties and thermal stability, can be tailored to some extent by different chemical and physical treatments [99]. Therefore, their application as adsorbents, catalysts or catalysts supports has gained much attention in recent years. Clinoptilolite is most abundant naturally occurring zeolite. The effect of Ni loading on its catalytic properties has been studied by Nimwattanakul et al. [96]. The catalyst with 8 wt.% Ni showed the highest catalytic activity and considerable stability in DRM reaction at 700°C. Jabbour et al. [97] reported that Ni supported on diatomite was a promising cheap catalyst for DRM reaction. However, the presented results showed that catalyst exhibited slight deactivation during 12h tests, and thus authors suggested that application of promoters might increase catalyst stability. The acid treated, expanded and raw vermiculites were examined by Liu et al. [98]. The best catalytic performance, which authors attributed to its interlayer structure, was registered for expanded vermiculite with 12wt.% Ni. It is worth mentioning that the authors carried out catalytic test in the presence of oxygen, and thus the enhanced stability of materials may be explained by in-situ removal of carbon deposits via combustion.

Carbon materials

Catalytic activity of nickel loaded carbon materials, activated carbon (AC) and carbon nanotubes (CNs), in DRM reaction was examined by Ma et al. [100]. Ni/AC catalyst had lower activity than Ni/CNs, which the authors explained by the collapse of activated carbon structure during the reaction. From the two studied NCs-based catalysts, better performance was shown by the sample into which nickel was introduced inside carbon nanotubes when compared to the sample with nickel crystallites present on the outside surfaces of carbon nanotubes. This was explained by differences in electric density difference between interior and exterior surfaces of CNs and the confinement effect of CNs. The introduction of nickel on and into CNs influenced also the type of carbon deposits present after reaction. Amorphous carbon and graphitic carbon were found, respectively, for the former and the latter catalyst.

Comparison of the supports

A direct comparison of the influence of the supports on catalytic performance in DRM reaction is rather hard, because as presented e.g. in Table 7 the catalysts were studied under different reaction conditions (temperature, mass of catalyst, GHSV, flow, CH₄/CO₂ molar ratio), were prepared via different methods (impregnation, co-precipitation, sol-gel method) and underwent different pretreatment procedures (calcination conditions, reduction conditions). All these parameters influence size of metallic nickel particles, the interactions of active phase with the support, and thus may have negative or positive effect on catalyst activity and resistance to the formation of coke. This is why articles describing tests carried out under the same conditions over different supports for Ni-based catalyst in DRM reaction are presented in Table 8.

Tomishige et al. [104] studied the effect of preparation methods (impregnation and co-precipitation) on the performance of Ni/MgO and Ni/Al₂O₃ catalysts. The higher activity was registered for the catalyst supported on magnesia. The best catalyst turned out to be co-precipitated Ni/MgO, which showed the highest conversions of methane and carbon dioxide, and no carbon deposition on the catalyst surface after DRM reaction. The resistance to carbon formation followed the same sequence as that for catalytic activity and was related to the surface basicity and nickel particle size.

Kang et al. [105] compared the performance of nickel supported on alumina and mixed magnesia-alumina. The addition of magnesia to alumina had a beneficial effect on the stability of the catalyst. The authors stated that the formation of carbon deposits during DRM reaction caused fluctuations of CH₄ and CO₂ conversions. The addition of magnesia increased catalyst stability and no fluctuation in CH₄ and CO₂ conversions were observed up to 150h TOS. As reported earlier [88], nickel supported on magnesia or alumina alone was very strongly bonded to the support, due to the formation of NiO-MgO solid solution and NiAl₂O₄ spinel phase, respectively, which resulted in lower activity of the catalysts. The addition of appropriate amount of magnesia resulted in the formation of MgAl₂O₄ spinel phase, and thus weakened the interaction between the support and active phase leading to the increase of activity. At the same time, basicity also increased, which improved the resistance to coke formation and thus enhanced catalyst stability.

Khajeh Talkhoncheg and Haghghi [106] compared catalytic performance of Ni supported on Al₂O₃, CeO₂ and clinoptilolite. In the tested temperature range 550-850°C, the best catalytic performance was observed for alumina supported catalyst. The authors attributed that to the highest value of specific surface area, small crystallite size, and good dispersion and particle size distribution of Ni. Ni/clinoptilolite catalysts exhibited slightly higher specific surface area than Ni/CeO₂, fine particle size and possessed the benefits of natural zeolite-like structure and thus showed performance better than ceria supported catalyst and similar to the that of Ni/Al₂O₃ at 850°C. The other advantage of clinoptilolite was that the cost of mining and treatment of this mineral was lower than the cost of the preparation of alumina catalyst. Therefore, the application of clinoptilolite catalyst in DRM reaction could be beneficial from economic point of view. Unfortunately, carbon formation over the tested catalysts was not discussed.

Nickel supported on SiO₂, TiO₂, MgO and activated carbon was investigated by Bradford et al. [103,107]. The initial activity of tested catalyst expressed as turnover frequency (TOF), followed the sequence: TiO₂ > activated carbon > SiO₂ > MgO. The catalytic activity of tested materials also followed the ability of the catalysts to activate C-H bond cleavage in methane via electron donation to anti-bonding orbitals in methane. However, only Ni/MgO catalyst, although the least active, did not show deactivation up to 44h TOS. For Ni/TiO₂ deactivation was attributed to the formation of TiO_x species which migrated to nickel crystallites and may have caused blockage of DRM active sites. At the same time, the blockage of active sites by carbon deposits and sintering of nickel species were found responsible for the loss of catalytic activity for Ni/TiO₂, Ni/AC and Ni/SiO₂ catalyst. The authors concluded that the type of support strongly influenced the properties of the catalysts in e.g. electron-donating ability, basicity, metal-support interactions, and thus can suppress carbon-forming reactions. The carbon formation resistivity over the tested catalysts followed the sequence: Ni/MgO > Ni/TiO₂ >> Ni/SiO₂. The low amount of carbon deposits formed on MgO and TiO₂ was attributed, among others, to strong metal support interactions. The high amount of whisker-type carbon deposits was observed over Ni/SiO₂ catalyst, with no metal-support interactions. Ni/MgO catalyst formed NiO-MgO solid solution, thus stabilizing surface Ni-Ni bonds and preventing carbon diffusion into nickel particles, which is believed to be the first stage of whisker-type carbon deposits formation. The authors showed that the type of the support influenced the stabilization of different CH_x intermediates formed via dissociative methane adsorption. The reported values of CH_x were equal to CH_{2.7} for Ni/MgO, CH_{2.4} for Ni/Al₂O₃, CH_{1.9} for Ni/TiO₂ and CH₁ for Ni/SiO₂ [108], which follows the sequence of the catalyst resistance to coke formation.

The catalytic activity of Ni supported on alumina and alumina mixed with MgO, ZrO₂ and SiO₂ prepared via plasma method was investigated by Damyanova et al. [109]. The most beneficial in DRM reaction was the application of MgAl₂O₄ support, which exhibited the highest conversions of CH₄ and CO₂ equal, respectively, to 75 and 81%, as well as values of H₂/CO molar ratio closest to unity. The mixed ZrO₂-Al₂O₃ catalyst showed performance similar to that of the alumina-supported catalyst, while the lowest conversions were observed for

SiO₂-Al₂O₃ support. However, only Ni/MgAl₂O₄ catalyst was stable. Catalytic activity followed the same sequence as catalyst resistance to coke formation. The best performance of MgAl₂O₄ catalyst was ascribed to the high number of exposed metal sites, as the catalysts exhibited the smallest Ni particles (ca. 5.1nm) and the highest dispersion. Additionally, according to the H₂-TPR profiles, the applied catalyst reduction conditions were most probably insufficient for the complete reduction of NiO to metallic nickel for these catalysts. Thus, the coexistence of Ni²⁺ and Ni⁰ species on the catalyst surface might have facilitated the activation of CH₄ and CO₂, and further enhanced the activity and coke resistance.

Similar observations were reported by Zhang et al. [110], who recently compared catalytic activity of Ni supported on MgO, Al₂O₃, MgO-Al₂O₃, ZrO₂, SiO₂ and TiO₂ in DRM reaction. The highest conversions and stable performance was observed only for Ni supported on a mixed alumina-magnesia catalyst. Ni/SiO₂ catalyst, which exhibited the highest metal dispersion and the highest specific surface area, lost its high initial activity due to the sintering of active phase. The lowest conversions were observed for Ni/TiO₂ catalyst, while other tested samples showed significant decrease in activity with TOS.

Luengnaruemitchai et al. [95] studied different zeolites (zeolite A, zeolite Y, zeolite X, ZSM-5). The tested samples, with the exception of zeolite Y, showed high initial conversions of both methane and CO₂, but the decrease in catalytic activity with TOS was observed. The highest conversions and stable performance was shown by zeolite Y, but at the same time this catalyst exhibited the highest amount of carbon deposits after reaction, though they did not affect the catalytic performance. On the contrary, small increase in CH₄ and CO₂ conversions with TOS was observed, suggesting that carbon deposits formed in the reaction might be not poisonous. However, during the long-term stability tests they may lead to reactor plugging. Interestingly, the obtained values of H₂/CO molar ratios for the zeolite-supported catalysts were higher than 1. When compared to other studies, this clearly indicates that the application of zeolite strongly influences the reaction chemistry, as in case of other type of catalysts usually H₂/CO molar ratios lower than 1 were observed (Table 7).

Table 8 The effect of support on the catalytic activity of different Ni-based catalyst. Catalytic tests carried out in a fixed-bed reactor and at atmospheric pressure.

Ni content/ preparation ¹	Support	Reaction conditions	Activity sequence	Ref.
3 mol.%/CP and IMP	Al ₂ O ₃ , MgO	Temp. 850°C, m _{cat} =100mg, CH ₄ /CO ₂ =1/1, W/F=1.2g _{cat} h/mol; Reduction: in H ₂ at 850°C for 0.5h	NiO-MgO(CP) > Ni/MgO (IMP) > NiO-Al ₂ O ₃ (CP)	[104]
10 wt.%/CP-MBSL	Al ₂ O ₃ , MgO-Al ₂ O ₃	Temp. 700-800°C, m _{cat} =100mg CH ₄ /CO ₂ /He=1/1/1,	MgO-Al ₂ O ₃ > Al ₂ O ₃	[105]
nd/ IMP	CeO ₂ , Al ₂ O ₃ , clinoptilolite	Temp. 550-850°C, m _{vat} =100mg, CH ₄ /CO ₂ =1/1, GHSV=24dm ³ /gh Reduction: in H ₂ /N ₂ =1/9 at 700°C for 1h	Al ₂ O ₃ > Clinoptilolite > CeO ₂	[106]
ca. 1.3 wt.% for TiO ₂ ; 8 wt.% for SiO ₂ and AC; 10 wt.% for MgO /IMP, CP ²	MgO, TiO ₂ , SiO ₂ , activated carbon	Temp. 400-550°C, m _{cat} =5-50mg CH ₄ /CO ₂ /He=1/1/1.8, GHSV=10000- 2000 h ⁻¹ Reduction: in H ₂ at 500°C for 1h ³	TiO ₂ > activated carbon > SiO ₂ > MgO ⁴	[103, 107]
10 wt.%/IMP	α-Al ₂ O ₃ , γ- Al ₂ O ₃ , CeO ₂ , La ₂ O ₃ , ZrO ₂	Temp. 550°C, m _{cat} =100mg, CH ₄ /CO ₂ =1, W/F=0.55g _{cat} h/mol; Reduction: in H ₂ at 327°C for 2.5h	γ-Al ₂ O ₃ > α- Al ₂ O ₃ > ZrO ₂ > CeO ₂ > La ₂ O ₃	[111]
4 wt.%/IMP	δ,θ-Al ₂ O ₃ , MgAl ₂ O ₄ , SiO ₂ - Al ₂ O ₃ , ZrO ₂ -	Temp. 650°C, m _{cat} =50mg, CH ₄ /CO ₂ /N ₂ =1/1/3, Reduction: in H ₂ /N ₂ at 550°C for 1h	MgAl ₂ O ₄ > ZrO ₂ - Al ₂ O ₃ ≈ δ,θ- Al ₂ O ₃ >> SiO ₂ -	[109]

	Al ₂ O ₃		Al ₂ O ₃	
8 wt.%/IMP	SiO ₂ , MgO, TiO ₂ , ZrO ₂ , Al ₂ O ₃ , MgO Al ₂ O ₃ -MgO	Temp. 750°C, m _{cat} =100mg, CH ₄ /CO ₂ =1/1, Reduction: in H ₂ /N ₂ at 700°C for 1h	Al ₂ O ₃ -MgO > MgO > SiO ₂ > Al ₂ O ₃ > ZrO ₂ >> TiO ₂	[110]
7 wt.%/IMP	zeolite A, zeolite X, zeolite Y, ZSM- 5	Temp. 700°C, m _{cat} =200mg CH ₄ /CO ₂ =1/1, GHSV=30000 Reduction: in H ₂ at 600°C for 1h	Zeolite Y ≈ ZSM- 5 > zeolite X >> zeolite A	[95]
2 wt.%/IMP	α-Al ₂ O ₃ , ZrO ₂ , α-Al ₂ O ₃ -ZrO ₂	Temp. 600°C, m _{cat} =25mg CH ₄ /CO ₂ /N ₂ =1/1/6 Reduction: in H ₂ from 25 to 1000°C	α-Al ₂ O ₃ -ZrO ₂ > α-Al ₂ O ₃ > ZrO ₂	[101]

¹ Methods of preparation: IMP – incipient wetness impregnation; CP – co-precipitation; CP-MBSL – co-precipitation under multi-bubble sonolimescence conditions

² co-precipitation method was used only for Ni/MgO catalyst

³ Ni/MgO catalyst reduced at 850°C for 0.5h

⁴ Ni/MgO catalyst was tested at higher temperature than other catalysts

In general, all authors stated that the type of applied support has a significant influence on the state of nickel species on the catalyst surface. The strong interactions between support and active phase may result in the formation of inactive phases in DRM reaction, such as NiAl₂O₄ or MgO-NiO solid solution. On the other hand, too weak interactions between nickel species and their carrier promoted deactivation via sintering and formation of carbon deposits. From, discussed articles it may be concluded that the most beneficial effect on the catalyst activity is connected to mixed Al₂O₃-MgO support, which shows interactions between Ni phase and support of moderate strength and is characterized by high basicity.

4.2.2 The role of promoters

Suitable promoters are added to the catalyst in order to enhance its stability, selectivity and/or catalytic activity. The influence of a promoter on catalyst stability and activity may be explained by their ability to modify catalyst structure (type of active sites, additional sites). In DRM reaction, the application of different types of promoters is usually aimed at increasing catalyst stability rather than its activity. In general, the promoters in DRM reaction may be divided into three groups: (I) alkali or alkaline earth metals, such as K, Li, Mg, Ca, Ba, (ii) rare earth metals, such as Ce, Zr, La and (III) other metals, such as Au, Ag, Sn, Bi, As, Pb and Cu.

Alkali or alkaline earth metals are applied because of their basic properties, which enhance catalyst affinity towards CO₂, and thus can help to oxidize carbon deposits. Moreover, they can form solid solution with NiO, increasing in this way the interactions between the support and active phase, and thus resulting in the formation of small nickel crystallites upon reduction with H₂, as well as suppresses coking. Rare earth metal oxides (e.g. CeO₂ or ZrO₂) on the other hand, exhibit redox properties, and thus also promote oxidation of carbon deposits. Other metals can be also added to the catalyst and their role is to either modify existing active sites or to create new active sites, and form in this way a bimetallic catalyst. The role of promoter can differ depending on the amount applied, type of support and method of a promoter introduction. Large amounts of promoters usually decrease catalytic activity due to the coverage of active sites [72]. Tables 9 and 10 present short review of different promoters applied in DRM reaction over Ni-based catalysts.

Table 9 The effect of alkali and rare earth metal promoters on Ni-based catalysts in dry methane reforming.

Promoter	Loading (wt.%)	Support	Ni (wt.%)	Effect of promoter addition	Ref.
----------	----------------	---------	-----------	-----------------------------	------

ALKALI METALS					
K	1, 5, 10	γ -Al ₂ O ₃	20	Divides Ni surface into smaller ensembles; suppress carbon deposition;	[144]
K	0.2-5	γ -Al ₂ O ₃	10	Partially blocks Ni active sites, Promotes coke gasification; Decreases activity	[145]
K	0.125 ¹	MgO	nd	Suppress dissolution of carbon atoms in Ni crystallites; Decreases activity; Increases stability;	[89]
K, Li	0.5	CeO ₂	10	Improves stability, decreases activity and H ₂ /CO molar ratio; K can block Ni active sites; K catalyses C gasification	[140]
Mg	3	γ -Al ₂ O ₃	5, 10, 15, 20	Increases basicity of support; increases stability of the catalysts	[105]
Mg	2.5, 5	Al ₂ O ₃	15	Increased Ni dispersion; Decreased activity towards CH ₄	[146]
Ca				Increased Ni dispersion; Increased activity; Improved stability	
Ca	10 ²	γ -Al ₂ O ₃	17	Increases activity and stability	[147]
Ba	nd	Al ₂ O ₃	10	Improves reducibility of Ni; Inhibits formation of NiAl ₂ O ₄ spinel	[148]

Table 9 Continuation

Promoter	Loading (wt.%)	Support	Ni (wt.%)	Effect of promoter addition	Ref.
RARE EARTH METALS					
Ce	7	MgO	10	Improves Ni dispersion, Improves stability, increases activity	[93]
Ce	1, 5, 10	Al ₂ O ₃	5	Increases activity towards CH ₄ , Improves stability	[87]
Ce	3	Al ₂ O ₃	11.5	Improved dispersion of Ni particles; Decreased activity;	[149]
Ce	3, 5, 10	montmorillonite	10	Increases activity and stability	[114]
Ce	6	SBA-15	5	Improved catalyst activity	[150]
CeO ₂ -ZrO ₂	10	SBA-15	10	Improves stability, decreases activity towards CO ₂	[100, 151]
Zr	1, 2, 3, 4, 5, 6	clinoptilolite	8	Improves stability	[111]
Zr	1	α -Al ₂ O ₃	2	Promotes gasification of carbon deposits; Improves stability	[152]
Zr	5	SiO ₂	10	Enhanced reducibility; Improved catalytic activity;	[153]
La	0.25-15	SiO ₂	10	Increased dispersion of Ni; Improved interactions between Ni and SiO ₂ ; Improved stability and activity	[154]

¹ K_{at}/Ni_{at}=0.125;

² mol %

nd – no data

Osaki et al. [112] studied the effect of potassium addition into Ni/Al₂O₃ catalyst. The studies revealed that K⁺, due to its basic character, enhances adsorption of CO₂. However, the rate of CO₂ dissociation into CO and oxygen was not affected, suggesting that the increased stability of the catalyst was not caused by oxidation of carbon deposits through enhanced CO₂ adsorption. The obtained results showed that potassium was present on the nickel crystallites and divided them into smaller ensembles, thus nickel crystallites were too small to catalyze carbon-forming reactions. The coverage of nickel crystallites by potassium resulted also in decreased activity due to the blockage of active sites. Similar conclusions were drawn by Juan-Juan et al. [113] and Frusteri et al. [74], who investigated K-promoted Ni/MgO catalyst. Their studies showed that K addition resulted in electronic enrichment on the active sites and led to stronger interactions between Ni atoms and electron-acceptor oxygen intermediates adsorbed on the catalyst surface. This prevented dissolution of C atoms and as a consequence their nucleation and formation of carbon deposits. The addition of potassium decreased catalytic activity but largely improved catalyst stability. Such effect was also observed for both K and Li promoted Ni/CeO₂ catalyst [111].

Magnesia was tested as a promoter for nickel supported on alumina by several authors [90,114–116]. Generally, small additions of magnesium had double promotion effect. Firstly, it modified Ni-particles arrangement, due to the formation of MgAl₂O₄ spinel phase and the suppressed formation of inactive NiAl₂O₄. This can be ascribed to the fact that basic MgO is preferably reacting with acidic Al₂O₃, thereby inhibiting the reaction between NiO and alumina. Secondly, magnesia inhibited agglomeration of coke deposits by an effective CO₂ gasification. Both effects resulted in increased catalyst stability. However, the initial activity of catalyst was reported to be lower than for the unpromoted catalyst.

Sengupta et al. [114] compared Ni/Al₂O₃ catalyst promoted with Mg and Ca. The addition of Ca was more beneficial than Mg promotion, as the catalytic activity towards CO₂ and CH₄ and catalyst stability were improved for Ca-promoted material with respect to Mg-promoted and unpromoted catalysts. Catalysts characterization revealed that the Ca addition resulted in the formation of new active sites able to adsorb H₂ and CO₂. At the same time Mg had negative effect on CO₂ and CH₄ conversion. The beneficial effect of Ca addition into Ni/Al₂O₃ catalyst were also observed by Zhang et al. [117].

The application of Ba as a promoter to Ni/Al₂O₃ was investigated by Garcia-Dieguez et al. [118]. A small addition of barium did not influence catalyst activity or stability. However, it inhibited the formation of NiAl₂O₄ spinel phase, and thus improved reducibility of nickel species.

CeO₂ is one of the commonly used promoters in DRM reaction. Wang et al. [72] tested Ni/Al₂O₃ catalyst promoted with 1 to 10 wt.% Ce. The addition of Ce improved catalyst stability regardless of Ce content with respect to unpromoted catalyst, as with increasing content of Ce Ni dispersion increased as well. Similar observation was made by Yan et al. [115]. Moreover, the addition of CeO₂ prevented the formation of inactive NiAl₂O₄ phase and enhanced reducibility of the catalyst. The results of TG experiments after reaction revealed that the catalyst resistance to coking was increasing with the increasing content of ceria. Nevertheless, the authors stated that the optimal content of Ce addition should be between 2-5%, as some blockage of active sites could occur. Similar results were reported for Ni/MgO catalyst [78].

Studies carried out by Kaydouh et al. [119] showed the importance of the preparation method on the catalyst activity. The effect of order of Ni and Ce introduction into SBA-15 by impregnation method was investigated. When Ce was impregnated prior to Ni, the catalyst showed much better performance than in case when nickel was deposited first. The increased activity of the catalyst prepared by the former procedure was ascribed to the formation of smaller Ni crystallites.

Zirconia addition onto various Ni supported catalyst has been studied [96,120,121]. In general, it has been reported that zirconia addition enhances reducibility of nickel species, leading to higher activity of the catalyst [96,120,122]. Promotion by Zr had also a positive effect on catalyst stability for nickel supported on alumina and clinoptilolite catalysts. On the other hand, Yao et al. [122] observed monotonic decrease in catalyst

activity over Zr-promoted Ni/SiO₂ catalyst, which was caused by deposition of carbon deposits. The deactivation of catalyst was more evident at lower temperatures.

Albarazi et al. [85,123] promoted Ni/SBA-15 catalyst with ceria-zirconia, which was well dispersed inside pores of the support, creating in this way a micro-mesoporous catalytic system with a beneficial effect on DRM reaction. The promoted catalyst exhibited higher activity towards CH₄, and its stability was also enhanced. However, the activity towards CO₂ was slightly lower than for the unpromoted catalyst.

Zhu et al. [124] studied addition of La, Mg, Zn and Co into Ni/SiO₂ catalyst. The best performance was observed for 5wt.% La promoted catalyst, which exhibited excellent stability in DRM reaction within 30h. Similar stability was shown by Zn promoted catalyst. The high activity and stability for the former were attributed to high dispersion of small nickel crystallites on the support surface. Mg and Co addition did not improve catalyst stability significantly. The authors also observed that Mg and La addition decreased the contribution of RWGS reaction, increasing H₂/CO molar ratio.

Ay and Uner [58] investigated Ni, Co and Ni-Co ceria supported catalysts in DRM. Their results showed no beneficial influence of Co incorporation into Ni/CeO₂ in terms of CH₄ and CO₂ conversions. Both Ni/CeO₂ and Ni-Co/CeO₂ catalysts showed very similar activity. The loss in CH₄ and CO₂ conversions was observed at the beginning of the reaction. It was attributed to the deactivation of catalysts by carbon-forming reactions. However, the addition of Co into Ni/CeO₂ resulted in formation of less stable carbon deposits (lower temperature of oxidation of carbon deposits). It should be added that Co/CeO₂ sample exhibited very low activity compared to Ni and Ni-Co containing catalysts. The authors explained it by general lower activity of Co towards DRM and strong interactions of Co with the support. A thin layer of ceria over active metal crystallites was observed on TEM images, pointing to the blockage of active centres of DRM reaction for both active catalysts. On the other hand, increased catalytic activity in DRM was observed by Luisetto et al. [125] for Ni-Co bimetallic catalyst. Their research showed that Co-Ni alloy was formed on the catalyst surface. It modified catalytic properties of the material, and thus increased activity, selectivity and stability. Beneficial effect on catalytic activity of Co-Ni bimetallic catalyst supported on ZSM-5 zeolite was observed also by Estephane et al. [126]. The bimetallic catalyst showed higher activity and was more stable than monometallic nickel catalyst. It was attributed to a synergetic effect of cobalt on nickel species, and Co played a role of oxidation catalyst for the removal of catalytic coke.

Table 10 The effect of introduction of a second metal to Ni-based catalyst in DRM reaction.

Promoter	Loading (wt.%)	Support	Ni (wt.%)	Effect of promoter addition	Ref.
Co	4	CeO ₂	8	Improved stability by formation of easily oxidized carbon deposits	[58]
Co	3.75	CeO ₂	3.75	Increased activity and selectivity; Inhibits formation of carbon	[125]
Co	3.5	ZSM-5	3.5	Improved activity and selectivity; Inhibited formation of carbon	[126]
Cu	1	SiO ₂	8	Increased catalytic activity and stability. Stabilized Ni active sites; Inhibited deactivation by CH ₄ decomposition;	[127]
Fe	2	CeO ₂ -ZrO ₂	3	Increased activity; Catalyst quickly deactivated	[128]
Ag	0.3, 0.6, 2.4*	CeO ₂	10*	Lowered activity of Ni surfaces; promotes RWGS; Accelerated combustion of coke deposits	[79]
Pt	0.3	MgO	5	Improved catalytic activity, selectivity and stability	[129]
Pt	0.4	Al ₂ O ₃	10	Increased activity	[130]

Pt	1	Al ₂ O ₃	6	Improved activity and selectivity; Inhibited formation of carbon whisker-like deposits	[131]
Rh	0.5	CeO ₂ -ZrO ₂	4.5	Increased activity and stability;	[128]

*mol %

Nd – no data

Chen et al. [127] reported that the addition of Cu into Ni/SiO₂ catalyst significantly increased its stability. The copper addition stabilized the structure of active nickel sites on the catalyst surface, thus preventing the loss of catalytic activity by sintering of nickel species. Moreover, Cu inhibited deactivation arising from CH₄ decomposition reaction. Cu-Ni species which were formed on the catalyst surface, suppressed the formation of inactive carbon deposits during DRM reaction.

Yu et al. [79] studied the promotion of Ni/CeO₂ catalyst with Ag. This addition decreased the activity of the catalyst due to the partial blockage of Ni active sites, but significantly increased stability within 100h catalytic tests. The characterization of the catalyst showed that Ag species were present on the step sites on Ni surface and a part of Ag species was bonded with ceria support. The promotion with Ag also changed the type of catalytic coke from graphitic or whisker carbon to amorphous carbonaceous deposits, which may play an active role in DRM reaction and are easier to oxidize than graphitic carbon.

Small additions of Pt were reported to have a very beneficial effect on the performance of Ni-based catalyst in DRM reaction [129–131]. Ni-Pt catalysts supported on MgO or Al₂O₃ exhibited improved catalytic performance, higher selectivity towards H₂/CO molar ratio and minimal deposition of carbon deposits. Gould et al. [131] observed that no whiskers-type of carbon deposits were formed for the Pt-Ni catalyst supported on Al₂O₃ which was prepared by atomic layer deposition method. The enhanced catalytic performance of bimetallic catalyst was attributed to the fact that Ni-Pt surfaces formed Ni-terminated surfaces which were associated with higher DRM rates than Pt-terminated surfaces. Presence of Pt on the edges of Ni crystallites inhibited carbon diffusion and thus resulted in higher resistance for coking.

Koubaissy et al. [128] reported that Rh addition into Ni/CeO₂-ZrO₂ catalyst enhanced its stability and catalytic activity. However, carbon deposits were still present on the catalyst surface after DRM catalytic test. Thermogravimetric experiments revealed that the addition of Rh had influenced the type of carbon deposits formed during DRM reaction and resulted in the formation of amorphous active carbon, which did not decrease conversions of CH₄ and CO₂.

Effects of the different promoters on the similar nickel supported catalysts were tested by several authors in order to find out the best promoter [132–134]. Choi et al. [132] investigated the effect of 2wt.% Co, Cu, Zr, Mn, Mo, Ti, Ag or Sn on catalytic activity of nickel supported on commercial ICI 46-1 material composed of 13wt.% CaO, 6.5% K₂O, 12% MgO and Al₂O₃. The carrier contained high amounts of alkali oxides, and thus exhibited high basicity. The catalytic activity of the tested materials followed the sequence for promoters: Co, Cu, Zr > unpromoted catalyst > Mn > Ti > Mo > Ag > Sn. Although the catalysts promoted by Co, Cu and Zr exhibited higher activity, high amounts of carbon were formed during the DRM reaction. On the other hand, the addition of Mn, Mo and Ag resulted in good resistance to coking. It must be mentioned, however, that only in case of the Mn-promoted sample registered conversions of CH₄ and CO₂ were similar to those for unpromoted catalyst. This is why the authors stated that the best promotion effect was obtained for manganese.

Castro Luna et al. [133] studied Ni/Al₂O₃ catalysts promoted by 0.5wt.% of K, Ca, Mn or Sn. The DRM tests carried out at 750°C for 30h showed that the addition of promoters decreased catalytic activity with respect to the unpromoted sample. Moreover, only for the catalysts doped with K or Ca stable values of CH₄ and CO₂ conversions were registered, suggesting that samples did not exhibit deactivation. The performance of the tested catalysts followed the sequence: unpromoted catalyst > K > Ca > Sn > Mn.

The effect of Co, Ca, K, Ba, La, Mn or Ce promotion of Ni/MgO-ZrO₂ catalyst was studied by Fan et al. [134]. The activity of the prepared materials tested in DRM reaction at 750°C decreased in the order Ni-Co > Ni-

La \approx Ni-Ce > Ni-Ba > Ni-Mn > Ni-K > Ni-Ca. The best performance of Ni-Co catalyst was attributed to the Ni-Co solid solution which reduced coke formation and improved catalytic conversion. Ni-La and Ni-Ce catalysts showed similar performance. The activity of Ni-Ba and Ni-Mn catalyst dropped within 40h TOS. On the other hand, a fairly stable performance was shown by Ni-K and Ni-Ca catalysts. The activity sequence followed that of metal dispersion. Carbon deposits were present on all catalysts after 40h catalytic tests and the highest amount was registered for Ni-Mn catalyst.

4.2.3 Conclusions

The presented review of nickel based catalysts showed that the catalytic performance of materials in DRM reaction is dependent on a number of factors. It is rather hard to establish the best support and promoter, as reported materials were tested under different conditions, with different loadings of metals and were prepared by different methods. Nevertheless, general trends in catalysts for DRM process can be established.

Researchers are focusing on preparing materials with **high dispersion** and **small size nickel particles**, which can be achieved by increasing interactions between nickel species and support. On the other hand, too strong interactions can significantly decrease reducibility of nickel species, and thus have negative effect on activity. Moderate interactions between Ni and support with high dispersion of stable nickel species were reported for MgO-Al₂O₃ support (Table 7, 8).

The addition of promoters can drastically change catalytic properties of a material. The positive effect of basic oxides and materials with high oxygen storage capacity is stressed in literature. Another concept is to introduce a second metal into catalytic systems, in order to create synergetic effect between Ni and other metal species, and inhibit in this way coking, as well as increase material activity. However, the effect of promoter addition is dependent on the used support, preparation method and promoter loading (Table 9, 10).

4.3 Hydrotalcites

Hydrotalcite is a naturally occurring layered mineral, discovered in Sweden in 1842, of chemical formula: $Mg_6Al_2(OH)_{16}CO_3 \cdot 4H_2O$ [135]. The name hydrotalcite comes from its resemblance with talc ($Mg_3Si_4O_{10}(OH)_2$), and from the high water content of this mineral. Similarly as talc, hydrotalcite mineral can be easily crushed into a white powder. Hydrotalcite occurs in nature in foliated and contorted plates and/or fibrous masses [135]. From a crystallographic point of view this mixed magnesium and aluminium hydroxycarbonate possesses the trigonal structure of brucite, i.e. magnesium hydroxide $Mg(OH)_2$. Hydrotalcite layers are built of octahedral units in which divalent or trivalent cation is placed in the centre of an octahedron and six OH^- groups are placed in the corners of the octahedron (Fig. 7). Similarly as in brucite, octahedral units are linked by edges, forming in these way parallel layers. Depending on the arrangement of the layers, hydrotalcite structure may have rhombohedral or hexagonal symmetry, in which the unit cell is build up from three and two hydrotalcite layers, respectively. For both naturally occurring and synthetic hydrotalcites, the rhombohedral symmetry is generally more common [135–138].

In the hydrotalcite brucite-like layers, a part of the divalent magnesium cations has been isomorphously replaced by trivalent aluminium cations. Such substitution is possible due to the similar ionic radii of Mg^{2+} and Al^{3+} . Thanks to this substitution, the brucite-like layers of hydrotalcite are positively charged. This charge is compensated by carbonate anions present in the interlayer spaces. Water molecules complete the voids in the spaces between the hydrotalcite layers [135–138]. A schematic representation of hydrotalcite structure is presented in Fig. 8.

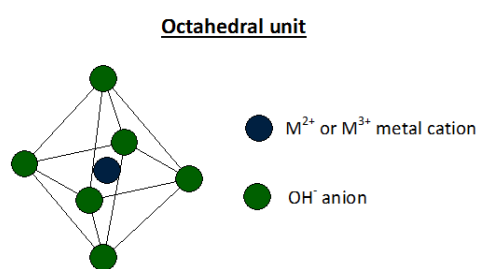


Fig. 7 The octahedral unit of brucite-like layers in an hydrotalcite structure.

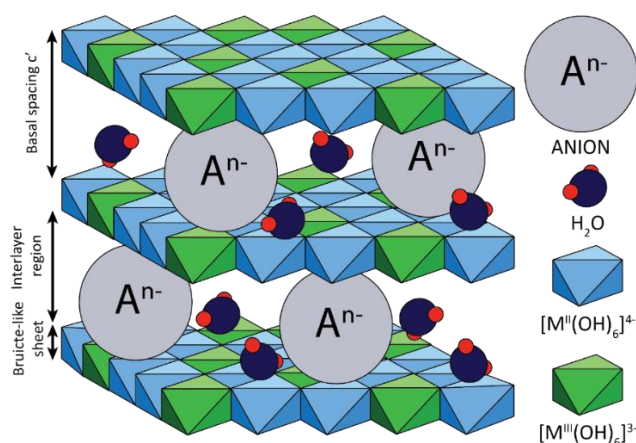
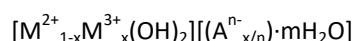


Fig. 8 Schematic representation of the hydrotalcite structure

Upon the discovery of hydrotalcites, similar mixed hydroxycarbonate of magnesium and iron were identified. Shortly, a large number of minerals with different compositions but the same hydrotalcite-like structure were developed. Currently, the name hydrotalcite (hydrotalcite-like compounds - HTs, layered double hydroxides – LDHs) is used to describe a large group of naturally occurring minerals and synthetic materials, which possess the typical layered structure of hydrotalcite. The general formula of such compounds can be represented as [136]:



where M^{2+} , M^{3+} - di- and tri-valent cations, A – interlayer anions, x – mole fraction of trivalent cations, the part $[M^{2+}_{1-x}M^{3+}_x(OH)_2]_2$ describes the composition of brucite-like layers and the part $[(A^{n-})_{x/n} \cdot mH_2O]$ describes composition of interlayer spaces.

4.4 Hydrotalcites as DRM catalysts

As reported in literature and briefly summarized within the previous section of this report, mixed **MgO-Al₂O₃** materials are promising supports for the preparation of Ni-containing catalysts for DRM. They gather all the advantages of the separated materials guaranteeing however a controlled interaction between

the Ni-phase and its carrier, thus preventing sintering of active material through avoiding the formation of inactive phases, i.e. NiAl_2O_4 or NiO-MgO solid solution. Moreover, Ni can be incorporated by different means, i.e. by means of ion exchange in the brucite-like structure through co-precipitation or simply by impregnation. Additionally, through anion exchange or reconstruction it is possible to introduce various promoters into catalytic system. The method of hydrotalcite synthesis and its composition have a significant effect on the properties of the obtained material. There is a number of various synthesis routes described in literature, which lead to hydrotalcite-like materials. The most widely used are co-precipitation, urea, sol-gel or salt-oxide methods. The obtained materials can be further modified by anion exchange and reconstruction, microwave or hydrothermal treatments. The specification of desired hydrotalcite determines the selection of appropriate synthesis route. There are three main routes leading to supported metal catalysts derived from hydrotalcites, shown schematically in Fig. 9. The first one involves synthesis of hydrotalcite precursor with desired metal cations present in brucite-like layers. In the second route, initial hydrotalcite undergoes ion exchange with anionic metal precursor containing desired metal. Third route involves the deposition of inorganic or organometallic precursors of metals on the calcined hydrotalcite material and the subsequent reconstruction of hydrotalcite structure. All preparation routes in the final stage involve the calcination and/or reduction resulting in the final supported metal catalyst.

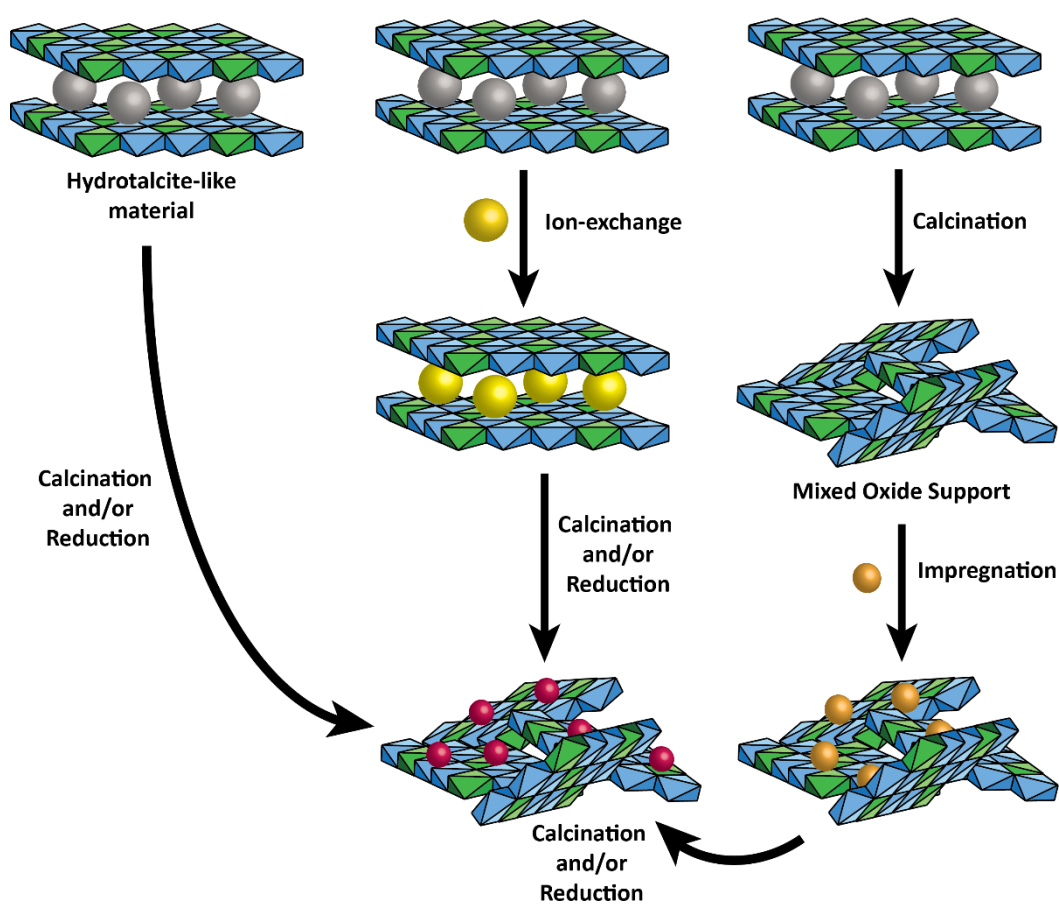


Fig. 9 A simplified representation of main routes leading to obtaining supported metal catalysts from hydrotalcite precursors

The methane and CO_2 conversions reported for several Ni-based catalytic systems, including hydrotalcite-derived materials are presented in Fig. 10. Note that the direct comparison of catalytic activity is not straightforward, since the values of methane and CO_2 conversions may depend on the specific reaction conditions used in the DRM experiments, and of course on Ni-content and on the preparation procedure of each catalyst. However, it is yet possible to conclude from Fig. 9 that the **hydrotalcite-derived catalysts are generally placed among the catalytic systems yielding the highest methane and CO_2 conversions of CH_4 in a wide range of reaction temperatures.**

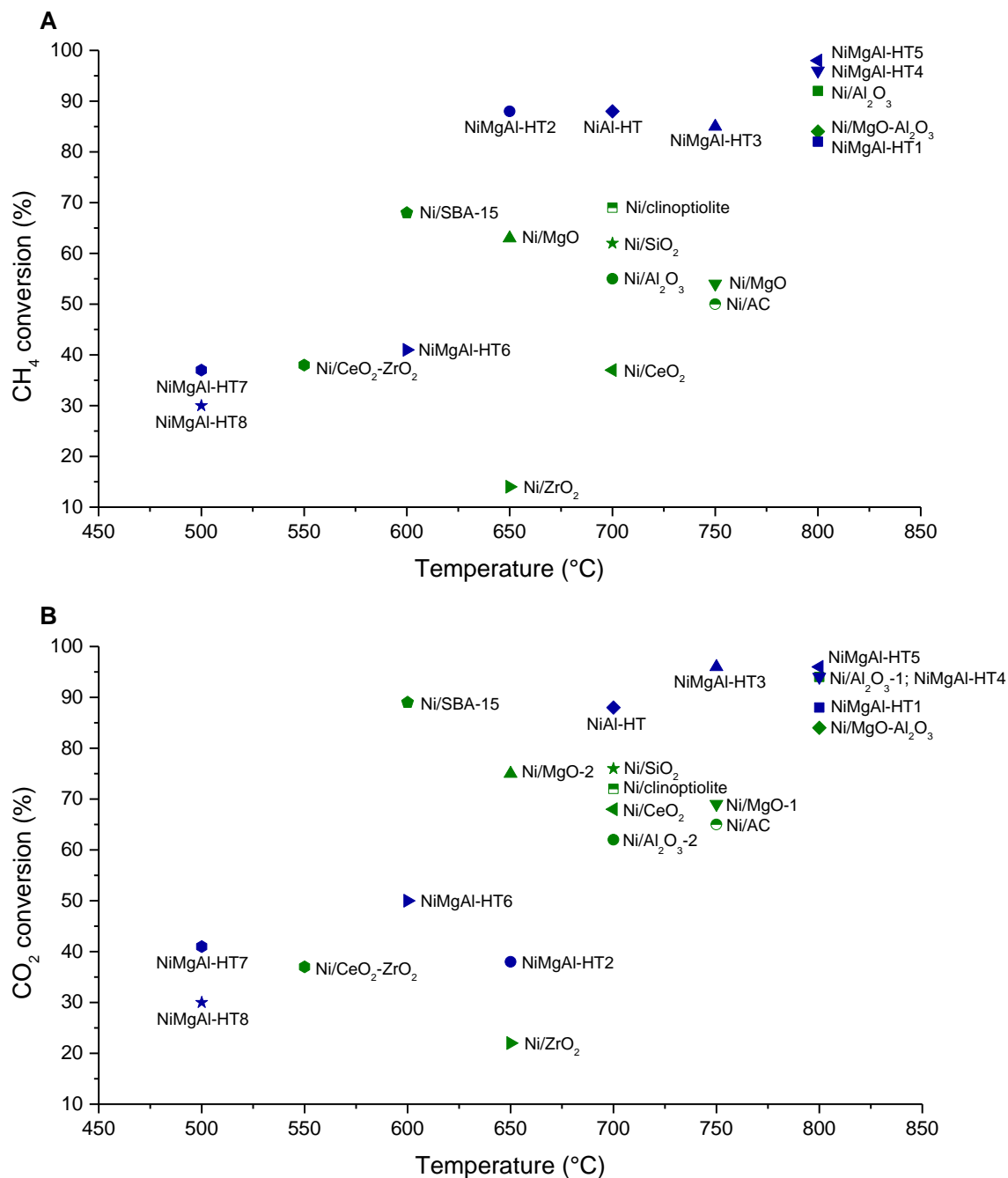


Fig. 10 Catalytic activity of nickel-based catalysts in dry reforming of methane: (A) CH₄ conversions and (B) CO₂ conversions, as a function of temperature;

Green symbols – catalysts Ni/support: Ni/Al₂O₃-1 [66], Ni/Al₂O₃-2 [67], Ni/MgO-1 [73], Ni/MgO-2 [77], Ni/MgO-Al₂O₃ [88], Ni/CeO₂ [81], Ni/ZrO₂ [101], Ni/CeO₂-ZrO₂ [92], Ni/SiO₂ [57], Ni/SBA-15 [102], Ni/clinoptilolite [96], Ni/AC [100]; Blue symbols – hydrotalcite-derived catalysts: NiMgAl-HT1 [139], NiMgAl-HT2 [140], NiMgAl-HT3 [141]; NiMgAl-HT4 [142]; NiMgAl-HT5 [143], NiMgAl-HT6 [144], NiMgAl-HT7 [145], NiMgAl-HT8 [146], NiAl-HT [147];

Moreover, these hydrotalcite-derived catalysts allow acceptable conversions at **low reaction temperatures, i.e. at 500°C**. Nickel-containing hydrotalcite-derived catalysts stand therefore as promising catalysts for DRM. This is a consequence of the particular physicochemical features of these materials, such as abundant but moderate strength basicity and controlled Ni-crystal size, which will be discussed in detail further in this review. This is the reason why the research on these type of materials is important, with an increasing amount of contributions being published each year in the last decades, and may contribute to the commercialization of the DRM process.

4.4.1 Ni/Mg/Al and Ni/Al hydrotalcite derived catalysts

The substitution of a part or all of Mg^{2+} cations by Ni^{2+} in the $Mg,Al-CO_3$ hydrotalcite structure results already in a catalytic system that, upon calcination, can be used in dry reforming. Table 11 contains a summary of the different DRM catalysts prepared from Ni/Mg/Al and Ni/Al hydrotalcites.

The work of Bhattacharyya et al. [148] contains most probably the earliest report on hydrotalcite-derived Ni/Al and Ni/Mg/Al mixed oxides for combined dry/steam reforming. They furthermore compared the catalytic activity of these hydrotalcite-derived materials to commercial NiO supported catalysts, proving that the use of both Ni/Al and Ni/Mg/Al catalysts resulted in very similar yields and conversions that those obtained in the presence of the commercial catalyst. Moreover the hydrotalcite-derived catalysts turned out to be more active under more severe reaction conditions (higher GHSV, and lower H_2O/CH_4 feed gas composition) and more resistant to coke formation. No further characterization data were nevertheless provided. Several researchers therefore continued the research on these promising materials. Basile et al. [149] prepared Ni/Mg/Al hydrotalcite-derived catalysts having Ni/Mg molar ratios around 1/6. These materials were tested in DRM at very low contact times. They showed very higher activity towards CO_2 and the formation of excess CO in the products of reaction, pointing to the simultaneous occurrence of reverse water gas shift reaction. These results are in good agreement with those presented by other authors [144,150,151] testing HTs-derived materials with low nickel content. On the contrary, the materials with high content of Ni in brucite-like layers were reported to promote CH_4 decomposition [140,152,153]. Therefore, the catalytic properties of hydrotalcite-derived materials (activity, stability, promotion of side reactions) are dependent on materials composition i.e. nickel content, Ni/Mg and Mg/Al molar ratio and will be discussed in the next subchapter. The temperature and duration of the calcination process has been as well considered, as reflected in Table 1. The temperature, duration and gas composition chosen for the reduction pre-treatment of the catalysts prior to DRM reaction is another important parameter strongly determining their activity. Once the periclase structure is formed, high reduction temperatures are generally needed, i.e. higher than $850^\circ C$, in order to reduce the Ni present in hydrotalcite-derived materials. However, no detailed information can be found regarding the influence of reduction conditions. The size of Ni crystals may vary as a consequence of their sintering at high temperatures. Further research is maybe needed in order to assess this important point.

4.4.2 Effect of Mg/Al, Ni/Mg and Ni/Al molar ratios

The influence of Mg/Al molar ratio in Ni/Mg/Al hydrotalcites was first examined by Zhu et al. [139]. These authors considered the variation of the Mg/Al molar ratio from 1/5 to 5. The results of catalytic tests showed that the performance of hydrotalcite-derived materials was dependent on the Mg/Al molar ratio, i.e. their activity increased with increasing Mg/Al ratios, pointing to a strong influence of the presence of MgO. Moreover, the catalyst containing the highest magnesium amount exhibited also the highest resistance to coke formation. However, it is important to remark that high Mg/Al ratios also resulted in the formation of a segregated $Mg_5(CO_3)_4(OH)_2 \cdot 3H_2O$ phase and that thus the catalytic activity of the catalyst prepared using the highest Mg/Al ratio may have been affected by the presence of isolated MgO.

Table 11 The summary of Ni/Mg/Al and Ni/Al hydrotalcite-based catalytic systems tested in dry reforming of methane

Type of catalyst	Method of hydrotalcite synthesis	Cations in HTs layers	Ni/Mg or Ni loading ¹⁾	M ²⁺ /M ³⁺	Calcination conditions	Reaction conditions				Conversion ²⁾		H ₂ /CO (-)	Ref.
						Temp. (°C)	CH ₄ /CO ₂	GHSV (h ⁻¹)	TOS (h)	CH ₄ (%)	CO ₂ (%)		
NiMgAl HTs	Co-precipitation at constant pH	Ni ²⁺ , Mg ²⁺ , Al ³⁺	1, 0.2	2, 3	nd	815	1.25	720	250	70	52	1.0	[148]
NiMgAl HT	Co-precipitation at constant pH	Ni ²⁺ , Mg ²⁺ , Al ³⁺	1/6	2.45	700, 900°C for 14h	750	1/1	nd	nd	29	50	nd	[149]
NiAl HT	Co-precipitation at constant pH	Ni ²⁺ , Al ³⁺	63 ¹⁾	4	550°C for 4h in air	550	2/1 ³⁾	20000	4	48	54	2.6	[152]
NiMgAl HT	Co-precipitation at constant pH	Ni ²⁺ , Mg ²⁺ , Al ³⁺	2.94	2	350, 600, 800, 1000°C	900	32/40 ³⁾	nd	10	74	nd	nd	[153, 154]
NiAl and NiMgAl HTs	Co-precipitation at constant pH	Ni ²⁺ , Al ³⁺	-	2	800°C for 6h in air	750	1/1 ³⁾	3·10 ⁵	8	68	90	0.7	[151]
NiMgAl HTs	Co-precipitation at constant pH	Ni ²⁺ , Mg ²⁺ , Al ³⁺	1/5, 1/3, 1	6, 4, 2, 2/3, 2/5	500°C for 10h in air	800	1/1	80000	30	82	88	nd	[139]
NiAl HTs	Co-precipitation at constant pH	Ni ²⁺ , Al ³⁺	-	2, 3, 5, 8, 10	300, 400, 500, 600, 700, 800°C for 6h	700	1/1 ³⁾	nd	10	88	88	1.0	[147]
NiAl HT	Co-precipitation at constant pH	Ni ²⁺ , Al ³⁺	44 ¹⁾	2	450°C for 4h	700	1/1 ³⁾	nd	30	94	94	0.9	[155]
NiMgAl HTs	Co-precipitation at constant pH	Ni ²⁺ , Mg ²⁺ , Al ³⁺	3, 6, 9, 12, 15, 18 ¹⁾	3	800°C for 5h	600	1/1 ³⁾	60000	25	41	50	0.7	[144]

Table 11 Continuation

Type of catalyst	Method of hydrotalcite synthesis	Cations in HTs layers	Ni/Mg or Ni loading ¹⁾	M ²⁺ /M ³⁺	Calcination conditions	Reaction conditions				Conversion ²⁾		H ₂ /CO (-)	Ref.
						Temp. (°C)	CH ₄ /CO ₂	GHSV (h ⁻¹)	TOS (h)	CH ₄ (%)	CO ₂ (%)		
NiMgAl HTs	Co-precipitation at constant pH	Ni ²⁺ , Mg ²⁺ , Al ³⁺	0.5, 1, 2, 5	0.4, 0.9, 2	400, 600, 800°C for 6h in air	650	1/2 ³⁾	45000 ₄₎	nd	83	38	1.2	[140]
NiMgAl HTs	Co-precipitation at constant pH	Ni ²⁺ , Mg ²⁺ , Al ³⁺	1, 5, 25, 50 ⁴⁾	2	600°C for 3h in air	900	32/40 ³⁾	nd	10	67	nd	0.8	[156]
NiMgAl and NiAl HTs	Co-precipitation at constant pH	Ni ²⁺ , Mg ²⁺ , Al ³⁺	3, 1, 0.33, 0.18, 0.06	3	550°C for 4h in air	550	1/1 ³⁾	20000	24	43	40	1.1	[150]

¹⁾ weight % of Ni loading;

²⁾ results obtained for the best catalyst;

³⁾ gases were diluted with inert gas;

⁴⁾ mol% of Ni loading

nd –no data

With respect to the influence of Ni loading and/or Ni/Al ratio, Touahra et al. [147] prepared hydrotalcite derived Ni/Al mixed oxides using different Ni/Al molar ratios (2, 3, 5, 8, 10), which were subsequently tested in DRM within the temperature range of 400-700°C. They observed an important influence of the calcination temperature, since NiAl₂O₄ spinel phase was detected in the catalysts calcined at 800°C, this fact being, according to the authors, the main reason for the higher stability of these materials in DRM. Moreover, the catalyst prepared using a Ni/Al ratio equal to 2 was showing the best overall catalytic performance. The work described the influence of Ni/Al molar ratio in terms of the final Ni particle size, which affected as well the stability of the material. Small Ni particles, i.e. around 6 nm size, are thus preferred. Let us note here that these catalysts were all pre-treated in pure H₂ at 750°C for 1 h. This work was continued by Abdelsadek et al. [155] who tested the activity and stability of Ni/Al = 2 hydrotalcite-derived materials in DRM for ca. 40 h, followed by an in-situ regeneration of catalyst by means of the hydrogasification of carbon deposits. These catalyst were pre-treated at 650°C in pure H₂ for 1 h, thus at lower temperature than the catalysts tested by Touahra and co-workers. The regeneration of the catalysts through hydrogasification resulted in an increase in DRM activity upon each cycle. The authors attributed this increase in activity to the formation a C-alpha type of carbon deposits upon DRM, Which may still result partial pore blockage but do not irreversibly poison the Ni-active sites.

Lin et. al. [144] studied the influence of nickel loading within the range of 3-18 wt.% in Ni/Mg/Al hydrotalcite-derived catalysts for DRM. The authors found that both CH₄ and CO₂ conversions increased with increasing Ni loading. However, the influence of side reactions, namely CH₄ decomposition and CO disproportionation, was more evident at low temperatures for the catalysts prepared using high nickel content. The 30 h-isothermal experiments, carried out at 600 and 750°C, showed that the stability of the catalysts was dependent on both reaction temperature and nickel content. At 750°C the stability of the catalysts improved with increasing nickel content. The opposite trend was observed at 600°C. In fact, coke deposition on the catalysts tested at 600°C increased with Ni loading. Increased Ni-contents favored the sintering of Ni particles, and thus the presence of bigger Ni particles resulted in the promotion of carbon-forming reactions. At 750°C, the amount of coke deposited decreased with increasing Ni content. The authors claimed that different types of carbons structures could be formed as a function of reaction temperature. The formation of encapsulating carbon, i.e. thick graphitic layers growing on the surface of Ni-particles, was considered to be responsible for carbon deactivation.

Perez-Lopez et al. [140] studied the effect of the composition and the calcination temperature in the preparation of Ni/Mg/Al hydrotalcite-derived catalysts, using different M²⁺/M³⁺ and Ni/Mg molar ratios. They observed that the catalytic performance of Ni/Mg/Al hydrotalcites was mostly affected by the M²⁺/M³⁺ molar ratio rather than by the Ni/Mg ratio. The best catalytic performance in DRM was obtained in the presence of the materials prepared using a Ni/Mg ratio between 1-5 and fixed M²⁺/M³⁺ ratio around 2, calcined at 600°C and reduced at 700°C. For a constant M²⁺/M³⁺ ratio, the surface area of the catalysts was found to be independent of Ni content, whereas when the Ni/Mg ratio was kept constant the surface area decreased drastically with the reduction of the M²⁺/M³⁺ ratio, i.e. an increase in Al content resulted in smaller surface areas. Two low M²⁺/M³⁺ are not sufficient in order to develop a spinel mixed oxide structure. However, the catalytic activity was found to be rather independent of surface area and mostly related to Ni crystal size and to Ni/Mg ratios. For a constant Ni/Mg ratio, the catalytic activity decreases as the M²⁺/M³⁺ decreased. The selectivity in DRM was found to be influenced by both Ni/Mg and M²⁺/M³⁺ ratios. The authors finally claimed that these differences were due to the simultaneous influence of these parameters in the Ni crystal size and in the acid-base properties of the surface. They moreover remarked the influence of the reduction temperature in the activity and selectivity in DRM for this kind of catalysts.

The influence of Ni/Mg molar ratio was further examined by Dudder et al. [156], who tested different catalysts containing 1, 5, 25 and 50 mol% Ni. The activity of these catalysts, evaluated in terms of methane conversion, increased with increasing Ni content, what was attributed to the increasing availability of Ni metal sites. In fact, the best catalytic performance was shown by the 50 mol% Ni-containing catalyst, which was moreover tested for 100 h, evidencing remarkable stability (around 6 % activity loss upon 100 h TOS). The type of formed carbon deposits was found to be dependent on both nickel content and reaction temperature. High temperature DRM favored formation of bulk graphitic forms of coke, while carbon nanofibers were formed at

lower reaction temperatures. However, Dudder and co-workers claimed that carbon species could be easily removed by O₂ and CO₂ either isothermally or using a temperature ramp, in order to regenerate the original catalytic activity.

Dębek et al. [150] have recently considered the influence of Ni/Mg molar ratio in low temperature DRM for hydrotalcite-derived materials. The Ni/Mg molar ratio considered were 3, 1, 0.33, 0.18 and 0.06. A Mg-free NiAl-HT catalyst was also prepared and tested. Similarly than in the studies carried out by Dudder et al. [156] methane conversion increased with increasing Ni content, whereas CO₂ conversion was found to be maximal for the catalyst containing ca. 20 wt.% Ni. Since methane and CO₂ conversion need to be coupled, and equal, in the case of treating equimolar CH₄/CO₂ mixtures, this catalyst was considered as the most effective within this series. Decoupled and far too high methane conversions point to the simultaneous occurrence of direct methane decomposition, resulting in carbon formation and thus contributing to a faster deactivation of the catalyst, if this is not avoided by regeneration. Direct methane decomposition activity experiments performed on these catalysts further confirmed this fact. Increasing Ni content also resulted in increased Ni crystal size upon reduction and thus promoted this important concomitant reaction. The authors therefore claimed that selectivity could be tailored by means of controlling Ni crystal size that, together with an increased presence of the highest number of basic sites, i.e. especially strong basic sites, can result in inhibited carbon formation through direct methane decomposition.

At the sight of the reported results it can be thus concluded that the Ni content and thus the Ni/Mg ratio, together with Ni/Al and Mg/Al molar ratios, can definitively determine the catalytic activity and selectivity of Ni-containing hydrotalcite-derived catalysts for DRM. DRM activity and selectivity can furthermore affect the stability of the catalysts and thus the different conversions and product distributions related to composition and preparation procedure can be related to the very different behaviors with TOS observed at different reaction temperatures. In general, increasing Ni content results in increased Ni particle or crystal sizes that, particularly at relative low or moderate temperatures, may result in the promotion of carbon forming reactions such as direct methane decomposition. Increasing Mg content can be linked to an increase in the overall basicity. Increasing basicity is generally seen as a positive fact, leading to enhanced stability.

4.4.3 Effect of the method of Ni introduction into HTs structure

The works discussed in the previous section refer to the incorporation of Ni-cations into the brucite-like structure of the hydrotalcite precursors. Nickel can be nevertheless incorporated into hydrotalcite structure by different means, i.e. not only within the brucite-type layers. In fact, the most commonly applied procedure for the preparation of Ni-containing hydrotalcite-derived materials is the co-precipitation of the different cations present in a solution of their corresponding nitrates, yielding a mixed hydroxide structure where Ni has been introduced in its brucite-like layers (e.g. see references cited in the previous section). Other less frequently used methods considered the incorporation of Ni into the interlayer spaces of the hydrotalcite structure, either by the so-called reconstruction method, either through “memory effect” or via ion-exchange. The latter must be carried out using an appropriate hydrotalcite precursor, since carbonate anions are closely packed in the interlayer spaces, and thus it is hard to exchange them by other type of anions [135]. Usually HTs containing monovalent anions between the rhombohedral layers (e.g. NO³⁻) are applied for ion-exchange modification. The third possibility is to incorporate nickel species on the surface of hydrotalcite crystallites via conventional impregnation or adsorption methods. Table 12 summarizes the hydrotalcite-derived catalysts prepared by means of these different Ni incorporation procedures, recently reported in the existing literature.

Guo et al. [141] used a conventional impregnation method to prepare nickel supported on MgAl₂O₄ spinels obtained from Mg/Al hydrotalcite precursors upon their calcination at 800°C. Their performance was compared to similarly prepared Ni/γ-Al₂O₃ and Ni/MgO-Al₂O₃ catalysts. Using the MgAl₂O₄ spinel as support resulted in a highly active catalytic system presenting acceptable stability, due to an enhance dispersion of Ni-particles together with the moderate interaction between active phase and support. Other works [88–90], already discussed within the previous sections, already evidence the advantages of using MgAl₂O₄ spinels as supports in the preparation of Ni-contained catalysts for DRM.

Shishido et al. [157] compared the DRM catalytic activity of a co-precipitated Ni/Mg/Al hydrotalcite-derived catalyst with the performance of 25.1 wt.% Ni impregnated MgAl₂O₄ (Mg/Al hydrotalcite-derived)

catalyst, and other conventional Ni/MgO and Ni/Al₂O₃ catalysts. Among them, the co-precipitated Ni/Mg/Al hydrotalcite-derived catalyst exhibited the highest activity at 800°C, what was explained in terms of the formation of highly dispersed and stable nickel species on the catalyst surface.

Tan et al. [158] studied the DRM performance of Ni/Mg/Al mixed oxides prepared from hydrotalcites, which were synthesized via a surfactant-assisted co-precipitation method. The authors used 3 different surfactants at the co-precipitation stage, in order to modify the properties of the resulting material, i.e. their texture, reducibility, structure and nickel distribution on the catalysts surface. The DRM catalytic experiments evidenced that the use of the different surfactants significantly affected the catalytic performance of materials. When co-precipitation was carried out in the presence of tetrapropylammonium hydroxide (TPAOH), the resulting material yielded increased CH₄ and CO₂ conversions. The charge properties and coordination abilities toward metal ions of the different surfactants influenced the metal particle size and promoted or restrained the growth of specific crystal planes. In this sense, the authors showed that both catalytic activity and stability were strongly affected by the exposure of Ni(200) crystal plane (identified XRD and HRTEM, i.e. FFT images). These Ni(200) planes were furthermore formed during reaction at high temperatures upon a slow release of Ni encapsulated within the support, and were assumed to responsible for the stabilization of the catalytic activity, without providing further details on the reaction mechanism. Nevertheless, all the tested catalysts showed a considerable decrease in their catalytic activity at 800°C over 40 h-DRM experiments.

Tsyganok et al. [159] proposed a new method of Ni introduction into hydrotalcite structure by co-precipitation of a Mg/Al hydrotalcite in a solution of stable [Ni(EDTA)]²⁻ chelates. The so-prepared materials evidenced the presence of nickel-EDTA species in the interlayer spaces of the pristine hydrotalcite structure. An important advantage of this method vis-à-vis the conventional co-precipitation of Ni/Mg/Al hydroxides is that the reduction pre-treatment is not required, still the stabilization of the catalytic systems needed from 30 to 90 min induction time. The catalyst showed stable performance during 150 h DRM tests at 800°C. Different forms of coke deposits were however found on the surface of the spent catalysts, pointing to the simultaneous occurrence of carbon forming reactions. However, carbon deposition did not seem to affect the catalytic activity. These materials yielded moreover higher conversion of CO₂ than of methane, pointing to the concomitant occurrence of RWGS reaction and thus influencing the product distribution.

Table 12 The summary of Ni/Mg/Al hydrotalcite-derived catalysts into which nickel was incorporated via various methods

Type of catalyst	Method of hydrotalcite synthesis	Cations in HTs layers	Ni/Mg or Ni loading ¹⁾	M ²⁺ /M ³⁺	Calcination conditions	Reaction conditions				Conversion ²⁾		H ₂ /CO (-)	Ref.
						Temp. (°C)	CH ₄ /CO ₂	GHSV (h ⁻¹)	TOS (h)	CH ₄ (%)	CO ₂ (%)		
Ni supported on MgAl HTs	Co-precipitation at constant pH	Mg ²⁺ , Al ³⁺	1, 3, 5, 10, 15 ¹⁾	nd	900°C for 5h	750	1/1	50000	10	85	96	0.9	[141]
NiMgAl HTs; Ni supported on MgAl HT	Co-precipitation at constant pH	Ni ²⁺ , Mg ²⁺ , Al ³⁺	1/2	3	650 and 850°C for 14h in air	800	1/1 ³⁾	54000	6	94	nd	nd	[157]
	Impregnation of Ni ²⁺ on MgAl HT	Mg ²⁺ , Al ³⁺	25.1 ¹⁾	3						92	nd	nd	
NiMgAl HTs	Surfactant assisted co-precipitation	Ni ²⁺ , Mg ²⁺ , Al ³⁺	10 ¹⁾	3	700°C for 6h	800	1/1	60000	35	47	62	nd	[158]
Ni introduced into MgAl HTs	Co-precipitation in [Ni(EDTA)] ²⁻	Mg ²⁺ , Al ³⁺	-	3	500°C for 16h in air	800	1/1 ³⁾	nd	150	98	95	1.0	[159]
Ni introduced into MgAl HTs and NiMgAl HTs	Co-precipitation in [Ni(EDTA)] ²⁻	Mg ²⁺ , Al ³⁺	1/7	3.5	500°C for 16h in air	800	1/1 ³⁾	nd	6	97	95	1.0	[143]
	Anion exchange	Mg ²⁺ , Al ³⁺	1/11	3.3						97	95	1.0	
	Reconstruction	Mg ²⁺ , Al ³⁺	1/11	3.6						97	94	1.0	
	Co-precipitation	Ni ²⁺ , Mg ²⁺ , Al ³⁺	1/5	2.5						98	96	1.0	
NiMgAl HTs	Sol-gel method	Ni ²⁺ , Mg ²⁺ , Al ³⁺	4, 15, 19 ¹⁾	nd	500, 650°C for 5h	800	1/1 ³⁾	2.94·10 ^{-5 5)}	8	96	94	nd	[142]

Table 12 Continuation

Type of catalyst	Method of hydrotalcite synthesis	Cations in HTs layers	Ni/Mg or Ni loading ¹⁾	M ²⁺ /M ³⁺	Calcination conditions	Reaction conditions				Conversion ²⁾		H ₂ /CO (-)	Ref.
						Temp. (°C)	CH ₄ /CO ₂	GHSV (h ⁻¹)	TOS (h)	CH ₄ (%)	CO ₂ (%)		
NiMgAl HTs	Sol-gel method	Ni ²⁺ , Mg ²⁺ , Al ³⁺	15 ¹⁾	0.25-19	750°C for 5h in air	800	1/1 ³⁾	36000	40	84	89	nd	[88]
	Co-precipitation at constant pH	Ni ²⁺ , Mg ²⁺ , Al ³⁺		2						84	89	nd	
NiAl HT and Ni supported on MgAl HT	Co-precipitation at constant pH	Ni ²⁺ , Al ³⁺	63 ¹⁾	4	550°C for 4h in air	550°C	2/1	20000	1	48	57	2.7	[160]
	Adsorption of [Ni(EDTA)] ²⁻⁻	Mg ²⁺ , Al ³⁺	0.8 ¹⁾	3						25	38	1.6	
NiMgAl HTs	Co-precipitation at constant pH	Ni ²⁺ , Mg ²⁺ , Al ³⁺	10 ¹⁾	1.5-9	800°C for 3h	800	1/1	nd	4	86	87	nd	[161]
NiMgAl HTs	Co-precipitation at constant pH	Ni ²⁺ , Mg ²⁺ , Al ³⁺	10 ¹⁾	3	500-800°C for 6h	800	1/1	8000	2000	92	95	0.9	[162]

¹⁾ weight % of Ni loading;

²⁾ results obtained for the best catalyst;

³⁾ gases were diluted with inert gas;

⁴⁾ mol% of Ni loading

nd –no data

In a subsequent work, Tsyganok et al. [143] compared the DRM catalytic performance of Ni-containing hydrotalcite-derived catalysts prepared following different routes, such as: co-precipitation of Mg^{2+} and Al^{3+} with pre-synthesized $[Ni(EDTA)]^{2-}$ complexes; anion exchange reaction of NO_3^{2-} ions in the hydrotalcite interlayer spaces with $[Ni(EDTA)]^{2-}$ chelate in aqueous solution; calcination of Mg/Al hydrotalcite at moderate temperature, followed by reconstruction of hydrotalcite layered structure in an aqueous solution of $[Ni(EDTA)]^{2-}$; and traditional co-precipitation of Ni^{2+} , Mg^{2+} and Al^{3+} with CO_3^{2-} . In spite of the differences in Ni crystal size, all the catalysts prepared using $[Ni(EDTA)]^{2-}$ chelates showed stable performance and high conversions of both CH_4 and CO_2 . The highest amount of deposited carbon was indeed found for the catalyst prepared through traditional co-precipitation. Dębek et al. [160] also studied the effect of nickel introduction into hydrotalcite-based catalytic systems, and compared the performance of Ni/Al mixed oxides with Mg/Al hydrotalcite into which nickel was introduced via the adsorption of $[Ni(EDTA)]^{2-}$ complexes. The results showed that both catalysts were active in DRM at 550°C. However, the material into which nickel was introduced by means of the adsorption of $[Ni(EDTA)]^{2-}$ chelates exhibited higher activity per gram of active material, with the respect to the catalysts into which nickel was introduced into the brucite-like layers of the pristine hydrotalcite via the conventional co-precipitation method.

Though conventional impregnation of $MgAl_2O_4$ spinels derived from the calcination of Mg/Al hydrotalcites already yields good results in the preparation of Ni-containing hydrotalcite-derived catalysts for DRM, the co-precipitation of Ni/Mg/Al hydroxides can lead as well to an uncomplicated synthesis of highly performing hydrotalcite-derived materials. Other methods, such as the incorporation of **Ni-species in the form of $[Ni(EDTA)]^{2-}$ chelates need to be further explored**, since they may offer important advantages, such as bypassing the reduction pre-treatment of the catalyst. However, the surface of the catalysts and the state of Ni species may change upon TOS, and indeed, relatively long induction periods seem to be needed.

4.4.4 Influence of the air-calcination temperature

The thermal stability of hydrotalcite-like materials is an important issue, since the products of their thermal decomposition of layered double hydroxides (LDHs) find application not only in DRM catalysis but also in various branches of industry. Although hydrotalcite-like materials may greatly differ in their composition, they exhibit similar thermal decomposition behaviour [50]. This usually comprises four consequent steps [163]: (i) the removal of water physically adsorbed on the external surfaces of the crystallites (below 100°C), (ii) the removal of interlayer water (up to 250°C), (iii) the removal of hydroxyl groups from the layers as water vapour and (iv) the decomposition of the interlayer anions (up to 500°C). The steps (iii) and (iv) usually overlap. Thermal treatments up to 500°C are normally associated with the loss of ca. 40 wt.% of the initial weight and have been reported for several hydrotalcite-like materials, which differed in composition [135,163–166]. As a result of this thermal decomposition, the lamellar structure of hydrotalcites collapses and a new phase of periclase-like mixed nano-oxides is obtained, i.e. analogous to the cubic form of MgO where the different oxides appear mixed and exhibit crystal sizes in the order of several nanometers [136].

Water, together with the gaseous products of anion decomposition, are released during the thermal treatment of the hydrotalcite structure, can create channels in brucite-like layers and lead to the formation of additional porosity, mostly within the range of mesopores. Thus, the mixed-oxides obtained upon calcination are usually characterized by higher specific surface areas, in comparison to their parental hydrotalcite materials [135]. Upon further heating, the periclase-like structure of the mixed oxides may undergo structural further changes, leading to the formation of stable spinel phase. This phenomenon is dependent on material composition and usually takes place at high temperatures (above 700°C). However, e.g. the formation of $MgFe_2O_4$ spinel was reported for Mg-Fe- CO_3 hydrotalcite already upon heating at 350°C [136]. Therefore, selection of appropriate calcination temperature is an important factor that may determine catalytic activity in DRM. A summary of different works considering and discussing the effect of calcination temperature in the DRM performance of hydrotalcite-derived catalysts is presented in Table 13.

Table 13 The effect of calcination temperature on HTs-derived materials in DRM

Type of catalyst/Method ¹⁾	Calcination conditions	Effect of calcination temperature	Ref.
---------------------------------------	------------------------	-----------------------------------	------

NiAl HTs/CP	300, 400, 500, 600, 700 and 800°C for 6h	Calcination temperature <500°C has minimal effect of activity; Increase in calcination temperature resulted in increased activity and stability	[147]
NiMgAl HTs/CP	400, 600, 800°C for 6h	Calcination temperature had a small influence on the activity and selectivity	[140]
NiMgAl HTs/SG	500, 650°C for 5h	Moderate calcination temperatures prevent formation of spinel phase. Higher calcination temperature resulted in the increased stability	[142]
NiMgAl HT/CP	500, 600, 700, 800°C for 6h	No significant effect of calcination temperature on performance in DRM was observed	[162]
NiMgAl HT/CP	350, 600, 800, 1000°C	Calcination at 800 and 1000°C resulted in formation of spinel phase. The optimal calcination temperature was selected to be 600°C	[153,154]

¹⁾Method of HTs synthesis: CP-co-precipitation; SG-sol-gel method

Thouahra et al. [147] examined the influence of the calcination temperature on the performance of Ni/Al catalysts. They concluded that the use of calcination temperatures below 500°C did not practically affect the catalytic activity. In this way, the catalysts calcined at 300 and 400°C exhibited very similar values of specific surface area and Ni particle size. On the contrary, calcination temperatures above 500°C could strongly influence the final catalytic properties of the prepared materials, due to the formation of different spinel phases, which resulted in increased interaction between Ni and Al. A decrease in Ni particle size with increasing calcination temperature was thus observed. The highest stability and activity was recorded by Ni/Al catalyst calcined at 700°C. The studies carried out by Perez-Lopez et al. [140] evidenced however that for Ni/Mg/Al hydrotalcite-derived catalysts, the calcination temperature had a minimal effect on the catalytic activity. Similar results, presented by Li et al. [162], showed that calcination temperature did not significantly affect the catalytic activity of Ni/Mg/Al hydrotalcite-derived catalysts containing 10 wt.% Ni. These authors observed however that crystal size of the periclase-like phase of mixed oxides increased with increasing calcination temperature. The formation of NiAl₂O₄ spinel phase was however not observed and the catalysts calcined at 600, 700 and 800°C exhibited very similar performance in DRM at 800°C. It seems therefore that the presence of Mg inhibited the formation of mixed spinel phases in these materials.

Gonzalez et al. [142] considered the sol-gel preparation of Ni/Mg/Al hydrotalcite-derived mixed oxides with 4, 15 and 19 wt.% Ni. They studied the influence of moderate calcination temperatures (500-650°C) in order to avoid the formation of spinel structures. The resulted materials also promoted side reactions, such as CH₄ decomposition, Boudouard reaction and RWGS. The best catalytic performance was observed for the catalyst containing 19% Ni and calcined at 650°C. The calcination temperature influenced the amount of carbon formed during reaction, i.e. it decreased with increasing calcination temperature. Mette et al. [153,154] investigated performance of Ni/Mg/Al hydrotalcite-derived catalysts with high Ni loading (55 wt.%) calcined and reduced in various conditions. Calcination at 800 and 1000°C resulted in the formation of spinel phases, inactive in DRM. Authors confirmed that temperature 600°C is sufficient to obtain an amorphous, fully dehydrated and carbonate-free NiMgAl mixed oxide, whose catalytic activity in DRM might be further tailored by the subsequent modification of reduction temperature. The most active and stable catalysts for DRM at 900°C was the one prepared via calcination at 600°C, followed by reduction at 800°C.

4.4.5 Effect of the addition of different promoters

Ce-promotion

Ceria is well known for its high oxygen storage capacity associated linked to the redox transformation between Ce³⁺ and Ce⁴⁺ [79,92]. Therefore, the application of ceria as a promoter for hydrotalcite-derived catalysts in DRM reaction may be beneficial, due to easier removal of carbon deposits via oxidation by oxygen anions. Moreover, nickel can dissolve in the fluorite structure of CeO₂. The Ni-O-Ce bond is stronger than Ni-O

bond in the NiO crystal, thus leading to increased metal-support interactions in ceria-supported Ni systems, resulting in the formation of small Ni particles. The comparison of different methods of ceria introduction into Ni/Mg/Al hydrotalcite-derived mixed oxides reported in literature is presented in Table 14.

The addition of cerium to Ni/Mg/Al hydrotalcites was widely studied by Daza et al., who investigated the effect of the method for the introduction of cerium [167], Ce loading [145,146,168] and the general hydrotalcite preparation procedure [169]. The authors compared the DRM catalytic performance registered for a non-promoted Ni/Mg/Al catalysts and for Ce-promoted co-precipitated catalysts (containing 5 wt.% Ce) prepared through co-precipitation in solutions of Na_2CO_3 , $[\text{Ni}(\text{EDTA})]^{2-}$ and $[\text{Ce}(\text{EDTA})]^-$ [167]. In all cases, the ceria-promoted catalysts exhibited higher activity than the non-promoted catalyst. The promoting effect of ceria was attributed to the increase of reducibility of nickel species without observing in all cases a simultaneous reduction in the resulting Ni particle size. The best catalytic performance was observed for the catalyst obtained by conventional co-precipitation in Na_2CO_3 , with average CH_4 and CO_2 conversions after 200 h TOS equal to ca. 78% and 87%, respectively. Moreover, it was observed that the catalysts prepared using low Ni content and prepared via co-precipitation in solution of $[\text{Ni}(\text{EDTA})]^{2-}$ complexes exhibited similar performance to the samples loaded with much higher Ni content. This was attributed to the formation of very small nickel crystallites (smaller than 5nm), in the presence of Ce and specially for this catalysts prepared in the presence of $[\text{Ni}(\text{EDTA})]^{2-}$ complexes.

Daza et al. [168] also studied the influence of Ce content in Ni/Mg/Al hydrotalcite-derived catalysts. Ceria was introduced into hydrotalcite structure by reconstruction method using $[\text{Ce}(\text{EDTA})]^-$ complexes. The Ce and nominal loading was equal to 0, 1, 3, 5 or 10 wt.%. Ce-promoted materials exhibited an increase in total basicity with increasing ceria content, upon their calcination and reduction. Using X-ray photoelectron spectroscopy (XPS), the authors further confirmed the coexistence of Ce_2O_3 and CeO_2 on the catalyst surface. During DRM CO_2 can be adsorbed on Ce_2O_3 sites, yielding CO and CeO_2 in a redox cycle. The produced CeO_2 can further react with deposited carbon, regenerating both Ce_2O_3 and CO_2 . This proposed mechanism may explain the increase in total basicity and the increased stability of Ce-promoted catalysts and is in good agreement with results presented recently by Lino et al. [170]. In general, higher conversions of CH_4 than CO_2 were observed for ceria containing samples, which may be explained by the conversion of methane into light hydrocarbons or simply due to direct methane decomposition. The amount of Ce introduced did not have significant influence on CH_4 and CO_2 conversions and H_2/CO molar ratio. However, it influenced the formation of carbon deposits. The smallest amounts of catalytic coke were formed on the samples loaded with small amounts of Ce, between 1-3 wt.%. Thus, the authors stated that the optimal nominal amount for Ce promotion was 3 wt.% [146].

Similar conclusions were driven in another study of the same authors, where ceria was introduced into the hydrotalcite-derived catalytic system at the co-precipitation [145]. Catalysts prepared using different Al/Ce molar ratios were studied. The reducibility of the catalysts increased with increasing ceria content, i.e. decreasing Al/Ce ratios, which resulted in the formation of bigger Ni crystallites, and thus had a negative effect on the catalysts stability. The same authors also compared the performance of Ni/Mg/Al hydrotalcites synthesized via co-precipitation and self-combustion in glycine methods [84]. Mixed oxides obtained through calcination of the resulting hydrotalcites underwent additionally reconstruction in presence of a solution of $[\text{Ce}(\text{EDTA})]^-$ complexes. The catalyst prepared from the self-combusted hydrotalcite showed enhanced performance. Its higher activity was related by the authors to its higher specific surface area, pore volume and total basicity.

Table 14 Methods of ceria introduction into Ni/Mg/Al hydrotalcite derived mixed oxides tested in DRM

Method of hydrotalcite synthesis	Method of Ce introduction into HT structure	Ni/Mg	Ce content (wt.%)	Calcination conditions	Ref.
Co-precipitation in solution of Na_2CO_3 , $[\text{Ce}(\text{EDTA})]^-$ or $[\text{Ni}(\text{EDTA})]^{2-}$	At co-precipitation stage in form of Ce^{3+} cations or $[\text{Ce}(\text{EDTA})]^-$	1/2	5	500°C for 16h in air	[167]

Co-precipitation at constant pH	Reconstruction method with solution of [Ce(EDTA)] ⁻	2	0, 1, 3, 5, 10	500°C for 16h in air	[168]
Co-precipitation at constant pH	Reconstruction method with solution of [Ce(EDTA)] ⁻	2	0, 1, 3, 10	500°C for 16h in air	[146]
Co-precipitation at constant pH	At co-precipitation stage in form of Ce ³⁺ cations	2	24, 9, 4, 1, 5 ¹⁾	500°C for 16h in air	[145]
Co-precipitation at constant pH and self-combustion method	Reconstruction method with solution of [Ce(EDTA)] ⁻	2	3	500°C for 16h in air	[169]
Co-precipitation at constant pH	At co-precipitation stage in form of Ce ³⁺ cations and by impregnation	20 ²⁾	1-10 ¹⁾	500°C for 4h	[171]
Co-precipitation at constant pH	Adsorption from the solution of [Ce(EDTA)] ⁻	0.6 ²⁾	1.15	550°C for 4h	[172]
Co-precipitation at constant pH	Adsorption from the solution of [Ce(EDTA)] ⁻	1/3	3.7	550°C for 4h	[173–175]
Co-precipitation at constant pH	At co-precipitation stage in form of Ce ³⁺ cations	10, 25 ²⁾	5	650°C for 5h	[170]

¹⁾ Al/Ce molar ratio

²⁾ weight % of Ni

Recently, Ce-promoted Ni/Mg/Al hydrotalcite-derived catalysts have been as well considered by Ren et al. [171], who investigated DRM reaction at moderate pressure (0.5 MPa). The results confirmed important anti-coking benefits of ceria addition. However, the effect of Ce-promotion depended on the amount and the method of ceria introduction. The Ce-impregnated catalysts were more effective in the formation of coke deposits than the co-precipitated ones, which was associated to the higher content of Ce³⁺ on the catalyst surface and to an increased presence of lattice defects in the CeO₂ present in the former catalysts. These materials were very active in DRM and showed an initial CH₄ conversion at 750°C very close to the thermodynamic equilibrium limit. However, carbon deposition was observed over the catalyst surface. The amount of coke deposited, and thus the deactivation of catalyst, increased with increasing of Ce loading. These results are in agreement with those reported by Daza et al. [168], who also reported that high loading of ceria may have negative effect on catalyst stability, due to the enhanced reducibility of nickel species, leading to the formation of bigger crystallites on the catalyst surface.

Dębek et al. [173,175] proposed a method of Ce addition into HTs structure via adsorption from a solution of [Ce(EDTA)]⁻ complexes. Ce addition resulted in an increased reducibility of the nickel species and in the introduction of new strong (low coordinated) oxygen species and intermediate (Lewis acid-base pairs) strength basic sites, which increased the CO₂ adsorption capacity. The DRM activity of these materials consequently increased, especially in terms of CO₂ conversion. Instead, Ce promotion lowered CH₄ conversion with respect to unpromoted catalyst, what was attributed to the partial inhibition of direct methane decomposition. These authors concluded that Ce-promotion could change selectivity of the process and moreover determine type of carbon deposits, i.e. amorphous or graphitic, formed upon the DRM reaction. In a subsequent work [172], they proved that the effect of ceria promotion is also dependent on the method of Ni introduction. The incorporation of Ni species via adsorption of [Ni(EDTA)]²⁻ complexes, followed by ceria promotion resulted in increased activity, stability and selectivity and yielded an stoichiometric syngas as reaction product, in comparison to the non-promoted catalyst.

Other promoters

The use of different promoters of NiMgAl hydrotalcite-derived catalysts, other than cerium, has been as well reported in the literature published in the last years. Table 15 contains a summary of these published works, the promoter used and the results observed upon their addition to the hydrotalcite-derived catalysts.

Table 15 The effect of promoters on the performance of NiMgAl hydrotalcite derived catalysts in DRM.

Promoter	Catalyst	Promoter loading (wt.%)/Method ¹⁾	Effect of addition	Ref.
La	NiMgAl-HT	0, 0.04, 0.11, 0.18 ²⁾ /CP	Increased stability and activity	[176]
La	NiMgAl-HT	1.1, 2/CP	Increased stability and decreased activity	[177,178]
La	NiMgAl-HT	0, 1, 2, 4/CP	Increased activity, selectivity and stability	[179]
La Rh	10 wt.% Ni impregnated on MgAl-HT	10/IMP 1/IMP	Increased reducibility of Ni; Promotes carbon formation	[180]
CeZrO ₂	NiMoMgAl-HT	0, 5, 10, 15, 20/CP	Increased catalyst activity; Promotes reducibility of Ni	[181]
Ru	5 wt.% Ni supported on MgAl-HT	0.1/RE	Inhibits sintering; Increased activity and stability	[182]
Co	NiMgAl and NiCoMgAl-HTs	1, 4 ³⁾ /CP	Increased activity and stability	[144]
Co	NiCoMgAl-HTs	2.76-12.9/CP	nd ⁴⁾	[183]
Zr	NiMgAl-HT	3/CP	Decreased reducibility; formation of small Ni crystallites; Increased stability	[174,184,185]

¹⁾ Preparation methods: IMP – Impregnation; CP – Co-precipitation; RE-reconstruction in the solution of [Mⁿ⁺(EDTA)]⁽⁴⁻ⁿ⁾⁻ chelates

²⁾ nominal La/Al molar ratio

³⁾ nominal Ni/Co molar ratio

⁴⁾ nd- no data, since performance of catalyst was not compared to reference Ni-based sample

Yu et al. [176] investigated the addition of La into Ni/Mg/Al hydrotalcite-derived catalysts. The effect of lanthanum was positive on both catalyst stability and activity, within the temperature range 600-700°C. La-addition increased total basicity and surface Ni content of the catalyst, resulting in a considerable suppression of coking. The best catalytic performance was registered for the sample with a nominal La/Al molar ratio of 0.11, which at 700°C yielded CH₄ and CO₂ conversions equal to 76 and 72%, respectively. A similar positive effect of lanthanum addition, in terms of catalyst stability, was observed by Serrano-Lotina et al. [177,178]. However, a decrease in the catalytic activity with TOS was still observed, assigned to the decrease in Ni crystallinity in the La-promoted catalyst. Liu et al. [179], on the other hand, reported an enhanced catalytic activity towards CH₄ conversion, which was explained in terms of the increase of Ni particle size and the simultaneous promotion of direct methane decomposition. However, the amounts of carbon deposited on the surface of the catalysts were lower than expected. Though the formation of oxycarbonate species (La₂O₂CO₃), La-promotion contributed to the gasification of amorphous carbon deposits. The optimal La content was found to be ca. 4 wt%. The different results obtained upon La-promotion of these Ni-containing hydrotalcite-derived catalysts are most probably a result of using different La-loads and different La incorporation methods. Moreover, the conditions chosen for the calcination and pre-treatment of these materials surely further determine its catalytic behaviour in DRM.

Lucredio et al. [186] studied La and/or Rh addition into Ni supported on MgAl-hydrotalcite. The results showed that the addition of both La and Rh resulted in increased reducibility of nickel species. Thus more Ni active sites were formed on the catalyst surface. Indeed, the catalyst promoted with both Rh and La showed higher activity in terms of CO₂ conversion, However, a negative effect of promoters addition was observed, as Rh and La promoted samples exhibited higher amounts of carbon deposited after 6 h TOS at 750°C.

The DRM catalytic activity of Ni/Mg/Al hydrotalcite-derived catalysts promoted with Ru was studied by Tsyganok et al. [182]. The addition of small amounts of Ru into the catalyst structure by means of a reconstruction method had a highly positive effect on the catalytic performance. Ru-promotion inhibited the sintering of Ni crystallites, thus enhancing the stability of the promoted catalyst. Moreover, the authors showed that a better performance of both catalysts was achieved when hydrotalcite samples were calcined/reduced in situ, and concluded that calcination prior to the reaction may result in sintering of NiO.

Molybdenum has been as well used in the preparation of Ni-containing bimetallic hydrotalcite-derived catalysts for DRM. The presence of Mo is thought to stabilize Ni-species. Li et al. [181] prepared Ni-Mo/Mg(Al)O hydrotalcite derived catalysts that they further promoted using Ce and Zr. These catalysts showed poor selectivity and were found to be considerably active in the RWGS reaction at 800°C. The however authors confirmed the formation of a complex support of Ce_{0.8}Zr_{0.2}-Mg(Al)O, whose presence was beneficial in terms of catalytic activity. They further stated that the cycling of Ce⁴⁺/Ce³⁺ contributes to the oxidation of carbon deposits at temperatures higher than 900°C, in agreement with the results about Ce promotion discussed previously discussed in this review. No details are however provided regarding the role of Mo in this bimetallic catalyst.

Long et al. [187] investigated the activity of Ni-Co bimetallic hydrotalcite-derived catalysts for DRM. The results showed that the addition of Co in an appropriate amount had a positive effect on the catalytic performance. The catalysts were characterized by XRD, XPS, TEM and N₂ adsorption techniques. The sample with Ni/Co molar ratio equal to 4 showed the highest conversions of CO₂ and CH₄ and a stable performance in DRM at 700°C up to 100h TOS. This was explained by synergetic interactions between Ni and Co, which resulted in the formation of highly dispersed small Ni crystallites. On the contrary, Zhang et al. [183] reported the best performance of Ni-Co hydrotalcite-derived catalysts for Ni/Co molar ratios close to unity. The authors, however, noted that the amount of metals had also effect on the catalyst performance, and catalysts with low content of Ni (1.83-3.61 wt.%) and Co (2.76-4.43 wt.%) showed better performance.

As explained before, Li et al. [181] considered the simultaneous use of Ce and Zr as promoters. Dębek et al. [174,184] also considered the utilisation of Ce, Zr and Ce-Zr as promoters of Ni/Mg/Al hydrotalcite derived catalysts for DRM at low temperatures, i.e. 550°C. The characterization of the materials evidenced that Ce-species were present as a separate phase on the materials surface, while Zr⁴⁺ cations were successfully incorporated into the brucite-like layers of catalysts precursors. The presence of the promoters was found to strongly determine both the activity and the selectivity of these catalysts. The characterization of the spent catalysts showed that Ce addition led to the formation of higher amount of carbon deposits with respect to the non-promoted catalysts. However, the type of carbon deposits formed depended on the promoter used, and lower amounts of undesired graphitic carbon were observed over Ce-promoted samples in comparison to non-promoted catalyst. Moreover, Ce-promoted samples showed lower activity towards direct methane decomposition. Zirconia addition further inhibited this important side reaction, favouring the interaction of methane with CO₂ together with other important parallel reactions, such as reverse Boudouard reaction. Though lower conversions of both methane and CO₂ were measured for Zr-containing samples, almost no carbon was deposited on the catalysts surface upon 5h of DRM reaction at 550°C. Carbon nanotubes were formed upon direct methane decomposition on Ni-containing catalysts. The physicochemical characterization of the catalysts showed the formation of narrower porosity, resulting in higher surface areas for Zr-promoted catalysts. The XRD and TEM measurements confirmed the formation of small Ni crystallites (around 4 nm) in these two catalysts, which were considerably smaller than for the non-promoted sample (around 12 nm). Due to the active site size-selective character of the different reactions involved in DRM, such small Ni crystallites were not active in direct methane decomposition and favoured other side reactions, i.e. reverse Boudouard reaction. Moreover, the presence of Zr was found to promote the adsorption of CO₂ on weak and moderate

strength basic sites, resulting in a favoured interaction of adsorbed CO₂ with methane, and thus enhancing selectivity towards DRM. There is no doubt that the very beneficial effect is connected to the synergetic effect between Zr and Ni species present in HTs brucite-like layers. Zr promotion seems to be the guarantee of stable DRM HTs-derived catalyst, however, further research in this area is still needed.

4.4.6 Conclusions

The present review aims to contain an overview of the recent advances in the use of nickel-containing hydrotalcite-derived catalysts for dry reforming of methane (DRM). The reviewed literature evidences that the catalytic activity, selectivity and stability of such materials is dependent on various factors including: the content of nickel in brucite-like layers, the method of nickel incorporation, the molar ratios of Ni/Mg, Ni/Al and M²⁺/M³⁺ and the use of different promoters. Moreover, the catalytic behaviour strongly depends on the conditions chosen for the calcination and reduction pre-treatment of the catalysts. In general, **hydrotalcite-derived catalyst showed in general high activity and adequate stability** at relatively high temperatures, i.e. above 700°C. However, the formation of carbonaceous deposits was still commonly observed. The extent of carbon formation, coking of the catalyst surface and deactivation depend on the physicochemical features of the catalyst. No general agreement can be found in the literature, about the key properties warranting a good catalytic stability. However, it is generally believed that Ni sintering and/or the presence of bigger Ni particle/crystals enhance direct methane decomposition, resulting in carbon formation. Some works remark that the carbon deposited can be easily removed via oxidation or hydrogasification. **A further evaluation of the consequences of these regeneration thermal treatments on the state and properties of the Ni-phase is needed. The incensement of materials stability in low temperature DRM seems to be the most challenging aspect, as low temperature DRM might be powered by non-emitting energy sources, such as renewables or small nuclear reactors.** The proposed solutions in literature include the use of different promoters, such as Ce, La, Zr, as well as other metals, such as Co and Mo. The presence of these promoters increase nickel-support interactions, preventing in this way sintering of nickel species and inhibiting i C-forming side reactions. Very promising results were obtained for hydrotalcite-derived catalysts containing Zr species in the brucite-like layers. Further research however essential in order to obtain stable and active catalysts, which will enable commercialization of DRM process for chemical valorization of CO₂.

5. Future plans

5.1 Bimetallic hydrotalcite-derived catalyst

As reported in subsection 4.4 the hydrotalcite-derived catalyst were proven to be very effective systems in DRM reaction. However, the research on their application in CO₂ methane reforming needs to be further developed. The recent publications in the topic showed that the addition of a second metal to Ni-containing hydrotalcite-derived materials and obtaining in this way bimetallic catalyst might be one of possible ways of addressing the problem of stability of Ni-based catalysts. Basing on literature review the authors of this report propose the addition of Co, Cu, Fe, Mn or Mo as the second metal. The discussion and literature review regarding similar materials is presented below.

5.1.2 Co, Cu, Fe, Mn, Mo promoters of Ni-based catalysts for dry methane reforming

The theoretical and experimental studies confirmed that Fe and Co themselves are active in catalyzing dry reforming reaction [48,51]. The activity of iron-based catalyst was reported to be higher than that of Ni, however, Fe catalyst is much more prone to coking [52].

Long et al. [187] investigated Ni-Co bimetallic hydrotalcite-derived catalysts in DRM. The results showed that the addition of an appropriate amount of Co had a positive effect on catalyst performance. The sample with Ni/Co molar ratio equal to 4 showed the highest conversions of CO₂ and CH₄ and a stable performance in DRM at 700°C up to 100h TOS. This was explained by synergetic interactions between Ni and Co, which resulted in the formation of highly dispersed small Ni crystallites. On the contrary, Zhang et al. [183] reported the best performance of Ni-Co hydrotalcite-derived catalysts for Ni/Co molar ratios close to unity. The authors noted, however, that the amount of metals also affected the catalyst performance, and the catalysts with low content of Ni (1.83-3.61 wt.%) and Co (2.76-4.43 wt.%) showed better performance.

The effect of Cu promotion on Ni clay-based catalyst was investigated by Liu et al. [188]. The Cu-promoted catalyst showed much higher conversions of CH₄ and CO₂ than Fe-promoted and unpromoted materials. This was attributed to the activity of copper in reverse water gas shift reaction and methanol synthesis process, which may influence overall DRM activity. On the other hand, the authors observed decreased basicity of Cu-promoted catalysts, which may influence deposition of carbon deposits. Ashok et al. [189] investigated Ni/Cu/Al hydrotalcites for direct methane decomposition. Their studies showed that the addition of copper inhibited the tested reaction. Thus, the addition of Cu into hydrotalcites may increase their resistance to coking.

Ni-Fe/MgAl₂O₄ catalysts for CO₂ methane reforming were studied by Theofanidis et al. [190,191]. The Fe promoted material showed higher resistance to coking than the unpromoted sample. The authors explained this phenomenon by redox properties of Fe₂O₃, as upon DRM reaction FeO_x species were formed which helped to oxidize carbon deposits by iron oxide lattice oxygen.

Mn-promotion was investigated by Gou et al. [192] on Ni-Mn/Al₂O₃ catalyst. The Mn promotion increased CH₄ conversion by 10% and decreased catalyst deactivation rate with respect to the unpromoted catalyst. Additionally, Mn addition increased basicity of the materials which may explain increased coking resistance ability of Mn-promoted sample. On the other hand, Yao et al. [122] observed that the addition of Mn to Ni/SiO₂ catalyst promoted the dispersion of Ni species leading to smaller particle size of NiO on the fresh Ni/SiO₂ catalyst. Additionally, the authors also observed the formation of NiMnO₄ spinel phase, which increased interactions between nickel and support. Similar results were reported by Touahra et al. [193] for Mn promoted Ni/Al hydrotalcite-derived catalysts. In general, all authors attributed enhanced catalytic performance of Ni-Mn catalysts to the formation of MnO_x species, which exhibit multiple valence states with a superior performance in oxidation-reduction cycles. Thus lattice oxygen of MnO_x may participate in the oxidation of carbon deposits increasing in this way both activity and stability.

Mo-promotion of Ni/Al₂O₃ catalyst for propane dry reforming showed stable performance of such material, which was attributed to the anti-coking properties of molybdenum [194]. These results were

confirmed by the study of Yao et al. [195] who investigated Ni-Mn/Al₂O₃ catalyst in methane dry reforming. The authors observed that the Mo promotion effect was greatly dependent on the applied reduction temperature which affected the formation of either Ni-Mo alloy or Ni⁰ separated phase. For the catalyst reduced at 700°C the formation of Ni⁰ separate phase and enhanced activity were observed.

As it was presented above there is a huge potential in the application of bimetallic catalysts in CO₂ utilization processes. However, there are still a lot of questions and open problems, such as: (i) how introduction of second metal to Ni-based catalyst influence its surface properties (acidity, basicity, as well as their balance, porosity, dispersion of nickel species), (ii) how the effect of addition of second metal is influenced by the method of catalyst preparation, (iii) how stability of the materials is influenced during long-term stability tests, (iv) how to increase activity of CO₂ methanation catalysts at low reaction temperatures and (v) how the regeneration of DRM catalysts influences its performance? The answer to these questions is of high scientific value, as it may, firstly, allow to tailor the properties of hydrotalcite-like materials, which may lead to their new applications, and, secondly, will result in novel materials of definite, combined properties. The mentioned properties were until now selectively introduced into such materials.

5.2 Long-term stability tests and catalysts regeneration

Another important aspect of the research concerns the determination of the thermal stability and catalytic stability of the hydrotalcite-derived materials in long stability tests and the possibility of their **regeneration**. These tests will be performed for selected samples, which show the best catalytic performance.

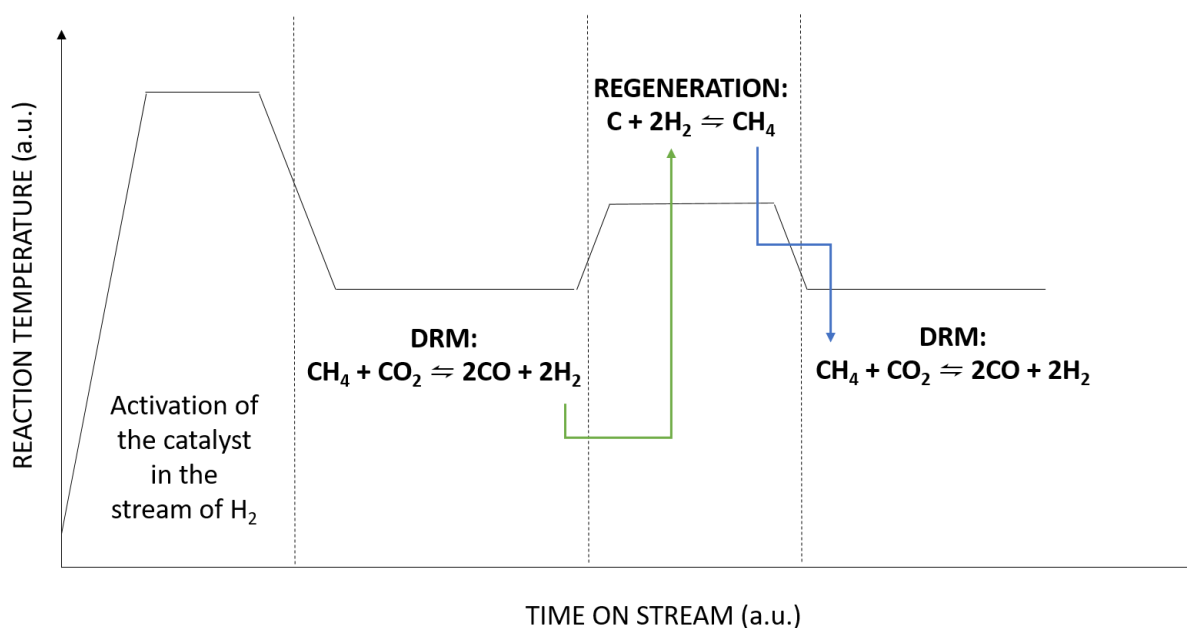


Fig. 11 Schematic representation of the combined DRM/hydrogenation cycles

The catalytic stability is crucial in potential industrial applications. This is particularly important for the dry reforming process, where the deactivation of the catalysts due to carbon deposit formation is the main factor limiting the introduction of the process on industrial scale. The presented research on nickel-based catalysts applied in DRM showed that although the application of the second metal increased materials stability, the carbon species were still formed. It seems thus that the coking of dry reforming catalyst is inevitable. One of the possible solution to that problem might be to combine stability tests with regeneration cycles through hydrogenation of the carbon deposits. This method was proposed by Abdelsadek et al. [155] for Ni/Al hydrotalcite catalysts. The regeneration of catalyst surface by gasification of carbonaceous deposits may be realized via application of several gasification agents i.e. O₂, CO₂, CO, H₂O and H₂. The work of Theofanidis et al. [190] showed that complete gasification of coke by CO₂ is not possible due to thermodynamic limitations. On the other hand, gasification with O₂ results in oxidation of Ni species, which generates the need of catalyst

reduction before next dry reforming cycle. Therefore, the **gasification by H₂** seems to be the most beneficial because:

- (i) hydrogen is the product of DRM and may be recycled to the reactor for regeneration,
- (ii) hydrogen as the reducing agent may also reduce NiO species, increasing in this way catalyst activity, and
- (iii) the product of coke hydrogenation is methane, which may be recycled to the reactor for dry reforming cycle or burnt in order to power endothermic DRM.

The schematic representation of the DRM/regeneration cycles is shown in Fig. 11. Since there is very few studies on this subject, the research in this area will greatly increase the knowledge about regeneration of DRM catalysts and may contribute to the development of science in the field of new (novel) materials.

- [24] M. Halmann, A. Steinfeld, Thermoneutral tri-reforming of flue gases from coal- and gas-fired power stations, *Catal. Today*. 115 (2006) 170–178. doi:10.1016/j.cattod.2006.02.064.
- [25] M. Halmann, A. Steinfeld, Fuel saving, carbon dioxide emission avoidance, and syngas production by tri-reforming of flue gases from coal- and gas-fired power stations, and by the carbothermic reduction of iron oxide, *Energy*. 31 (2006) 3171–3185. doi:10.1016/j.energy.2006.03.009.
- [26] L. Pino, A. Vita, F. Cipiti, M. Laganà, V. Recupero, Hydrogen production by methane tri-reforming process over Ni–ceria catalysts: Effect of La-doping, *Appl. Catal. B Environ.* 104 (2011) 64–73. doi:10.1016/j.apcatb.2011.02.027.
- [27] C. Song, W. Pan, Tri-reforming of methane: a novel concept for catalytic production of industrially useful synthesis gas with desired H₂/CO ratios, *Catal. Today*. 98 (2004) 463–484. doi:10.1016/j.cattod.2004.09.054.
- [28] P.M. Mortensen, I. Dybkjær, Industrial scale experience on steam reforming of CO₂-rich gas, *Appl. Catal. Gen.* 495 (2015) 141–151. doi:10.1016/j.apcata.2015.02.022.
- [29] L. Więclaw-Solny, Łabojko, G., Babiński, P., Możliwości przemysłowego wykorzystania ditlenku węgla - badania nad zastosowaniem CO₂ w procesie otrzymywania gazu syntezowego, *Polityka Energ.* 12 (2009).
- [30] R.E. Reitmeier, K. Atwood, H. Bennett, H. Baugh, Production of Synthetic Gas - Reaction of Light Hydrocarbons with Steam and Carbon Dioxide, *Ind. Eng. Chem.* 40 (1948) 620–626. doi:10.1021/ie50460a010.
- [31] C. Teuner, Neumann, P., Von Linde, F., The Calcor Standard and Calcor Economy Processes, *Oil Gas Eur. Mag.* 3 (2001) 44–46.
- [32] 40 years in catalysis, *Catal. Today*. 111 (2006) 4–11. doi:10.1016/j.cattod.2005.10.016.
- [33] J.T. Richardson, S.A. Paripatyadar, Carbon dioxide reforming of methane with supported rhodium, *Appl. Catal.* 61 (1990) 293–309. doi:10.1016/S0166-9834(00)82152-1.
- [34] J.H. McCrary, G.E. McCrary, T.A. Chubb, J.J. Nemecek, D.E. Simmons, An experimental study of the CO₂–CH₄ reforming-methanation cycle as a mechanism for converting and transporting solar energy, *Sol. Energy*. 29 (1982) 141–151. doi:10.1016/0038-092X(82)90176-1.
- [35] T.A. Chubb, Characteristics of CO₂–CH₄ reforming-methanation cycle relevant to the solchem thermochemical power system, *Sol. Energy*. 24 (1980) 341–345. doi:10.1016/0038-092X(80)90295-9.
- [36] M.K. Nikoo, N.A.S. Amin, Thermodynamic analysis of carbon dioxide reforming of methane in view of solid carbon formation, *Fuel Process. Technol.* 92 (2011) 678–691. doi:10.1016/j.fuproc.2010.11.027.
- [37] I. Istadi, Nor Aishah Saidina Amin, Co-Generation of C₂ Hydrocarbons and Synthesis Gases from Methane and Carbon Dioxide: a Thermodynamic Analysis, *J. Nat. Gas Chem.* 14 (2005) 140–150.
- [38] Y. Li, Y. Wang, X. Zhang, Z. Mi, Thermodynamic analysis of autothermal steam and CO₂ reforming of methane, *Int. J. Hydrog. Energy*. 33 (2008) 2507–2514. doi:10.1016/j.ijhydene.2008.02.051.
- [39] R.Y. Chein, Y.C. Chen, C.T. Yu, J.N. Chung, Thermodynamic analysis of dry reforming of CH₄ with CO₂ at high pressures, *J. Nat. Gas Sci. Eng.* 26 (2015) 617–629. doi:10.1016/j.jngse.2015.07.001.
- [40] A. Shamsi, C.D. Johnson, Effect of pressure on the carbon deposition route in CO₂ reforming of 13CH₄, *Catal. Today*. 84 (2003) 17–25. doi:10.1016/S0920-5861(03)00296-7.
- [41] Y. Sun, T. Ritchie, S.S. Hla, S. McEvoy, W. Stein, J.H. Edwards, Thermodynamic analysis of mixed and dry reforming of methane for solar thermal applications, *J. Nat. Gas Chem.* 20 (2011) 568–576. doi:10.1016/S1003-9953(10)60235-6.
- [42] M.A. Soria, C. Mateos-Pedrero, A. Guerrero-Ruiz, I. Rodríguez-Ramos, Thermodynamic and experimental study of combined dry and steam reforming of methane on Ru/ ZrO₂-La₂O₃ catalyst at low temperature, *Int. J. Hydrog. Energy*. 36 (2011) 15212–15220. doi:10.1016/j.ijhydene.2011.08.117.
- [43] Ş. Özkara-Aydinoğlu, Thermodynamic equilibrium analysis of combined carbon dioxide reforming with steam reforming of methane to synthesis gas, *Int. J. Hydrog. Energy*. 35 (2010) 12821–12828. doi:10.1016/j.ijhydene.2010.08.134.
- [44] X. Wang, N. Wang, J. Zhao, L. Wang, Thermodynamic analysis of propane dry and steam reforming for synthesis gas or hydrogen production, *Int. J. Hydrog. Energy*. 35 (2010) 12800–12807. doi:10.1016/j.ijhydene.2010.08.132.
- [45] F. Solymosi, G. Kutsán, A. Erdöhelyi, Catalytic reaction of CH₄ with CO₂ over alumina-supported Pt metals, *Catal. Lett.* 11 (1991) 149–156. doi:10.1007/BF00764080.
- [46] A.T. Ashcroft, A.K. Cheetham, J.S. Foord, M.L.H. Green, C.P. Grey, A.J. Murrell, P.D.F. Vernon, Selective oxidation of methane to synthesis gas using transition metal catalysts, *Nature*. 344 (1990) 319. doi:10.1038/344319a0.

- [47] S. Barama, C. Dupeyrat-Batiot, M. Capron, E. Bordes-Richard, O. Bakhti-Mohammedi, Catalytic properties of Rh, Ni, Pd and Ce supported on Al-pillared montmorillonites in dry reforming of methane, *Catal. Today*. 141 (2009) 385–392. doi:10.1016/j.cattod.2008.06.025.
- [48] Z. Hou, P. Chen, H. Fang, X. Zheng, T. Yashima, Production of synthesis gas via methane reforming with CO₂ on noble metals and small amount of noble-(Rh-) promoted Ni catalysts, *Int. J. Hydrog. Energy*. 31 (2006) 555–561. doi:10.1016/j.ijhydene.2005.06.010.
- [49] J.R. Rostrupnielsen, J.H.B. Hansen, CO₂-Reforming of Methane over Transition Metals, *J. Catal.* 144 (1993) 38–49. doi:10.1006/jcat.1993.1312.
- [50] A.I. Tsyganok, M. Inaba, T. Tsunoda, S. Hamakawa, K. Suzuki, T. Hayakawa, Dry reforming of methane over supported noble metals: a novel approach to preparing catalysts, *Catal. Commun.* 4 (2003) 493–498. doi:10.1016/S1566-7367(03)00130-4.
- [51] K. Asami, X. Li, K. Fujimoto, Y. Koyama, A. Sakurama, N. Kometani, Y. Yonezawa, CO₂ reforming of CH₄ over ceria-supported metal catalysts, *Catal. Today*. 84 (2003) 27–31. doi:10.1016/S0920-5861(03)00297-9.
- [52] M.J. Hei, H.B. Chen, J. Yi, Y.J. Lin, Y.Z. Lin, G. Wei, D.W. Liao, CO₂-reforming of methane on transition metal surfaces, *Surf. Sci.* 417 (1998) 82–96. doi:10.1016/S0039-6028(98)00663-3.
- [53] A.T. Ashcroft, A.K. Cheetham, M.L.H. Green, P.D.F. Vernon, Partial oxidation of methane to synthesis gas using carbon dioxide, *Nature*. 352 (1991) 225. doi:10.1038/352225a0.
- [54] P.D.F. Vernon, M.L.H. Green, A.K. Cheetham, A.T. Ashcroft, Partial oxidation of methane to synthesis gas, and carbon dioxide as an oxidising agent for methane conversion, *Catal. Today*. 13 (1992) 417–426. doi:10.1016/0920-5861(92)80167-L.
- [55] Y.H. Hu, E. Ruckenstein, Catalytic Conversion of Methane to Synthesis Gas by Partial Oxidation and CO₂ Reforming, in: *Adv. Catal.*, Academic Press, 2004: pp. 297–345. doi:10.1016/S0360-0564(04)48004-3.
- [56] Y.H. Hu, *Advances in Catalysts for CO₂ Reforming of Methane*, in: *Adv. CO₂ Convers. Util.*, American Chemical Society, 2010: pp. 155–174. doi:10.1021/bk-2010-1056.ch010.
- [57] V.C.H. Kroll, H.M. Swaan, C. Mirodatos, Methane Reforming Reaction with Carbon Dioxide Over Ni/SiO₂Catalyst: I. Deactivation Studies, *J. Catal.* 161 (1996) 409–422. doi:10.1006/jcat.1996.0199.
- [58] H. Ay, D. Üner, Dry reforming of methane over CeO₂ supported Ni, Co and Ni–Co catalysts, *Appl. Catal. B Environ.* 179 (2015) 128–138. doi:10.1016/j.apcatb.2015.05.013.
- [59] J.H. Edwards, A.M. Maitra, The chemistry of methane reforming with carbon dioxide and its current and potential applications, *Fuel Process. Technol.* 42 (1995) 269–289. doi:10.1016/0378-3820(94)00105-3.
- [60] S. Wang, G.Q. (Max) Lu, G.J. Millar, Carbon Dioxide Reforming of Methane To Produce Synthesis Gas over Metal-Supported Catalysts: State of the Art, *Energy Fuels*. 10 (1996) 896–904. doi:10.1021/ef950227t.
- [61] M.-S. Fan, A.Z. Abdullah, S. Bhatia, Catalytic Technology for Carbon Dioxide Reforming of Methane to Synthesis Gas, *ChemCatChem*. 1 (2009) 192–208. doi:10.1002/cctc.200900025.
- [62] M. Usman, W.M.A. Wan Daud, H.F. Abbas, Dry reforming of methane: Influence of process parameters—A review, *Renew. Sustain. Energy Rev.* 45 (2015) 710–744. doi:10.1016/j.rser.2015.02.026.
- [63] B. Abdullah, N.A. Abd Ghani, D.-V.N. Vo, Recent advances in dry reforming of methane over Ni-based catalysts, *J. Clean. Prod.* 162 (2017) 170–185. doi:10.1016/j.jclepro.2017.05.176.
- [64] Y. Wang, L. Yao, S. Wang, D. Mao, C. Hu, Low-temperature catalytic CO₂ dry reforming of methane on Ni-based catalysts: A review, *Fuel Process. Technol.* 169 (2018) 199–206. doi:10.1016/j.fuproc.2017.10.007.
- [65] N.A.K. Aramouni, J.G. Touma, B.A. Tarboush, J. Zeaiter, M.N. Ahmad, Catalyst design for dry reforming of methane: Analysis review, *Renew. Sustain. Energy Rev.* 82 (2018) 2570–2585. doi:10.1016/j.rser.2017.09.076.
- [66] A. Becerra, M. Dimitrijewits, C. Arciprete, A.C. Luna, Stable Ni/Al₂O₃ catalysts for methane dry reforming, *Granul. Matter.* 3 (2001) 79–81. doi:10.1007/PL00010890.
- [67] J.-H. Kim, D.J. Suh, T.-J. Park, K.-L. Kim, Effect of metal particle size on coking during CO₂ reforming of CH₄ over Ni–alumina aerogel catalysts, *Appl. Catal. Gen.* 197 (2000) 191–200. doi:10.1016/S0926-860X(99)00487-1.
- [68] Y. Chen, J. Ren, Conversion of methane and carbon dioxide into synthesis gas over alumina-supported nickel catalysts. Effect of Ni–Al₂O₃ interactions, *Catal. Lett.* 29 (1994) 39–48. doi:10.1007/BF00814250.
- [69] A. Bhattacharyya, V.W. Chang, CO₂ Reforming of Methane to Syngas: Deactivation Behavior of Nickel Aluminate Spinel Catalysts, in: B. Delmon, G.F. Froment (Eds.), *Stud. Surf. Sci. Catal.*, Elsevier, 1994: pp. 207–213. doi:10.1016/S0167-2991(08)62742-1.

- [70] E. Baktash, P. Littlewood, R. Schomäcker, A. Thomas, P.C. Stair, Alumina coated nickel nanoparticles as a highly active catalyst for dry reforming of methane, *Appl. Catal. B Environ.* 179 (2015) 122–127. doi:10.1016/j.apcatb.2015.05.018.
- [71] M.A. Goula, N.D. Charisiou, K.N. Papageridis, A. Delimitis, E. Pachatouridou, E.F. Iliopoulou, Nickel on alumina catalysts for the production of hydrogen rich mixtures via the biogas dry reforming reaction: Influence of the synthesis method, *Int. J. Hydrog. Energy.* 40 (2015) 9183–9200. doi:10.1016/j.ijhydene.2015.05.129.
- [72] S. Wang, G.Q. (Max) Lu, Role of CeO₂ in Ni/CeO₂–Al₂O₃ catalysts for carbon dioxide reforming of methane, *Appl. Catal. B Environ.* 19 (1998) 267–277. doi:10.1016/S0926-3373(98)00081-2.
- [73] L. Li, L. Zhang, Y. Zhang, J. Li, Effect of Ni loadings on the catalytic properties of Ni/MgO(111) catalyst for the reforming of methane with carbon dioxide, *J. Fuel Chem. Technol.* 43 (2015) 315–322. doi:10.1016/S1872-5813(15)30007-4.
- [74] F. Frusteri, L. Spadaro, F. Arena, A. Chuvilin, TEM evidence for factors affecting the genesis of carbon species on bare and K-promoted Ni/MgO catalysts during the dry reforming of methane, *Carbon.* 40 (2002) 1063–1070. doi:10.1016/S0008-6223(01)00243-3.
- [75] R. Zanganeh, M. Rezaei, A. Zamaniyan, Preparation of nanocrystalline NiO–MgO solid solution powders as catalyst for methane reforming with carbon dioxide: Effect of preparation conditions, *Adv. Powder Technol.* 25 (2014) 1111–1117. doi:10.1016/j.appt.2014.02.015.
- [76] R. Zanganeh, M. Rezaei, A. Zamaniyan, Dry reforming of methane to synthesis gas on NiO–MgO nanocrystalline solid solution catalysts, *Int. J. Hydrog. Energy.* 38 (2013) 3012–3018. doi:10.1016/j.ijhydene.2012.12.089.
- [77] M. Jafarbegloo, A. Tarlani, A.W. Mesbah, S. Sahebdehfar, One-pot synthesis of NiO–MgO nanocatalysts for CO₂ reforming of methane: The influence of active metal content on catalytic performance, *J. Nat. Gas Sci. Eng.* 27 (2015) 1165–1173. doi:10.1016/j.jngse.2015.09.065.
- [78] M. Khajenoori, M. Rezaei, F. Meshkani, Dry reforming over CeO₂-promoted Ni/MgO nano-catalyst: Effect of Ni loading and CH₄/CO₂ molar ratio, *J. Ind. Eng. Chem.* 21 (2015) 717–722. doi:10.1016/j.jiec.2014.03.043.
- [79] M. Yu, Y.-A. Zhu, Y. Lu, G. Tong, K. Zhu, X. Zhou, The promoting role of Ag in Ni-CeO₂ catalyzed CH₄-CO₂ dry reforming reaction, *Appl. Catal. B Environ.* 165 (2015) 43–56. doi:10.1016/j.apcatb.2014.09.066.
- [80] X. Du, D. Zhang, L. Shi, R. Gao, J. Zhang, Morphology Dependence of Catalytic Properties of Ni/CeO₂ Nanostructures for Carbon Dioxide Reforming of Methane, *J. Phys. Chem. C.* 116 (2012) 10009–10016. doi:10.1021/jp300543r.
- [81] T. Odedairo, J. Chen, Z. Zhu, Metal–support interface of a novel Ni–CeO₂ catalyst for dry reforming of methane, *Catal. Commun.* 31 (2013) 25–31. doi:10.1016/j.catcom.2012.11.008.
- [82] M. Németh, Z. Schay, D. Srankó, J. Károlyi, G. Sáfrán, I. Sajó, A. Horváth, Impregnated Ni/ZrO₂ and Pt/ZrO₂ catalysts in dry reforming of methane: Activity tests in excess methane and mechanistic studies with labeled ¹³CO₂, *Appl. Catal. Gen.* 504 (2015) 608–620. doi:10.1016/j.apcata.2015.04.006.
- [83] F. Huang, R. Wang, C. Yang, H. Driss, W. Chu, H. Zhang, Catalytic performances of Ni/mesoporous SiO₂ catalysts for dry reforming of methane to hydrogen, *J. Energy Chem.* 25 (2016) 709–719. doi:10.1016/j.jechem.2016.03.004.
- [84] J. Zhang, F. Li, Coke-resistant Ni@SiO₂ catalyst for dry reforming of methane, *Appl. Catal. B Environ.* 176–177 (2015) 513–521. doi:10.1016/j.apcatb.2015.04.039.
- [85] A. Albarazi, P. Beaunier, P. Da Costa, Hydrogen and syngas production by methane dry reforming on SBA-15 supported nickel catalysts: On the effect of promotion by Ce_{0.75}Zr_{0.25}O₂ mixed oxide, *Int. J. Hydrog. Energy.* 38 (2013) 127–139. doi:10.1016/j.ijhydene.2012.10.063.
- [86] Z. Zhang, X.E. Verykios, Carbon dioxide reforming of methane to synthesis gas over Ni/La₂O₃ catalysts, *Appl. Catal. Gen.* 138 (1996) 109–133. doi:10.1016/0926-860X(95)00238-3.
- [87] S.S. Kim, S.M. Lee, J.M. Won, H.J. Yang, S.C. Hong, Effect of Ce/Ti ratio on the catalytic activity and stability of Ni/CeO₂–TiO₂ catalyst for dry reforming of methane, *Chem. Eng. J.* 280 (2015) 433–440. doi:10.1016/j.cej.2015.06.027.
- [88] J.-E. Min, Y.-J. Lee, H.-G. Park, C. Zhang, K.-W. Jun, Carbon dioxide reforming of methane on Ni–MgO–Al₂O₃ catalysts prepared by sol–gel method: Effects of Mg/Al ratios, *J. Ind. Eng. Chem.* 26 (2015) 375–383. doi:10.1016/j.jiec.2014.12.012.
- [89] L. Xu, H. Song, L. Chou, Ordered mesoporous MgO–Al₂O₃ composite oxides supported Ni based catalysts for CO₂ reforming of CH₄: Effects of basic modifier and mesopore structure, *Int. J. Hydrog. Energy.* 38 (2013) 7307–7325. doi:10.1016/j.ijhydene.2013.04.034.

- [90] Z. Alipour, M. Rezaei, F. Meshkani, Effect of Ni loadings on the activity and coke formation of MgO-modified Ni/Al₂O₃ nanocatalyst in dry reforming of methane, *J. Energy Chem.* 23 (2014) 633–638. doi:10.1016/S2095-4956(14)60194-7.
- [91] M. Abdollahifar, M. Haghghi, A.A. Babaluo, Syngas production via dry reforming of methane over Ni/Al₂O₃–MgO nanocatalyst synthesized using ultrasound energy, *J. Ind. Eng. Chem.* 20 (2014) 1845–1851. doi:10.1016/j.jiec.2013.08.041.
- [92] M. Radlik, M. Adamowska-Teyssier, A. Krztoń, K. Kozieł, W. Krajewski, W. Turek, P. Da Costa, Dry reforming of methane over Ni/Ce_{0.62}Zr_{0.38}O₂ catalysts: Effect of Ni loading on the catalytic activity and on H₂/CO production, *Comptes Rendus Chim.* 18 (2015) 1242–1249. doi:10.1016/j.crci.2015.03.008.
- [93] A. Kambolis, H. Matralis, A. Trovarelli, C. Papadopoulou, Ni/CeO₂–ZrO₂ catalysts for the dry reforming of methane, *Appl. Catal. Gen.* 377 (2010) 16–26. doi:10.1016/j.apcata.2010.01.013.
- [94] I. Luisetto, S. Tuti, C. Battocchio, S. Lo Mastro, A. Sodo, Ni/CeO₂–Al₂O₃ catalysts for the dry reforming of methane: The effect of CeAlO₃ content and nickel crystallite size on catalytic activity and coke resistance, *Appl. Catal. Gen.* 500 (2015) 12–22. doi:10.1016/j.apcata.2015.05.004.
- [95] A. Luengnaruemitchai, A. Kaengsilalai, Activity of different zeolite-supported Ni catalysts for methane reforming with carbon dioxide, *Chem. Eng. J.* 144 (2008) 96–102. doi:10.1016/j.cej.2008.05.023.
- [96] W. Nimwattanukul, A. Luengnaruemitchai, S. Jitkarnka, Potential of Ni supported on clinoptilolite catalysts for carbon dioxide reforming of methane, *Int. J. Hydrog. Energy.* 31 (2006) 93–100. doi:10.1016/j.ijhydene.2005.02.005.
- [97] K. Jabbour, N. El Hassan, A. Davidson, P. Massiani, S. Casale, Characterizations and performances of Ni/diatomite catalysts for dry reforming of methane, *Chem. Eng. J.* 264 (2015) 351–358. doi:10.1016/j.cej.2014.11.109.
- [98] Y. Liu, Z. He, L. Zhou, Z. Hou, W. Eli, Simultaneous oxidative conversion and CO₂ reforming of methane to syngas over Ni/vermiculite catalysts, *Catal. Commun.* 42 (2013) 40–44. doi:10.1016/j.catcom.2013.07.034.
- [99] C.E. Daza, A. Kiennemann, S. Moreno, R. Molina, Dry reforming of methane using Ni–Ce catalysts supported on a modified mineral clay, *Appl. Catal. Gen.* 364 (2009) 65–74. doi:10.1016/j.apcata.2009.05.029.
- [100] Q. Ma, D. Wang, M. Wu, T. Zhao, Y. Yoneyama, N. Tsubaki, Effect of catalytic site position: Nickel nanocatalyst selectively loaded inside or outside carbon nanotubes for methane dry reforming, *Fuel.* 108 (2013) 430–438. doi:10.1016/j.fuel.2012.12.028.
- [101] F. Pompeo, N.N. Nichio, O.A. Ferretti, D. Resasco, Study of Ni catalysts on different supports to obtain synthesis gas, *Int. J. Hydrog. Energy.* 30 (2005) 1399–1405. doi:10.1016/j.ijhydene.2004.10.004.
- [102] M.E. Gálvez, A. Albarazi, P. Da Costa, Enhanced catalytic stability through non-conventional synthesis of Ni/SBA-15 for methane dry reforming at low temperatures, *Appl. Catal. Gen.* 504 (2015) 143–150. doi:10.1016/j.apcata.2014.10.026.
- [103] M.C.J. Bradford, M.A. Vannice, Catalytic reforming of methane with carbon dioxide over nickel catalysts I. Catalyst characterization and activity, *Appl. Catal. Gen.* 142 (1996) 73–96. doi:10.1016/0926-860X(96)00065-8.
- [104] K. Tomishige, O. Yamazaki, Y. Chen, K. Yokoyama, X. Li, K. Fujimoto, Development of ultra-stable Ni catalysts for CO₂ reforming of methane, *Catal. Today.* 45 (1998) 35–39. doi:10.1016/S0920-5861(98)00238-7.
- [105] K.-M. Kang, H.-W. Kim, I.-W. Shim, H.-Y. Kwak, Catalytic test of supported Ni catalysts with core/shell structure for dry reforming of methane, *Fuel Process. Technol.* 92 (2011) 1236–1243. doi:10.1016/j.fuproc.2011.02.007.
- [106] S. Khajeh Talkhonchek, M. Haghghi, Syngas production via dry reforming of methane over Ni-based nanocatalyst over various supports of clinoptilolite, ceria and alumina, *J. Nat. Gas Sci. Eng.* 23 (2015) 16–25. doi:10.1016/j.jngse.2015.01.020.
- [107] M.C.J. Bradford, M.A. Vannice, Catalytic reforming of methane with carbon dioxide over nickel catalysts II. Reaction kinetics, *Appl. Catal. Gen.* 142 (1996) 97–122. doi:10.1016/0926-860X(96)00066-X.
- [108] T. Osaki, H. Masuda, T. Mori, Intermediate hydrocarbon species for the CO₂–CH₄ reaction on supported Ni catalysts, *Catal. Lett.* 29 (1994) 33–37. doi:10.1007/BF00814249.
- [109] S. Damyanova, B. Pawelec, K. Arishtirova, J.L.G. Fierro, Ni-based catalysts for reforming of methane with CO₂, *Int. J. Hydrog. Energy.* 37 (2012) 15966–15975. doi:10.1016/j.ijhydene.2012.08.056.
- [110] R. Zhang, G. Xia, M. Li, Y. Wu, H. Nie, D. Li, Effect of support on the performance of Ni-based catalyst in methane dry reforming, *J. Fuel Chem. Technol.* 43 (2015) 1359–1365. doi:10.1016/S1872-5813(15)30040-2.

- [111] M.M. Barroso-Quiroga, A.E. Castro-Luna, Catalytic activity and effect of modifiers on Ni-based catalysts for the dry reforming of methane, *Int. J. Hydrog. Energy*. 35 (2010) 6052–6056. doi:10.1016/j.ijhydene.2009.12.073.
- [112] T. Osaki, T. Mori, Role of Potassium in Carbon-Free CO₂ Reforming of Methane on K-Promoted Ni/Al₂O₃ Catalysts, *J. Catal.* 204 (2001) 89–97. doi:10.1006/jcat.2001.3382.
- [113] J. Juan-Juan, M.C. Román-Martínez, M.J. Illán-Gómez, Effect of potassium content in the activity of K-promoted Ni/Al₂O₃ catalysts for the dry reforming of methane, *Appl. Catal. Gen.* 301 (2006) 9–15. doi:10.1016/j.apcata.2005.11.006.
- [114] S. Sengupta, G. Deo, Modifying alumina with CaO or MgO in supported Ni and Ni–Co catalysts and its effect on dry reforming of CH₄, *J. CO₂ Util.* 10 (2015) 67–77. doi:10.1016/j.jcou.2015.04.003.
- [115] Z.-F. Yan, R.-G. Ding, X.-M. Liu, L.-H. Song, Promotion Effects of Nickel Catalysts of Dry Reforming with Methane, *Chin. J. Chem.* 19 (2001) 738–744. doi:10.1002/cjoc.20010190806.
- [116] M. García-Diéguez, C. Herrera, M.Á. Larrubia, L.J. Alemany, CO₂-reforming of natural gas components over a highly stable and selective NiMg/Al₂O₃ nanocatalyst, *Catal. Today*. 197 (2012) 50–57. doi:10.1016/j.cattod.2012.06.019.
- [117] Z.L. Zhang, X.E. Verykios, Carbon dioxide reforming of methane to synthesis gas over supported Ni catalysts, *Catal. Today*. 21 (1994) 589–595. doi:10.1016/0920-5861(94)80183-5.
- [118] M. García-Diéguez, M.C. Herrera, I.S. Pieta, M.A. Larrubia, L.J. Alemany, NiBa catalysts for CO₂-reforming of methane, *Catal. Commun.* 11 (2010) 1133–1136. doi:10.1016/j.catcom.2010.06.008.
- [119] M.-N. Kaydouh, N. El Hassan, A. Davidson, S. Casale, H. El Zakhem, P. Massiani, Effect of the order of Ni and Ce addition in SBA-15 on the activity in dry reforming of methane, *Comptes Rendus Chim.* 18 (2015) 293–301. doi:10.1016/j.crci.2015.01.004.
- [120] F. Pompeo, N.N. Nichio, M.M.V.M. Souza, D.V. Cesar, O.A. Ferretti, M. Schmal, Study of Ni and Pt catalysts supported on α -Al₂O₃ and ZrO₂ applied in methane reforming with CO₂, *Appl. Catal. Gen.* 316 (2007) 175–183. doi:10.1016/j.apcata.2006.09.007.
- [121] L. Yao, J. Shi, H. Xu, W. Shen, C. Hu, Low-temperature CO₂ reforming of methane on Zr-promoted Ni/SiO₂ catalyst, *Fuel Process. Technol.* 144 (2016) 1–7. doi:10.1016/j.fuproc.2015.12.009.
- [122] L. Yao, J. Zhu, X. Peng, D. Tong, C. Hu, Comparative study on the promotion effect of Mn and Zr on the stability of Ni/SiO₂ catalyst for CO₂ reforming of methane, *Int. J. Hydrog. Energy*. 38 (2013) 7268–7279. doi:10.1016/j.ijhydene.2013.02.126.
- [123] A. Albarazi, M.E. Gálvez, P. Da Costa, Synthesis strategies of ceria–zirconia doped Ni/SBA-15 catalysts for methane dry reforming, *Catal. Commun.* 59 (2015) 108–112. doi:10.1016/j.catcom.2014.09.050.
- [124] J. Zhu, X. Peng, L. Yao, J. Shen, D. Tong, C. Hu, The promoting effect of La, Mg, Co and Zn on the activity and stability of Ni/SiO₂ catalyst for CO₂ reforming of methane, *Int. J. Hydrog. Energy*. 36 (2011) 7094–7104. doi:10.1016/j.ijhydene.2011.02.133.
- [125] I. Luisetto, S. Tuti, E. Di Bartolomeo, Co and Ni supported on CeO₂ as selective bimetallic catalyst for dry reforming of methane, *Int. J. Hydrog. Energy*. 37 (2012) 15992–15999. doi:10.1016/j.ijhydene.2012.08.006.
- [126] J. Estephane, S. Aouad, S. Hany, B. El Khoury, C. Gennequin, H. El Zakhem, J. El Nakat, A. Aboukaïs, E. Abi Aad, CO₂ reforming of methane over Ni–Co/ZSM5 catalysts. Aging and carbon deposition study, *Int. J. Hydrog. Energy*. 40 (2015) 9201–9208. doi:10.1016/j.ijhydene.2015.05.147.
- [127] H.-W. Chen, C.-Y. Wang, C.-H. Yu, L.-T. Tseng, P.-H. Liao, Carbon dioxide reforming of methane reaction catalyzed by stable nickel copper catalysts, *Catal. Today*. 97 (2004) 173–180. doi:10.1016/j.cattod.2004.03.067.
- [128] B. Koubaissy, A. Pietraszek, A.C. Roger, A. Kiennemann, CO₂ reforming of methane over Ce-Zr-Ni-Me mixed catalysts, *Catal. Today*. 157 (2010) 436–439. doi:10.1016/j.cattod.2010.01.050.
- [129] F. Meshkani, M. Rezaei, Nanocrystalline MgO supported nickel-based bimetallic catalysts for carbon dioxide reforming of methane, *Int. J. Hydrog. Energy*. 35 (2010) 10295–10301. doi:10.1016/j.ijhydene.2010.07.138.
- [130] M. García-Diéguez, E. Finocchio, M.Á. Larrubia, L.J. Alemany, G. Busca, Characterization of alumina-supported Pt, Ni and PtNi alloy catalysts for the dry reforming of methane, *J. Catal.* 274 (2010) 11–20. doi:10.1016/j.jcat.2010.05.020.
- [131] T.D. Gould, M.M. Montemore, A.M. Lubers, L.D. Ellis, A.W. Weimer, J.L. Falconer, J.W. Medlin, Enhanced dry reforming of methane on Ni and Ni-Pt catalysts synthesized by atomic layer deposition, *Appl. Catal. Gen.* 492 (2015) 107–116. doi:10.1016/j.apcata.2014.11.037.

- [132] J.-S. Choi, K.-I. Moon, Y.G. Kim, J.S. Lee, C.-H. Kim, D.L. Trimm, Stable carbon dioxide reforming of methane over modified Ni/Al₂O₃ catalysts, *Catal. Lett.* 52 (1998) 43–47. doi:10.1023/A:1019002932509.
- [133] A.E. Castro Luna, M.E. Iriarte, Carbon dioxide reforming of methane over a metal modified Ni-Al₂O₃ catalyst, *Appl. Catal. Gen.* 343 (2008) 10–15. doi:10.1016/j.apcata.2007.11.041.
- [134] M.-S. Fan, A.Z. Abdullah, S. Bhatia, Utilization of Greenhouse Gases through Dry Reforming: Screening of Nickel-Based Bimetallic Catalysts and Kinetic Studies, *ChemSusChem.* 4 (2011) 1643–1653. doi:10.1002/cssc.201100113.
- [135] F. Cavani, F. Trifirò, A. Vaccari, Hydrotalcite-type anionic clays: Preparation, properties and applications., *Catal. Today.* 11 (1991) 173–301. doi:10.1016/0920-5861(91)80068-K.
- [136] C. Forano, U. Costantino, V. Prévot, C.T. Gueho, Chapter 14.1 - Layered Double Hydroxides (LDH), in: F. Bergaya, G. Lagaly (Eds.), *Dev. Clay Sci.*, Elsevier, 2013: pp. 745–782. doi:10.1016/B978-0-08-098258-8.00025-0.
- [137] D.G. Evans, R.C.T. Slade, Structural Aspects of Layered Double Hydroxides, in: *Layer. Double Hydroxides*, Springer, Berlin, Heidelberg, n.d.: pp. 1–87. doi:10.1007/430_005.
- [138] V. Rives, D. Carriazo, C. Martín, Heterogeneous Catalysis by Polyoxometalate-Intercalated Layered Double Hydroxides, in: *Pillared Clays Relat. Catal.*, Springer, New York, NY, 2010: pp. 319–397. doi:10.1007/978-1-4419-6670-4_12.
- [139] Y. Zhu, S. Zhang, B. Chen, Z. Zhang, C. Shi, Effect of Mg/Al ratio of NiMgAl mixed oxide catalyst derived from hydrotalcite for carbon dioxide reforming of methane, *Catal. Today.* 264 (2016) 163–170. doi:10.1016/j.cattod.2015.07.037.
- [140] O.W. Perez-Lopez, A. Senger, N.R. Marcilio, M.A. Lansarin, Effect of composition and thermal pretreatment on properties of Ni–Mg–Al catalysts for CO₂ reforming of methane, *Appl. Catal. Gen.* 303 (2006) 234–244. doi:10.1016/j.apcata.2006.02.024.
- [141] J. Guo, H. Lou, H. Zhao, D. Chai, X. Zheng, Dry reforming of methane over nickel catalysts supported on magnesium aluminate spinels, *Appl. Catal. Gen.* 273 (2004) 75–82. doi:10.1016/j.apcata.2004.06.014.
- [142] A.R. González, Y.J.O. Asencios, E.M. Assaf, J.M. Assaf, Dry reforming of methane on Ni–Mg–Al nanospheroid oxide catalysts prepared by the sol–gel method from hydrotalcite-like precursors, *Appl. Surf. Sci.* 280 (2013) 876–887. doi:10.1016/j.apsusc.2013.05.082.
- [143] A.I. Tsyganok, T. Tsunoda, S. Hamakawa, K. Suzuki, K. Takehira, T. Hayakawa, Dry reforming of methane over catalysts derived from nickel-containing Mg–Al layered double hydroxides, *J. Catal.* 213 (2003) 191–203. doi:10.1016/S0021-9517(02)00047-7.
- [144] X. Lin, R. Li, M. Lu, C. Chen, D. Li, Y. Zhan, L. Jiang, Carbon dioxide reforming of methane over Ni catalysts prepared from Ni–Mg–Al layered double hydroxides: Influence of Ni loadings, *Fuel.* 162 (2015) 271–280. doi:10.1016/j.fuel.2015.09.021.
- [145] C.E. Daza, S. Moreno, R. Molina, Co-precipitated Ni–Mg–Al catalysts containing Ce for CO₂ reforming of methane, *Int. J. Hydrog. Energy.* 36 (2011) 3886–3894. doi:10.1016/j.ijhydene.2010.12.082.
- [146] C.E. Daza, C.R. Cabrera, S. Moreno, R. Molina, Syngas production from CO₂ reforming of methane using Ce-doped Ni-catalysts obtained from hydrotalcites by reconstruction method, *Appl. Catal. Gen.* 378 (2010) 125–133. doi:10.1016/j.apcata.2010.01.037.
- [147] F. Touahra, M. Sehaïlia, W. Ketir, K. Bachari, R. Chebout, M. Trari, O. Cherifi, D. Halliche, Effect of the Ni/Al ratio of hydrotalcite-type catalysts on their performance in the methane dry reforming process, *Appl. Petrochem. Res.* 6 (2016) 1–13. doi:10.1007/s13203-015-0109-y.
- [148] A. Bhattacharyya, V.W. Chang, D.J. Schumacher, CO₂ reforming of methane to syngas: I: evaluation of hydrotalcite clay-derived catalysts, *Appl. Clay Sci.* 13 (1998) 317–328. doi:10.1016/S0169-1317(98)00030-1.
- [149] F. Basile, L. Basini, M.D. Amore, G. Fornasari, A. Guarinoni, D. Matteuzzi, G.D. Piero, F. Trifirò, A. Vaccari, Ni/Mg/Al Anionic Clay Derived Catalysts for the Catalytic Partial Oxidation of Methane: Residence Time Dependence of the Reactivity Features, *J. Catal.* 173 (1998) 247–256. doi:10.1006/jcat.1997.1942.
- [150] R. Dębek, M. Motak, D. Duraczyska, F. Launay, M.E. Galvez, T. Grzybek, P.D. Costa, Methane dry reforming over hydrotalcite-derived Ni–Mg–Al mixed oxides: the influence of Ni content on catalytic activity, selectivity and stability, *Catal. Sci. Technol.* 6 (2016) 6705–6715. doi:10.1039/C6CY00906A.
- [151] B. Djebbari, V.M. Gonzalez-Delacruz, D. Halliche, K. Bachari, A. Saadi, A. Caballero, J.P. Holgado, O. Cherifi, Promoting effect of Ce and Mg cations in Ni/Al catalysts prepared from hydrotalcites for the dry reforming of methane, *React. Kinet. Mech. Catal.* 111 (2014) 259–275. doi:10.1007/s11144-013-0646-2.

- [152] R. Dębek, K. Zubek, M. Motak, M.E. Galvez, P. Da Costa, T. Grzybek, Ni–Al hydrotalcite-like material as the catalyst precursors for the dry reforming of methane at low temperature, *Comptes Rendus Chim.* 18 (2015) 1205–1210. doi:10.1016/j.crci.2015.04.005.
- [153] K. Mette, S. Kühn, A. Tarasov, H. Düdder, K. Kähler, M. Muhler, R. Schlögl, M. Behrens, Redox dynamics of Ni catalysts in CO₂ reforming of methane, *Catal. Today.* 242 (2015) 101–110. doi:10.1016/j.cattod.2014.06.011.
- [154] K. Mette, S. Kühn, H. Düdder, K. Kähler, A. Tarasov, M. Muhler, M. Behrens, Stable Performance of Ni Catalysts in the Dry Reforming of Methane at High Temperatures for the Efficient Conversion of CO₂ into Syngas, *ChemCatChem.* 6 (2014) 100–104. doi:10.1002/cctc.201300699.
- [155] Z. Abdelsadek, M. Sehailia, D. Halliche, V.M. Gonzalez-Delacruz, J.P. Holgado, K. Bachari, A. Caballero, O. Cherifi, In-situ hydrogasification/regeneration of NiAl-hydrotalcite derived catalyst in the reaction of CO₂ reforming of methane: A versatile approach to catalyst recycling, *J. CO₂ Util.* 14 (2016) 98–105. doi:10.1016/j.jcou.2016.03.004.
- [156] H. Düdder, K. Kähler, B. Krause, K. Mette, S. Kühn, M. Behrens, V. Scherer, M. Muhler, The role of carbonaceous deposits in the activity and stability of Ni-based catalysts applied in the dry reforming of methane, *Catal. Sci. Technol.* 4 (2014) 3317–3328. doi:10.1039/C4CY00409D.
- [157] T. Shishido, M. Sukenobu, H. Morioka, R. Furukawa, H. Shirahase, K. Takehira, CO₂ reforming of CH₄ over Ni/Mg–Al oxide catalysts prepared by solid phase crystallization method from Mg–Al hydrotalcite-like precursors, *Catal. Lett.* 73 (2001) 21–26. doi:10.1023/A:1009066017469.
- [158] P. Tan, Z. Gao, C. Shen, Y. Du, X. Li, W. Huang, Ni-Mg-Al solid basic layered double oxide catalysts prepared using surfactant-assisted coprecipitation method for CO₂ reforming of CH₄, *Chin. J. Catal.* 35 (2014) 1955–1971. doi:10.1016/S1872-2067(14)60171-6.
- [159] A.I. Tsyganok, K. Suzuki, S. Hamakawa, K. Takehira, T. Hayakawa, Mg–Al Layered Double Hydroxide Intercalated with [Ni(edta)]₂- Chelate as a Precursor for an Efficient Catalyst of Methane Reforming with Carbon Dioxide, *Catal. Lett.* 77 (2001) 75–86. doi:10.1023/A:1012739112430.
- [160] R. Dębek, K. Zubek, M. Motak, P.D. Costa, T. Grzybek, Effect of nickel incorporation into hydrotalcite-based catalyst systems for dry reforming of methane, *Res. Chem. Intermed.* 41 (2015) 9485–9495. doi:10.1007/s11164-015-1973-x.
- [161] Z. Hou, T. Yashima, Meso-porous Ni/Mg/Al catalysts for methane reforming with CO₂, *Appl. Catal. Gen.* 261 (2004) 205–209. doi:10.1016/j.apcata.2003.11.002.
- [162] N. Li, C. Shen, P. Tan, Z. Zuo, W. Huang, Effect of phase transformation on the stability of Ni-Mg-Al catalyst for dry reforming of methane, *IJC- Vol54A10 Oct.* 2015. (2015). <http://nopr.niscair.res.in/handle/123456789/32852> (accessed January 18, 2018).
- [163] V. Rives, Characterisation of layered double hydroxides and their decomposition products, *Mater. Chem. Phys.* 75 (2002) 19–25. doi:10.1016/S0254-0584(02)00024-X.
- [164] Y. Lwin, M.A. Yarmo, Z. Yaakob, A.B. Mohamad, W. Ramli Wan Daud, Synthesis and characterization of Cu–Al layered double hydroxides, *Mater. Res. Bull.* 36 (2001) 193–198. doi:10.1016/S0025-5408(01)00491-3.
- [165] S. Kannan, A. Dubey, H. Knozinger, Synthesis and characterization of CuMgAl ternary hydrotalcites as catalysts for the hydroxylation of phenol, *J. Catal.* 231 (2005) 381–392. doi:10.1016/j.jcat.2005.01.032.
- [166] S. Velu, K. Suzuki, M.P. Kapoor, S. Tomura, F. Ohashi, T. Osaki, Effect of Sn Incorporation on the Thermal Transformation and Reducibility of M(II)Al-Layered Double Hydroxides [M(II) = Ni or Co], *Chem. Mater.* 12 (2000) 719–730. doi:10.1021/cm9904685.
- [167] C.E. Daza, J. Gallego, J.A. Moreno, F. Mondragón, S. Moreno, R. Molina, CO₂ reforming of methane over Ni/Mg/Al/Ce mixed oxides, *Catal. Today.* 133–135 (2008) 357–366. doi:10.1016/j.cattod.2007.12.081.
- [168] C.E. Daza, J. Gallego, F. Mondragón, S. Moreno, R. Molina, High stability of Ce-promoted Ni/Mg–Al catalysts derived from hydrotalcites in dry reforming of methane, *Fuel.* 89 (2010) 592–603. doi:10.1016/j.fuel.2009.10.010.
- [169] C.E. Daza, S. Moreno, R. Molina, Ce-incorporation in mixed oxides obtained by the self-combustion method for the preparation of high performance catalysts for the CO₂ reforming of methane, *Catal. Commun.* 12 (2010) 173–179. doi:10.1016/j.catcom.2010.09.012.
- [170] A.V.P. Lino, E.M. Assaf, J.M. Assaf, Hydrotalcites derived catalysts for syngas production from biogas reforming: Effect of nickel and cerium load, *Catal. Today.* 289 (2017) 78–88. doi:10.1016/j.cattod.2016.08.022.
- [171] H.-P. Ren, Y.-H. Song, W. Wang, J.-G. Chen, J. Cheng, J. Jiang, Z.-T. Liu, Z.-W. Liu, Z. Hao, J. Lu, Insights into CeO₂-modified Ni–Mg–Al oxides for pressurized carbon dioxide reforming of methane, *Chem. Eng. J.* 259 (2015) 581–593. doi:10.1016/j.cej.2014.08.029.

- [172] R. Dębek, A. Gramatyka, M. Motak, P.D. Costa, Produkcja gazu syntezowego w reakcji suchego reformingu metanu na katalizatorach hydrotalkitowych, Syngas production by dry reforming of methane over hydrotalcite-derived catalysts, *Przem. Chem.* 93 (2014) 2026–2032.
- [173] R. Dębek, M. Radlik, M. Motak, M.E. Galvez, W. Turek, P. Da Costa, T. Grzybek, Ni-containing Ce-promoted hydrotalcite derived materials as catalysts for methane reforming with carbon dioxide at low temperature – On the effect of basicity, *Catal. Today*. 257 (2015) 59–65. doi:10.1016/j.cattod.2015.03.017.
- [174] R. Dębek, M.E. Galvez, F. Launay, M. Motak, T. Grzybek, P. Da Costa, Low temperature dry methane reforming over Ce, Zr and CeZr promoted Ni–Mg–Al hydrotalcite-derived catalysts, *Int. J. Hydrog. Energy*. 41 (2016) 11616–11623. doi:10.1016/j.ijhydene.2016.02.074.
- [175] R. Dębek, M. Motak, M.E. Galvez, P.D. Costa, T. Grzybek, Catalytic activity of hydrotalcite-derived catalysts in the dry reforming of methane: on the effect of Ce promotion and feed gas composition, *React. Kinet. Mech. Catal.* 121 (2017) 185–208. doi:10.1007/s11144-017-1167-1.
- [176] X. Yu, N. Wang, W. Chu, M. Liu, Carbon dioxide reforming of methane for syngas production over La-promoted NiMgAl catalysts derived from hydrotalcites, *Chem. Eng. J.* 209 (2012) 623–632. doi:10.1016/j.cej.2012.08.037.
- [177] A. Serrano-Lotina, L. Rodríguez, G. Muñoz, A.J. Martín, M.A. Folgado, L. Daza, Biogas reforming over La-NiMgAl catalysts derived from hydrotalcite-like structure: Influence of calcination temperature, *Catal. Commun.* 12 (2011) 961–967. doi:10.1016/j.catcom.2011.02.014.
- [178] A. Serrano-Lotina, L. Rodríguez, G. Muñoz, L. Daza, Biogas reforming on La-promoted NiMgAl catalysts derived from hydrotalcite-like precursors, *J. Power Sources*. 196 (2011) 4404–4410. doi:10.1016/j.jpowsour.2010.10.107.
- [179] H. Liu, D. Wierzbicki, R. Debek, M. Motak, T. Grzybek, P. Da Costa, M.E. Gálvez, La-promoted Ni-hydrotalcite-derived catalysts for dry reforming of methane at low temperatures, *Fuel*. 182 (2016) 8–16. doi:10.1016/j.fuel.2016.05.073.
- [180] A.F. Lucrédio, J.D.A. Bellido, E.M. Assaf, Effects of adding La and Ce to hydrotalcite-type Ni/Mg/Al catalyst precursors on ethanol steam reforming reactions, *Appl. Catal. Gen.* 388 (2010) 77–85. doi:10.1016/j.apcata.2010.08.026.
- [181] C. Li, P.-J. Tan, X.-D. Li, Y.-L. Du, Z.-H. Gao, W. Huang, Effect of the addition of Ce and Zr on the structure and performances of Ni–Mo/CeZr–MgAl(O) catalysts for CH₄–CO₂ reforming, *Fuel Process. Technol.* 140 (2015) 39–45. doi:10.1016/j.fuproc.2015.08.020.
- [182] A.I. Tsyganok, M. Inaba, T. Tsunoda, K. Uchida, K. Suzuki, K. Takehira, T. Hayakawa, Rational design of Mg–Al mixed oxide-supported bimetallic catalysts for dry reforming of methane, *Appl. Catal. Gen.* 292 (2005) 328–343. doi:10.1016/j.apcata.2005.06.007.
- [183] J. Zhang, H. Wang, A.K. Dalai, Effects of metal content on activity and stability of Ni-Co bimetallic catalysts for CO₂ reforming of CH₄, *Appl. Catal. Gen.* 339 (2008) 121–129. doi:10.1016/j.apcata.2008.01.027.
- [184] R. Dębek, M. Motak, M.E. Galvez, T. Grzybek, P. Da Costa, Influence of Ce/Zr molar ratio on catalytic performance of hydrotalcite-derived catalysts at low temperature CO₂ methane reforming, *Int. J. Hydrog. Energy*. 42 (2017) 23556–23567. doi:10.1016/j.ijhydene.2016.12.121.
- [185] R. Dębek, M. Motak, M.E. Galvez, T. Grzybek, P. Da Costa, Promotion effect of zirconia on Mg(Ni,Al)O mixed oxides derived from hydrotalcites in CO₂ methane reforming, *Appl. Catal. B Environ.* 223 (2018) 36–46. doi:10.1016/j.apcatb.2017.06.024.
- [186] A.F. Lucrédio, J.M. Assaf, E.M. Assaf, Reforming of a model sulfur-free biogas on Ni catalysts supported on Mg(Al)O derived from hydrotalcite precursors: Effect of La and Rh addition, *Biomass Bioenergy*. 60 (2014) 8–17. doi:10.1016/j.biombioe.2013.11.006.
- [187] H. Long, Y. Xu, X. Zhang, S. Hu, S. Shang, Y. Yin, X. Dai, Ni-Co/Mg-Al catalyst derived from hydrotalcite-like compound prepared by plasma for dry reforming of methane, *J. Energy Chem.* 22 (2013) 733–739. doi:10.1016/S2095-4956(13)60097-2.
- [188] H. Liu, L. Yao, H.B. Hadj Taief, M. Benzina, P. Da Costa, M.E. Gálvez, Natural clay-based Ni-catalysts for dry reforming of methane at moderate temperatures, *Catal. Today*. (2016). doi:10.1016/j.cattod.2016.12.017.
- [189] J. Ashok, M. Subrahmanyam, A. Venugopal, Hydrotalcite structure derived Ni–Cu–Al catalysts for the production of H₂ by CH₄ decomposition, *Int. J. Hydrog. Energy*. 33 (2008) 2704–2713. doi:10.1016/j.ijhydene.2008.03.028.
- [190] S.A. Theofanidis, R. Batchu, V.V. Galvita, H. Poelman, G.B. Marin, Carbon gasification from Fe–Ni catalysts after methane dry reforming, *Appl. Catal. B Environ.* 185 (2016) 42–55. doi:10.1016/j.apcatb.2015.12.006.

- [191] S.A. Theofanidis, V.V. Galvita, M. Sabbe, H. Poelman, C. Detavernier, G.B. Marin, Controlling the stability of a Fe–Ni reforming catalyst: Structural organization of the active components, *Appl. Catal. B Environ.* 209 (2017) 405–416. doi:10.1016/j.apcatb.2017.03.025.
- [192] F. Guo, J.-Q. Xu, W. Chu, CO₂ reforming of methane over Mn promoted Ni/Al₂O₃ catalyst treated by N₂ glow discharge plasma, *Catal. Today.* 256 (2015) 124–129. doi:10.1016/j.cattod.2015.02.036.
- [193] F. Touahra, M. Sehalia, D. Halliche, K. Bachari, A. Saadi, O. Cherifi, (MnO/Mn₃O₄)-NiAl nanoparticles as smart carbon resistant catalysts for the production of syngas by means of CO₂ reforming of methane: Advocating the role of concurrent carbothermic redox looping in the elimination of coke, *Int. J. Hydrog. Energy.* 41 (2016) 21140–21156. doi:10.1016/j.ijhydene.2016.08.194.
- [194] A. Siahvashi, D. Chesterfield, A.A. Adesina, Propane CO₂ (dry) reforming over bimetallic Mo–Ni/Al₂O₃ catalyst, *Chem. Eng. Sci.* 93 (2013) 313–325. doi:10.1016/j.ces.2013.02.003.
- [195] L. Yao, M.E. Galvez, C. Hu, P. Da Costa, Mo-promoted Ni/Al₂O₃ catalyst for dry reforming of methane, *Int. J. Hydrog. Energy.* 42 (2017) 23500–23507. doi:10.1016/j.ijhydene.2017.03.208.